博士論文（要約）

Phase-changing interfaces
for human-material interaction

（ヒューマン・マテリアル・インタラクションに向けた相変化インタフェース

Koya Narumi

鳴海 紘也

A doctoral dissertation

Graduate School of Information Scence and Technology

The University of Tokyo

December 2019

PHASE-CHANGING INTERFACES
for human-material interaction

ABSTRACT

In the last half-century, the way we interact with digital information has diverged drastically. The history of human computer-interaction (HCI) started by interfaces based on mechanical switches, punch cards, or texts (also known as character user interfaces, CUIs), with which only specialized technicians could solve mathematical problems such as ballistic calculation of missiles. Then the personal use of the computer gradually became accessible to non-professional users, thanks to the invention of graphical user interfaces (GUIs) and intuitive hardware such as a mouse. After the touch interfaces became pervasive, more and more people started to interact with computers in more intuitive ways with smartphones.

From this tendency, I speculate that as the number of interfaces increases around our daily objects and environments, interaction techniques will become more physical rather than digital, and absolutely, materials can directly and intellectually interact with humans. I believe this direction corresponds with the vision of ubiquitous computing, in which the interfaces weave themselves into our everyday life and disappear.

Standing on the idea of current shape-changing interfaces, I foresee the future where humans do not always interact with conventional computer interfaces, but also with the materials and objects around our living environment, via the physical properties of them, which I call as "human-material interaction (HMI)."

Especially, the research motivation of this thesis is to impart shape-changing interfaces the dynamic ability to leverage multiple "phases" of materials (*i.e.,* solid, liquid, gas, and viscoelastic solid-liquid states), that is, two types of "phase-changing interfaces" as embodiment of human-material interaction in order to extend the current design space of interaction that is typically limited within a single phase of the material. The first project was Liquid Pouch Motors, the novel actuation mechanism using liquid-to-gas phase change of the low boiling point liquid. We investigated basic motion, mathematical analysis, fabrication method, mechanical evaluation, and four applications leveraging large expansion and actuation of phase change

activated diverse heat source. The second project was Self-healing UI, the soft-bodied user interfaces made from self-healing materials that can restore mechanical and electrical integrity repeatedly just by making a physical connection. By tuning the rheological property of the self-healing materials, the interface device demonstrates unique properties of solid, solid-liquid, and liquid phases at the same time. We showed material preparation and device fabrication, as well as primitive sensing structures and design space with corresponding applications.

I believe human-material interaction and phase-changing interfaces proposed in this thesis will enrich and enlarge how we interact with our surrounding objects and environments in more diverse yet intuitive ways.

The following people served as readers for this thesis:

Toshihiko Yamasaki

Associate Professor, Department of Computer Science,
Graduate School of Information Science and Technology,
The University of Tokyo

Yoshihiro Kawahara

Professor, Department of Electrical Engineering and Information Systems,
Graduate School of Engineering,
The University of Tokyo

Takeo Igarashi

Professor, Department of Computer Science,
Graduate School of Information Science and Technology,
The University of Tokyo

Koji Yatani

Associate Professor, Department of Electrical Engineering and Information Systems,
Graduate School of Engineering,
The University of Tokyo

Ryuma Niiyama

Lecturer, Department of Electrical Engineering and Information Systems,
Graduate School of Information Science and Technology,
The University of Tokyo

ACKNOWLEDGMENTS

always seriously caring about me through my stay in CMU. Also, the friends around Morphing Matter Lab helped me enjoy unfamiliar foreign environments: Jack Forman, Zeyu Yan, Haolin Liu, Tingyu Cheng, Youngwook Do, Mohan Yeh, Jasio Santillan, Taylor Tabb, Yi-Chin Lee, Kuanren Qian, Rahul Sharma, Jenny Hu, Adrian Galvin, Ozguc Bertug Capunaman, Kashyap Nishtala, Jianxun Cui, Siyan Zhao, and Dr. Sovik Das. Especially, I grew up and got better as Morphers with Fang Qin, Humphrey Yan, Jianzhe Gu, and Danli Luo. Dr. Guanyun Wang, Dr. Ye Tao, Lea Albaugh, and Michael Rivera are, and will be, my most respectful friends as designers and engineers. In self-healing projects in CMU, I spend literally hundreds of days and nights with Siyuan Liu and Huai-Yu Cheng in Prof. Mohammad Islam's group to embody the magic of materials science into interfaces. The collaboration with Dr. Eric Markvicka from Prof. Carmel Majidi's group made me learn how the graduating Ph.D. candidates should be.

Outside CMU, I heavily owe my non-research life in Pittsburgh to Prof. Teruko Mitamura, Hikaru Mamiya, Tomonori Teraoka, Prof. Maki Sugimoto, Dr. Daisuke Kase, Dr. Keita Higuchi, Seita Kayukawa, Dr. Chieko Asakawa, sharing shelter, food, or drinks together.

Although there were not so many visible outputs, most of my projects were (and remain) highly inspired by the visionaries around me: Prof. Yasuaki Kakehi, Dr. Junichi Yamaoka, and Dr. Satoshi Nakamaru in Yasuaki Kakehi's Lab and Ryosuke Yamamura, Mercari, Inc. on material interaction; Prof. Tomohiro Tachi, Kai Suto, Prof. Kazuya Saito, and Yoshiyuki Miyamae on mathematics, engineering, and the art of origami; and Ryo Suzuki, Ken Nakagaki, and Prof. Takeo Igarashi on strong insight and passion to human-computer interaction.

CONTENTS

LIST OF FIGURES

LIST OF TABLES

INTRODUCTION

1.1 RESEARCH QUESTION

In the last half-century, the way we interact with digital information has diverged drastically. The history of human computer-interaction (HCI) started by interfaces based on mechanical switches, punch cards, or texts (also known as character user interfaces, CUIs), with which only specialized technicians could solve mathematical problems such as ballistic calculation of missiles. Then the personal use of the computer gradually became accessible to non-professional users, thanks to the invention of graphical user interfaces (GUIs) and intuitive hardware such as a mouse. After the touch interfaces became pervasive, more and more people started to interact with computers in more intuitive ways with smartphones.

From this tendency, I speculate that as the number of interfaces increases around our daily objects and environments, interaction techniques will become more physical rather than digital, and absolutely, materials can directly and intellectually interact with humans. I believe this direction corresponds with the vision of ubiquitous computing, in which the interfaces weave themselves into our everyday life and disappear.

Standing on the idea of current shape-changing interfaces, I foresee the future where humans do not always interact with conventional computer interfaces, but also with the materials and objects around our living environment, via the physical properties of them, which I call as "human-material interaction (HMI)." Especially, the research motivation of this thesis is to impart shape-changing interfaces the dynamic ability to leverage multiple "phases" of materials (*i.e.,* solid, liquid, gas, and viscoelastic solid-liquid states), as one embodiment of human-material interaction in order to extend the current design space of interaction that is typically limited within a single phase of the material.

Therefore, the research questions of this thesis are summarized as shown below:

1. What is human-material interaction (HMI)? What is the relationship between HCI and HMI? How can we leverage human-material interaction?

2. As one embodiment of HMI, how can we fabricate and make use of phase-changing interfaces?

1.2 BACKGROUND CONTEXT

1.2.1 *Human-computer Interaction – Transition from Digital to Physical*

In the history of computer science, human beings – living in the physical world – and computers – existing in the digital world – have been mediated via the system called *interfaces*, as shown in Figure 1. One of the oldest styles of them is character user interfaces (CUIs), where the digital bits of computers are translated from/into human languages and only a limited number of professional people have access to them. Next, as computers prevail for personal use, the majority of interfaces changed into graphical user interfaces (GUIs), where the digital information is presented as 2D shapes of icons, pointers, and drawings. After the invention of smartphones, then, the touch interfaces turned out to be a pervasive way to communicate with computers through haptic feedback.

Although there is no hierarchy among these types of interfaces and different interfaces still have their own niches depending on the use of the computers, it is not too much to say that **the more pervasive interfaces have the more physical ways of interaction for humans**; languages for CUIs are more logical and conceptual, while shape or touch is much more close to our primitive experiences. As the interfaces evolve more and more, the way we interact with computers can absolutely become identical with the way we interact with objects in our daily, thus the physical world.

The starting point of my research lies in the question "how can human-computer interaction get more close from the digital world to the physical world? What will it be like?"

Figure 1: The history of pervasive interfaces. The way we interact with digital information is getting closer to the physical world, from languages to shapes to haptics.
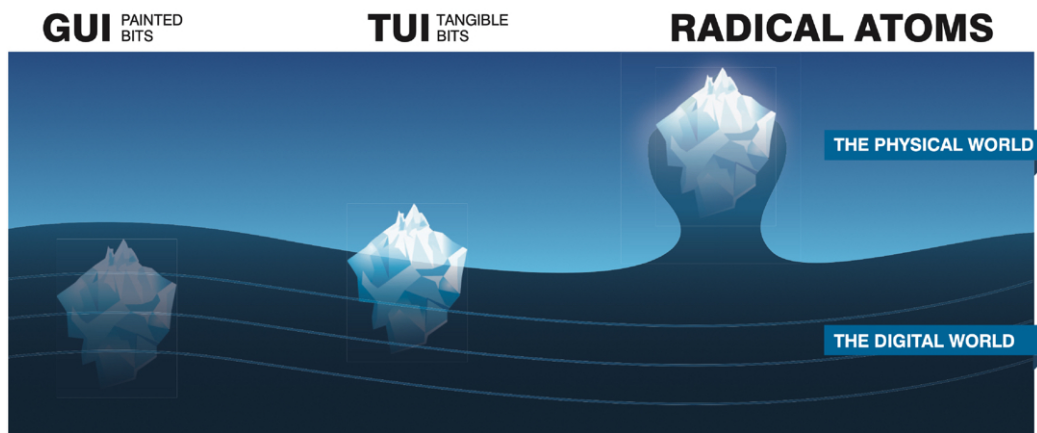
Figure 2: The vision of Radical Atoms [27]. The iceberg floats in the digital ocean, and is gradually pulled up to the side of the physical world. ©2012 ACM. Reprinted by permission.

As another type of analogy, Ishii *et al*. drew the relationship between the digital world and the physical world using the iceberg floating in the ocean [27]. In the GUIs, the iceberg completely sinks in the digital ocean, and humans cannot touch it from the physical world. In the case of tangible user interfaces (TUIs), users can touch the surface of the iceberg and change the digital information from the physical world. In the case of the Radical Atoms, then, the iceberg almost pops out of the ocean and users can grasp or knead the interfaces. This drawing also shows that human-computer interaction can potentially get closer to the physical side.

In this vision, however, the entity of interaction (the iceberg) is still strongly related to the digital world. My question here is "can physical objects distinct from the digital world interact with humans, when they are pulled completely up from the digital ocean?"

1.2.2   *Shape-changing Interfaces*

Recently, the researchers in HCI have been working on the domain called shape-changing interfaces, the interfaces that interact with humans through shape change of physical objects. Here, I will categorize the collection of these works by the "phases" of the materials (*e.g.,* solid, solid-liquid, liquid, and gas) composing each interface, and thereby clarify that **the shape-changing interfaces make more use of the material property of the objects for human interaction, rather than the computer control behind them**.

Solid shape-changing interfaces

Solid shape-changing interfaces are one of the most intensely investigated systems in HCI. They re-configure the relative position of many stiff objects (such as pins or voxels) to render multiple shapes, which in general result in precise, fast, and reproducible motion. Figure 3 shows the examples of solid shape-changing interfaces reconfiguring their shape.
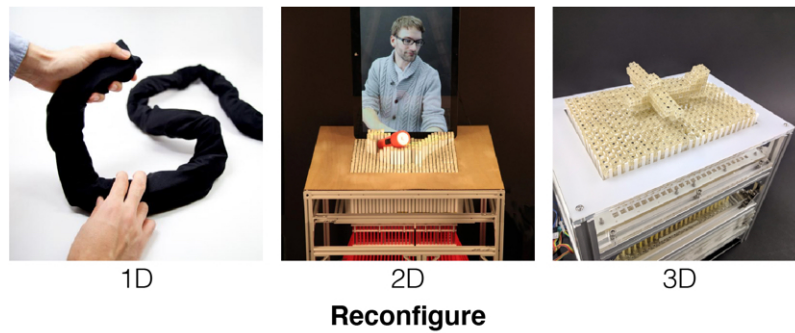
Figure 3: Examples of solid shape-changing interfaces. Each picture shows 1D [54], 2D [20], and 3D [75] reconfig-uration. Publication rights of these figures are reserved by the authors of "LineFORM", "inFORM", and "Dynablock" by Nakagaki et al., Follmer and Leithinger et al., and Suzuki et al., respectively. Reprinted from [54][20][75], permitted by the authors of each project.

1.2.2.2   *Solid-liquid shape-changing interfaces*

Solid-liquid materials like silicone rubbers and dough retain viscoelastic property; by tuning their property the interfaces can demonstrate large transformation or comfortable conformation to the skin or other objects thanks to their flexible and elastomeric nature, as shown in Figure 4.
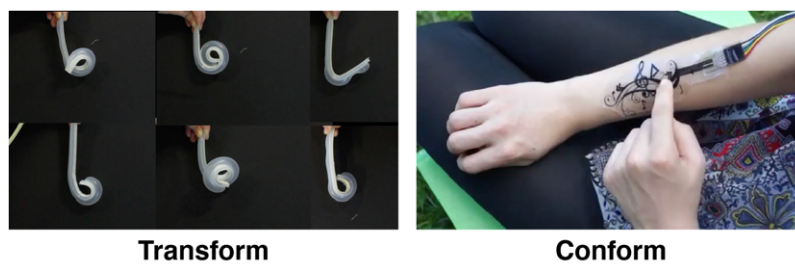
Figure 4: Examples of solid-liquid shape-changing interfaces. Each picture shows dynamic transformation [94] and smooth conformation to human skin [86]. Publication rights of these figures are reserved by the authors of "PneUI" and "iSkin" by Yao et al. and Weigel et al., respectively. Reprinted from [94][86], permitted by the authors of each project.

16

1.2.2.3 *Liquid shape-changing interfaces*

Although there are fewer reports compared to the two phases mentioned above, liquid shape-changing interfaces also exist as shown in Figure 5. For example, Programmable blobs [82] used magnetic fluid to display information breakable and healable. Also, a bubble display iteratively generates and breaks bubbles for a rewritable ambient display [24]. Programmable Droplets [80] controls the shape, number, and position of liquid metal or aqueous solutions by an electric field. In the video scenario, this showed that two droplets with different colors fused into a single droplet with a new color.
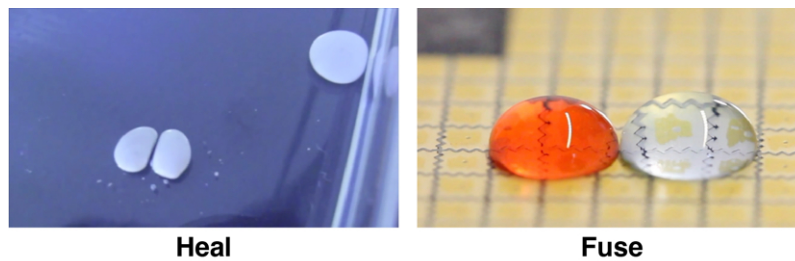
Figure 5: Examples of liquid shape-changing interfaces. Each picture shows two droplets made from the same material heal and break [82] and two droplets with different colors fuse into a new color [80]. Publication rights of these figures are reserved by the authors of "Programmable Blobs" and "Programmable Droplets for Interaction" by Wakita et al. and Umapathi et al., respectively. Reprinted from [82][80], permitted by the authors of each project.

From these examples, I can say that many ways of interaction by shape-changing interfaces (*i.e.,* reconfigure, transform, conform, heal, fuse, etc) are mainly enabled by the material phases, rather than the computer controlling the objects. This finding that the material property can potentially dominate interaction led to my proposal "human-material interaction" and "phase-changing interfaces" that I will explain in detail in the next chapter.

1.2.3 *Imaginary Interfaces with Invisible Computers*

As one of the ultimate goals of the way we interact with computers, researchers envisioned the computer "invisible" from users. Here I introduce two classic ideas.

1.2.3.1 *Ubiquitous computing*

Tracing back to the notion of ubiquitous computing proposed in 1999 [88], Mark Weiser mentioned:

> The most profound technologies are those that disappear. They weave themselves into the fabric of everyday life until they are indistinguishable from it.

1) Tear off a piece of perfect red.

2) ROLLING A BALL OF CLAY
Roll a ball of clay to let it snap to a perfect sphere.

3) A PERFECT SPHERE

4) SMASH IT INTO A PERFECT CYLINDER
Smash a ball into a perfect cylinder.

5) 6) ALL THE HOLES GET DRILLED TOGETHER
Draw eight dots and stick a pin into one of them to drill eight holes.

7) 8) WHOLE THING SPLITS DOWN THE LINE
Draw a line along the cut and tap it with a knife.

9) 10) TWO HALVES BEHAVE AS ONE
Split a piece in two even halves, then the operations performed on one part are mirrored in the other.

11) 12) CARVE AWAY SHADED AREA
Carve away shaded area with chisel and mirror it in another piece.

13) 14) INSERT SPEAKER + CIRCUIT
Insert materials and put two mirrored pieces together.

15) Final rattle created with Radical Atoms.

Figure 6: Perfect Red [8, 27]. Here, clay made from an "imaginary" material can not only change digital information physically, but more importantly, change its physical shape digitally. Source from [27]. ©2012 ACM. Reprinted by permission.

In this regard, the ultimate interfaces may hide or delete the existence of computers so that the daily objects pervasive around us can interact with humans without any intervention.

1.2.3.2 *Perfect Red*

Another imaginary vision of future interaction I refer to is called Perfect Red, proposed by Ishii et al. in 2012 [8, 27] (Figure 6). In this vision, for example, the user can tear off an imaginary clay and roll a ball on his/her palm. Then, the clay "reads" the user's intention and becomes a "perfect" sphere. The vision video [8] also shows this imaginary clay pieces can be perfectly cut, dug, or joined as if they were in the digital world.

What is interesting in this vision is that the imaginary clay acts as a digital object (*e.g.,* perfectly cut or healed on users' demands), but it is actually in the physical world and there is no visible computer connected to it. As I will explain in more detail in the next chapter, this imaginary interaction can now partly be achieved using the specific materials property and the computational fabrication technique developed in this decade.

1.2.4 *Conclusions of Backgrounds*

In this section, I visited the history of interfaces, originally mediated by languages in CUIs to more physical forms like shape in GUIs or touch in touch interfaces with the remark that the pervasive interfaces tend to have more physical ways of interaction. I also introduced the recent research domain of shape-changing interfaces and noted that the material properties of such interfaces affect the way we interact with them. Finally, the vision of ubiquitous computing and perfect red imply that future interfaces will be more pervasive to our everyday objects and environments and ultimately become indistinguishable with non-interactive objects.

Standing on this background context, from the next chapter, I will propose the notion of human-material interaction in which objects interacts with humans via the properties of the materials composing the objects. In this notion, the computer does not necessarily show up as an indispensable entity of human interaction. Also, as one embodiment of human-material interaction, I will propose phase-changing interfaces that can utilize phase change as a material property and show novel interaction unable to achieve with conventional shape-changing interfaces restricted to a certain static phase of the material.

1.3 THESIS CONTRIBUTION AND OVERVIEW

1.3.1 *Contribution*

In this thesis, the main contribution is as follows:

1. I proposed phase-changing interfaces that leverage multiple materials phases for interaction.

2. I proposed human-material interaction and described the difference between conventional human-computer interaction and hardware user interfaces through both high-level descriptions and two project examples.

3. I and coauthors proposed Liquid Pouch Motors that change their shape via liquid-to-gas phase change and described its basic motion, mathematical analysis, fabrication methods, mechanical evaluation, and four distinctive applications.

4. I and coauthors proposed Self-healing UI that works as if they were solid, solid-liquid, and liquid at the same time due to the intrinsic property of the self-healing material we used. We discussed the material preparation of the materials, device fabrication, mechanical/electrical evaluation along with its healing property, sensing primitives, and five applications based on design space that conventional shape-changing interfaces partly and individually achieved.

More visually, my contribution is summarized in Figure 7. I proposed two interfaces: (1) phase-switching interfaces that toggle between two phases on demand and (2) Phase-transcendent interfaces that work as if they are in multiple phases at the same time. These interfaces were implemented and confirmed through two projects of Liquid Pouch Motors and Self-healing UI, respectively. The relationship between these two research projects and conventional shape-changing interfaces is summarized in Figure 8.

1.3.2 *Statement of Multiple Authorship*

Seven projects are included in this thesis: Liquid Pouch Motors [P1], the electric phase-change actuator [P3], Papilion [P8], A LIVE UN LIVE [P9], Laser Pouch Motors [P2], SWCNTs-PBS elastomeric conductor [under submission], and Self-healing UI [P4]. These projects were done by a collaborative effort involving many individuals at The University of Tokyo, Keio University, Carnegie Mellon University, and ANREALAGE Inc. Therefore, I will partly use "we" in this thesis regarding the related chapters and sections.

1. Liquid Pouch Motors. I was in charge of ideation, writing, mechanical experiments, mathematical calculation and photo/video shooting as a first author [P1, P6, A3, A4, A5]. The application section of this journal publication overlaps with the project related to Liquid Pouch Motors below.

2. Electric phase-change actuator. I was in charge of story writing, experimental support, a few application productions, and photo/video shooting as a 2nd author [P3], while the main body of experiments and mathematical analysis were done by Kenichi Nakahara as a 1st author.

3. Papilion. I was in charge of the production of large numbers of Liquid Pouch Motors, construction, ideation, and exhibition as a 3rd contributor [P8], while the whole project was mainly led by Hiroki Sato.

4. A LIVE UN LIVE. I was in charge of ideation and technical support for ANREALGE [P9], while the project was mainly led by Kunihiro Morinaga, and the motors were implemented by Hiroki Sato and Dr. Tomohiro Akagawa.
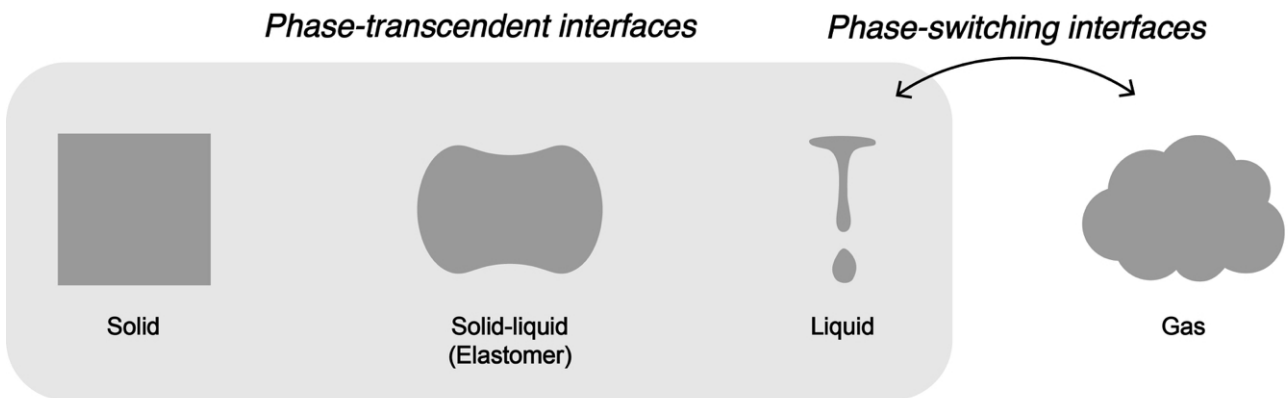
Figure 7: Summary of contribution in this thesis. Two types of interfaces were proposed that range from solid, solid-liquid, liquid, and gas all of which are the material phases we usually observe in our lives: (1) Phase-switching interfaces that toggle between two phases on demand, through the project Liquid Pouch Motors and (2) Phase-transcendent interfaces that work as if they are in multiple phases at the same time, through the project Self-healing UI.
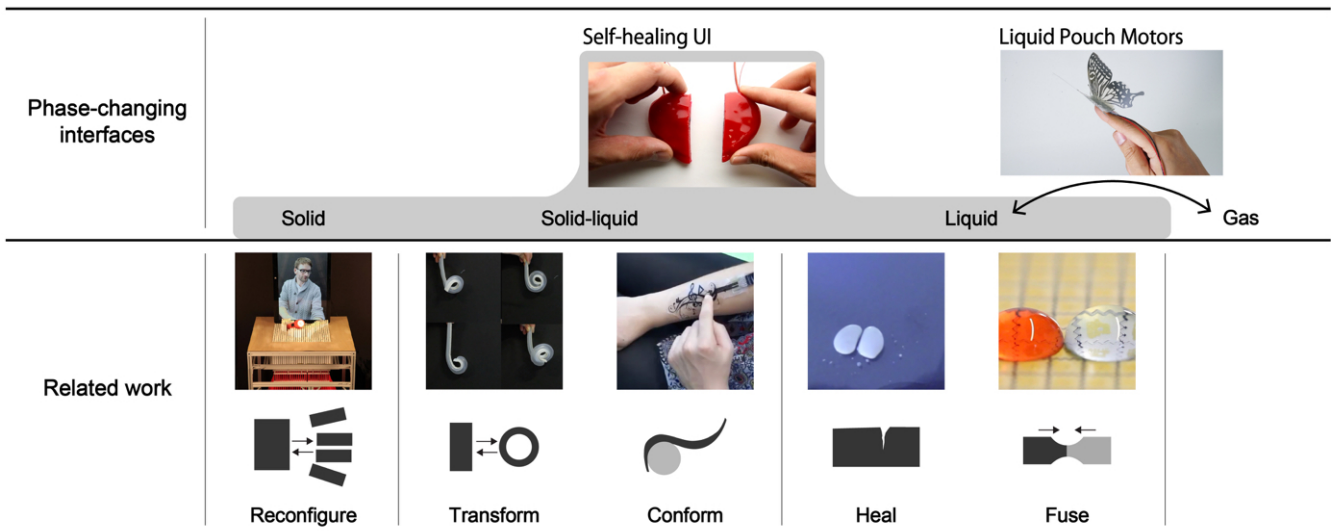
Figure 8: Relationship between our projects and conventional shape-changing interfaces. Liquid Pouch Motors bridge liquid and gas, while Self-healing UI covers the design space of solid, solid-liquid, and liquid shape-changing interfaces. Figures of related work were reprinted from [20],[94],[89],[82],[80], permitted by the authors (from left to right).

5. Laser Pouch Motors. I was in charge of ideation, writing, and experimental support as one of three co-1st authors [P2], while projector control was done by Takefumi Hiraki and the main body of the experiments was done by Kenichi Nakahara, the other co-1st authors.

6. SWCNTs-PBS elastomeric conductor. I was in charge of implementation and writing applications, macroscopic time-lapse imaging, and photo/video shooting as a 2nd author [under submission], while preparation of materials and evaluation was mainly done by Siyuan Liu.

7. Self-healing UI. I was in charge of ideation, material preparation, writing, development of sensing primitives, photo/video shooting, and application design and implementation as one of two co-1st authors [P4, P5, P7, A5, A6], while four applications were mainly implemented by Fang Qin, the other co-1st author.

1.3.3 *Overview of This Thesis*

This thesis is comprised of five chapters and one Appendix chapter followed by reference and the publication list.

In Chapter 1, I introduced research questions for this thesis, background contexts of HCI as a starting point of my proposal for this thesis. I also clarified the contribution of this thesis and my contribution to each project.

In Chapter 2, I defined, explained, and exemplified the concept of human-material interaction (HMI). I also introduced phase-changing interphases as one type of embodiment of HMI, which is followed by two implementations of phase-changing interfaces, Liquid Pouch Motors and Self-healing UI, from the next chapters.

In Chapter 3, first I explained the basic mechanism, fabrication, and mechanical evaluation of Liquid Pouch Motors as an example of phase-changing interfaces. Next, I demonstrated four applications of Liquid Pouch Motors: electric phase-change actuator, Papilion, A LIVE UN LIVE, and Laser Pouch Motors.

In Chapter 4, first I explained the SWCNTs aerogel-PBS project that is about developing elastomeric and conductive self-healing polymer in the context of materials science. Next, we applied the knowledge and experience we derived from the SWCNTs-PBS project to user interfaces. In order to explore more about fabrication and design space aspects, we changed the material from high performance yet expensive and time-consuming SWCNTs aerogel-PBS into lower performance yet cheaper and faster-to-prepare MWCNTs dispersion-PBS. Therefore, we described the preparation and fabrication for Self-healing UI again, as well as sensing primitives, design space, and applications.

In Chapter 5, I revisited two projects introduced in Chapter 3 and Chapter 4, and reorganized the projects with the vision firstly described in Chapter 1. This thesis was finally concluded with open questions and future direction left undone for human-material interaction.

2

HUMAN-MATERIAL INTERACTION & PHASE-CHANGING INTERFACES

In this chapter, I will define, explain, and exemplify the concept of human-material interaction and phase-changing interfaces that two research projects Liquid Pouch Motors (Chapter 3) and Self-healing UI (Chapter 4) share in common.

2.1 HUMAN-MATERIAL INTERACTION

2.1.1 *Definition*

Definition 1. *Human-material interaction is the interaction between humans and objects mediated by the physical properties of materials that compose the objects. The interface function is encoded in the material properties by means of computational fabrication and/or functional materials in a tunable way.*

This definition suggests that the computer does not always show up as an indispensable entity of interaction. Instead, human-material interaction directly leverages the physical property of the materials for interaction. In Figure 9 and Figure 10, I visually compared human-computer interaction and human-material interaction.

2.1.2 *Enabling Techniques*

From the definition above, human-material interaction apparently seems more naive and easier than conventional human-computer interaction. However, I note that recent development of two techniques – computational fabrication and functional materials – has highly contributed to achieving this seemingly primitive interaction:

2.1.2.1 *Computational Fabrication*

Computational fabrication is the technique that can precisely add, cut, subtract, or transform the materials according to the computer-aided design, which was democratized in this decade by the digital fabrication tools such as a 3D printer, a laser cutter, a CNC machine, and so on. The spread of computa-
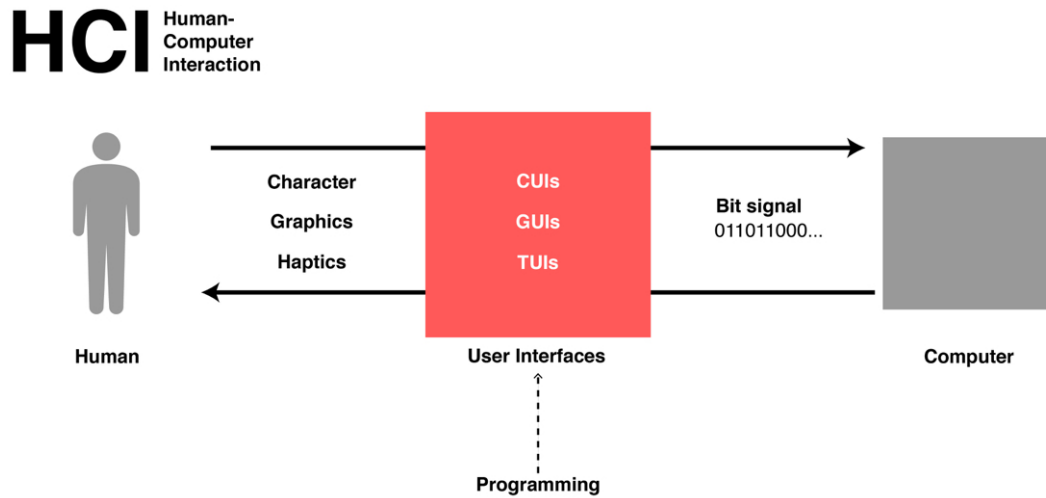
Figure 9: Human-computer interaction. User interfaces work as a translator between humans in the physical world and computers in the digital world. In this relationship, humans, interfaces, and computers exist almost independently. We can customize the function of interfaces extrinsically by programming.
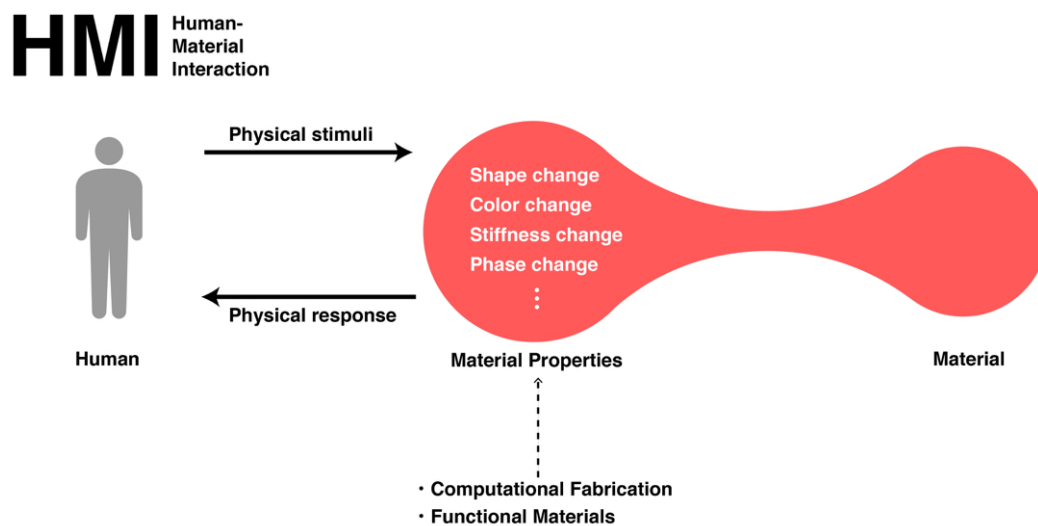
Figure 10: Human-material interaction. The material properties work as an input/output function between humans and the materials, both of which are in the physical world. In this relationship, the materials and their properties are strongly connected with each other. We can customize the function of materials' intrinsic properties by computational fabrication and/or functional materials.

tional fabrication has drastically lowered the obstacles for researchers to shape the objects and embed the material property only in the local region of the target.

2.1.2.2 *Functional Materials*

Functional materials are the specific types of materials that can be designed to be dynamic in terms of form and functions, recently drawing the attention of HCI researchers. For example, there are materials called thermochromic and photochromic inks that can change their color responding to heat and light, respectively (*c.f.*, both are easily available on the market these days). Or, there is a programmable transparency-changing material used in HCI [42, 70]. Also, there are some stiffness-changing materials using jamming transition [25, 42] or heat-responsive materials [53]. As shown in the previous chapter, shape change by the material property is also investigated in HCI. Especially, self-assembly of 2D sheets into 3D shapes is called 4D printing [4].

N.b., Many of the projects cited here use a computer to control the input stimuli. However, the main body of interaction proposed in such projects is typically allowed by the material properties and the computers only act as a "switch," contributing less than the materials themselves.

2.1.3 *Recent Examples*

Here I introduce the recent examples of human-material interaction. The first one is GelTouch [53], which achieves the interaction of stiffness-changing physical buttons by the heat-responsive property of the material. Another example is Metamaterial Mechanisms [26], which controls the kinesthetic feedback of the rotational structure, by controlling the density of materials by 3D printing. Morphlour changes the shape of boiled or baked food, by locally distributing the hydration/dehydration property of flour by computationally controlled stripe patterns [77]. Organic Primitives [29] controls their color, odor, and shape through pH-sensitive reactions of food-grade anthocyanin, vanillin, and chitosan, respectively. Kirigami Haptic Swatches [13] achieves the variable force-displacement properties of the haptic structure made from paper by computationally deciding the kirigami patterns.

I emphasize that all the examples except for GelTouch are even not connected to computers, yet still achieve interaction between humans and objects via the material properties. The interaction is embedded into daily objects like buttons, food, or the 3D printed thermoplastic through computational fabrication or functional materials, as defined above.

2.1.4   *Design Space*

To clarify the design space of human-material interaction, I compare it with the conventional approach of "human-device interaction," in which the interaction is achieved by assembling the pre-made components.

Figure 11 shows two types of the hierarchy of interaction, one for human-device interaction and the other for human-material interaction. The top priority is what kind of interaction it can afford. Interaction is constrained by devices that are made of/from some components or materials.

In this sense, the tunable properties of human-device interaction are determined at the level of devices, through changing mechanical or electrical parameters. When investigating human-device interaction, researchers typically do not have to care much about the components' fabrication process or small discrepancy on material properties, and they are allowed to focus more on computational control of the interaction.

On the other hand, human-material interaction considers the design parameter at the lower level of materials, where tunable parameters are more chemical and rheological as well as mechanical and electrical. When considering the material interaction, researchers can make use of the diverse physical properties conventionally hard to get.
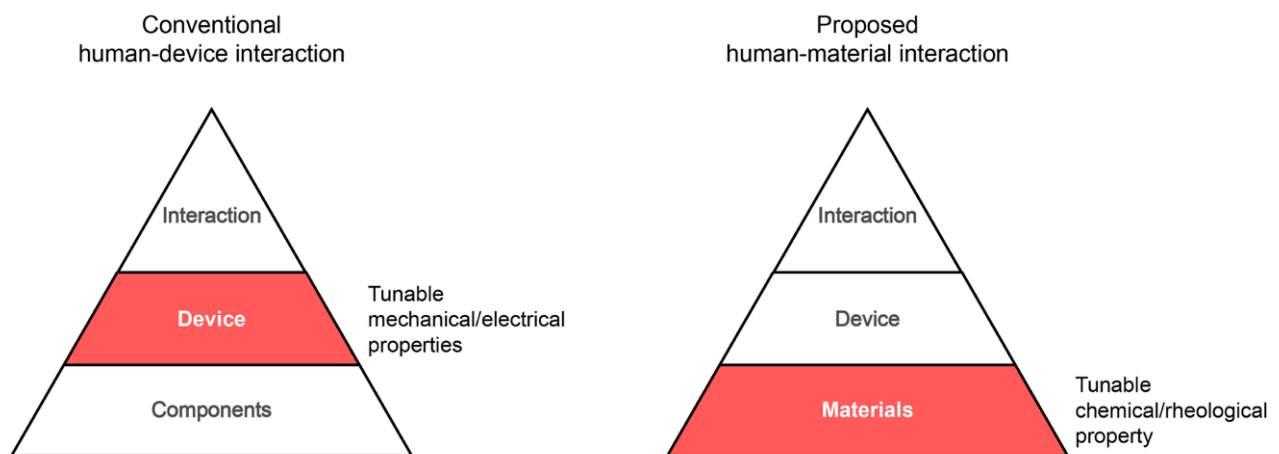
Figure 11: Human-device interaction (left) and human-material interaction (right). In human-device interaction, the design parameters lie at the level of devices, that are mainly on mechanical or electrical properties. On the other hand, in human-material interaction, the design parameters lie at the lower level of materials, which are mainly on chemical, rheological, or other physical properties.

For reference, I summarized the example space of human-material interaction I introduced above in Table 1. Please note that the material with tunable mechanical, electrical, chemical, and rheological properties varies in the field of materials science, so this table is much smaller than the complete set of what we can achieve with the current technical limitation of materials.

Table 1: Example space of human-material interaction

Tunable parameter	Category	Project
Stiffness	Mechanical	GelTouch [53], Self-healing UI [this thesis]
Motion	Mechanical	Metamaterial Mechanisms [26], Kirigami Haptic Swatches [13]
Shape	Mechanical	Thermorph [4], Morphlour [77]
Conductivity	Electrical	Self-healing UI [this thesis]
Color	Chemical	Squama [70], Organic Primitives [29]
Odor	Chemical	Organic Primitives [29]
Phase	Rheological	Liquid Pouch Motors, Self-healing UI [this thesis]

2.1.5 *Niche*

As I mentioned in the previous chapter, human-computer interaction and human-material interaction have their own pros and cons and therefore have different niches to work at. Table 2 shows the qualitative comparison of two interaction techniques. First, bits are in the digital world yet atoms are in the physical world, and thus HCI can extrinsically be modified, while HMI has embedded intrinsic properties. As the number of interfaces increases, they tend to be collective, connected to the network or power in the case of HCI, while each entity tends to be ambient and autonomous in case of HMI. Many of HCI are implemented into the screen or the device, while HMI can be implemented into daily objects. As for the speed and power, HCI is superior to HMI.

Therefore, I claim that HMI is more suitable for the context of ubiquitous computing rather than centralized or personal computing. HMI aims at working in an ambient and calm way, embedded into our daily objects and environments, such as shelter, clothe, food, and etc. On the other hand, conventional HCI largely dominates in terms of customizability, computing speed, and power.

2.2 PHASE-CHANGING INTERFACES

In this thesis, I investigated the phase change of materials for the target tunable property of human-material interaction, and proposed two types of phase-changing interfaces. As I previously showed in Figure 7 and Figure 8, I demonstrated (1) Liquid Pouch Motors as a phase-switching interface toggling between two materials phases and (2) Self-healing UI as a phase-transcendent interface having properties of multiple phases at the same time, respectively. These interfaces are unique in that they utilize the actual phase change, not the virtual display of multiple phases; in the field of HCI, researchers have explored two different strategies that display multiple material phases using dynamic pin displays.

Table 2: Qualitative comparison of HCI and HMI.

HCI		HMI
Digital	← - - - - - →	**Physical**
Extrinsic	← - - - - - →	**Intrinsic**
Collective	← - - - - - →	**Ambient**
Screen, device	← - - - - - →	**Daily objects**
Fast	← - - - - - →	**Slow**
Powerful	← - - - - - →	**Calm**

The first strategy is a metaphor of "data as gas and objects as solid". Leithinger *et al.* prepared both a shape-changing pin display and a see-through visual display [39]. This visual display overlays 3D graphics on a shape display. In this setup, they demonstrated a bidirectional transition between physical objects (equivalent to solid) and digital information (equivalent to gas) as *sublimation and deposition* and demonstrated how digital information and physical shape change are mediated.

The other strategy of displaying multiple material phases with pin displays is to reproduce the rheological properties of objects, as well as their shapes. Nakagaki *et al.* proposed the method to render rheological properties of objects (*e.g.,* flexibility, elasticity, and viscosity) by controlling the time-dependent displacement of each pin [56]. Although each pin is always just stiff, the display as a whole acts more diversely, such as viscose liquid and soft yet springy human bodies.

Although these research efforts drastically contributed to the fusion of flexible bits and stubborn atoms, there is still a clear discrepancy between the rendered material phases and the actual material phases; AR graphics can never become gas and the pin display can never become liquid. My research motivation is rather aiming at utilizing the actual physical property of materials to make use of multiple phases and their phase change for human-computer interaction.

From the next chapter, I will explain in detail about two phase-changing interfaces we developed through several projects.

LIQUID POUCH MOTORS

3.1 INTRODUCTION — SHAPE SWITCH BY PHASE SWTICH

3.2 RELATED WORK

3.3 LIQUID POUCH MOTORS

3.4 FABRICATION PROCESS

3.5 APPLICATION: ELECTRIC PHASE-CHANGE ACTUATOR

In the field of robotics, integrated fabrication of body structures, actuators, sensors, and electronic circuits into one robot system is an open problem. Existing approaches have difficulties in constructing electric actuators in the body with simple and rapid processes. We took advantage of Liquid Pouch Motors and proposed an electric phase-change actuator that consists of a printable fluidic actuator controlled by an inkjet-printed electric heater. The actuator can easily be integrated with origami robots. We theoretically analyzed the dynamics of electro-fluidic conversion in the actuator and compared it with actual measurement data. We then demonstrated example applications of a self-folding origami structure, a robot gripper with a printed touch sensor, and the butterfly and the flytrap robots as analogies of living things.

3.5.1 *Prototyping Functional Robots*

One of the main challenges for soft-robotics is to accelerate the prototyping processes from idea to implementation. Soft-robotics have the potential to integrate components in relatively fewer processes, while conventional robotic manufacturing requires a significant amount of time for complex manual assembly of constituent components. To embed actuators into the body structure, soft-robotic studies have mainly focused on fluidic approaches: silicone pneumatic channels with soft-lithography [48], shape deposition [12], embedded air tubes [14], jamming transition [9], and 3D-printed hydraulic actuators [47]. Despite such efforts, these methods still have limitations in terms of manufacturing cost and time.

To deal with this issue, Niiyama *et al.* proposed Pouch Motors, printable pneumatic actuators that consist of one or more inflatable gas-tight bladders made of two layers of plastic sheet bonded by

CNC heat drawing [58][59]. It allows both easy planar design and fast implementation of affordable actuators.

However, there are still some drawbacks when trying to build functional pneumatic robots, which possess not only body structures and actuators, but also sensors, antennas, and electric wiring. First, computation, communication, sensing, and powering are mainly conducted with electric energy, so robots have to prepare electric patterns in addition to pneumatic channels. Second, pneumatic actuation inevitably involves cumbersome components like compressors/pumps, tanks, and tubing. Third, although there exists some research on powering robots pneumatically using chemical reaction [63][85] or monopropellant power [21], they are difficult to control.

Therefore, we need to develop an electrically activated actuator which can be rapidly prototyped. Although electroactive polymers (EAPs) [35] and thermal actuation by shape memory actuators (SMAs) [43] can be considered as options of such an actuator, we focused on electrically driving Liquid Pouch Motors. Different from the conventional pneumatic actuators that need air tubes connected to them, Liquid Pouch Motors can be driven by electric heaters, which leads to good compatibility with flexible circuit. Furthermore, thin actuators do not interfere with the intrinsic flexibility of flexible substrates. Considering these benefits, we combined Liquid Pouch Motors with inkjet printable paper circuit to build an all-printed functional robot equipped with electric wiring, sensors, and actuators on it.

Several other groups have proposed actuators driven by the phase change of liquid, but they do not aim for prototyping use. Akagi *et al.* [2] and Tsuji *et al.* [79] report thin-film phase-change actuators driven by carbon-based conductive heater painted on laminated plastic, although none of their body, heater, or electric wiring are printable. Other groups' actuators involve a rigid body or a relatively complicated, time-consuming fabrication process [95][52][81]. Therefore the potential of Liquid Pouch Motors for the rapid fabrication of functional robots is considered to be large.

Here, we proposed an electric phase-change actuator, a printable actuator that extends Liquid Pouch Motors simply by attaching inkjet printed circuit on them. Not only does the system work as actuators, but the printed conductive traces function as an electric sensor and wiring.

The main contributions of this application are summarized as follows:

1. An electrically controlled, printable actuator is proposed.

2. Phase-changing actuation controlled by inkjet printed heater is modeled and measured.

3. Paper folding was demonstrated using phase-change actuation, which shows the feasibility of body formation.

4. A capacitive touch sensor and electrical wiring were inkjet printed and integrated with printed actuators, which shows the feasibility of sensor fabrication.

In the remainder of this section, we first describe the overview of an electric phase-change actuator. Then we discuss the theoretical model of its dynamic actuation and compare it with experimental results. In the section of fabrication, the process, cost, and takt time were illustrated. We also demonstrated the feasibility of our proposal with applications of the self-folding box, robotic hand, butterfly, and flytrap.

3.5.2 *Electric Phase-change Actuator*

As shown in Figure 12, an electric phase-change actuator is a combination of a printed electric circuit and Liquid Pouch Motors. When the solvent is heated by the electric circuit, it inflates and works as an actuator.
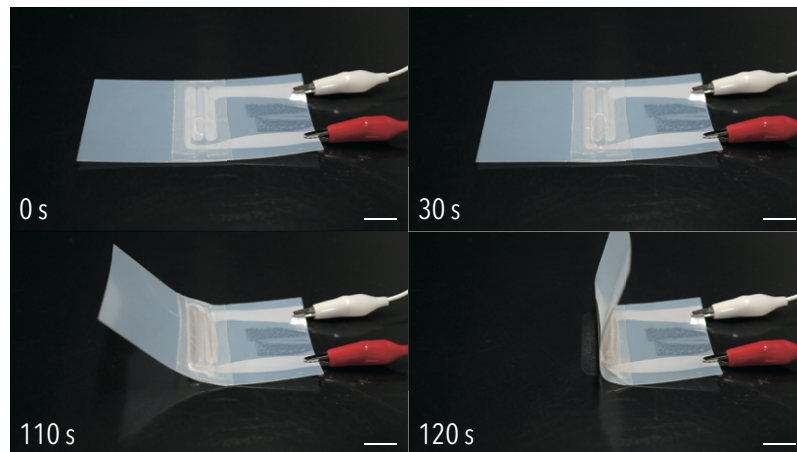
Figure 12: An electric phase-change actuator that shows primitive angular motion. It is composed of a printed conductive heater and Liquid Pouch Motors. The whole fabrication process completes in approximately 30 minutes with accessible equipment and materials. Scale bar: 1 cm (Figure reused from [P3]).

The circuit was composed of silver nano-particle ink on PET film, printed with an off-the-shelf inkjet printer. The pouch is also printable, using heat-drawing on a pile of polymer sheets as previously shown in Figure **??**A. Thus, the whole process is done with simple yet widely accessible material and fabrication methods.

3.5.3 *Theoretical Model*

In this section, we theoretically modeled two parameters of an electric phase-change actuator: moment and time response.

3.5.3.1 *Moment*

First, we assume that a pouch is filled with liquid, and the pressure is virtually zero when the heat is not applied. We also assume that the actuator performs movements in the same mechanism as Pouch Motors [58] when a pouch is heated and liquid evaporates.

Then, the volume of a pouch can be given as follows.

$$V(\theta) = \frac{L_0{}^2 D}{2} \left(\frac{\theta - \cos\theta \sin\theta}{\theta^2} \right) \tag{1}$$

Here, the size of a pouch L_0, D and angle θ are shown in Figure 13.

(a)   (b)
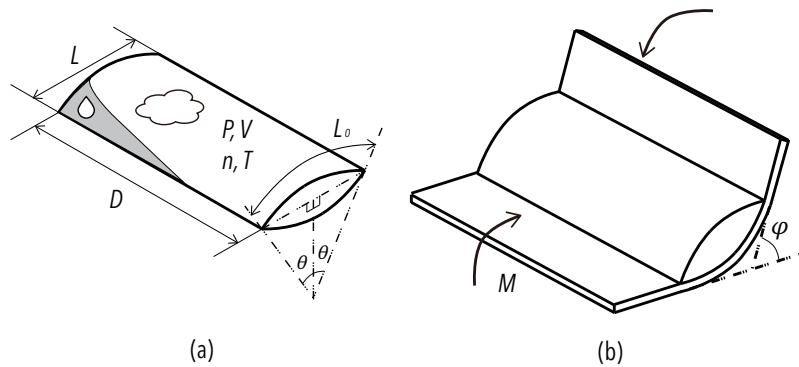
Figure 13: The model of electric phase-change actuators. a: A pouch filled with low boiling point liquid, some of which is in the state of liquid, and the rest of which is gas. b: Rotational actuation of the pouch, pasted on the substrate (Figure reused from [P3]).

Let the moment generated by an electric phase-change actuator be M. Then the energy conservation Equation 2 to a virtual rotation $d\phi$ is expressed as follows.

$$Md\phi = PdV \tag{2}$$

Now ϕ is expressed as $\phi = 2\theta$, so we obtain moment M as the following equation from Equation 1 and Equation 2,

$$M(\theta) = P\frac{dV}{d\phi} = P\frac{\frac{dV}{d\theta}}{\frac{d\phi}{d\theta}} = L_0{}^2 DP \frac{\cos\theta(\sin\theta - \theta\cos\theta)}{2\theta^3} \tag{3}$$

Thus, we can derive the following Equation 4 from Equation 1, Equation 3, and the state equation $PV = nRT$.

$$M(\theta) = nRT \frac{\cos\theta(\sin\theta - \theta\cos\theta)}{\theta(\theta - \cos\theta\sin\theta)} \tag{4}$$

The moment M takes negative value if $\theta > \frac{\pi}{2}$. Therefore, the maximum angle of rotation is $2\theta = \pi$ rad (*i.e.,* totally flat state). We note that the moment limitlessly increases if θ gets closer to zero. But

there is always some liquid or gas left in a pouch, so M never diverges to positive infinity in the actual situation.

Also, we note that pressure inside a pouch has an upper limit, which is decided by atmospheric pressure and stress of the pouch. Therefore, the amount of liquid that can evaporate has a limit regardless of the excessive heat.

3.5.3.2 *Time Response*

Next, we also need to analyze the time response of the actuator, since n and T in Equation 4 depend on the elapsed time from activation. Time response of the moment of an electric phase-change actuator can be calculated by simulating heat conduction among a heater, a pouch, and the air.

For simplicity, here I just introduce the result of the calculation below. To get the actual value of $M(\theta, t)$, we need to numerically solve $G(t)$ by substituting several parameters, while $F(\theta)$ can be analytically solved. For more mathematical detail, please refer to section a.1.

$$M(\theta, t) = RT_b n(t) \frac{\cos\theta(\sin\theta - \theta\cos\theta)}{\theta(\theta - \cos\theta\sin\theta)} \tag{5}$$

$$= \frac{NRT_b}{Q_v} F(\theta)G(t) \tag{6}$$

where

$$F(\theta) = \frac{\cos\theta(\sin\theta - \theta\cos\theta)}{\theta(\theta - \cos\theta\sin\theta)}$$

$$G(t) = c_2 t + \frac{c_1 C_h}{\alpha + \gamma} e^{-\frac{\alpha+\gamma}{C_h}t} - \frac{c_1 C_h}{\alpha + \gamma}$$

3.5.4 *Experiments*

In this section, we compared the theoretical model with experimental results.

3.5.4.1 $M(t)$ *and* $M(\theta)$

We evaluated the actuator's moment in two ways. Figure 14 shows the two experimental setups for moment measurement. In the first experiment, the moment of the actuator was measured while both sides of the actuator are kept horizontal (Figure 14a) to evaluate the moment as a function of t. Second, the moment of the fully evaporated state of the actuator was measured while the rotational angle of the

actuator is controlled (Figure 14b) to evaluate the moment as a function of θ. In these two experiments, the shape of the pouch was a rectangle, with a size of 80 mm x 25 mm, respectively. All the experiments in this section were done at the room temperature of 27 °C, and we assumed that the pressure inside a pouch reaches its upper limit, since there was always some liquid left throughout all the experiments.
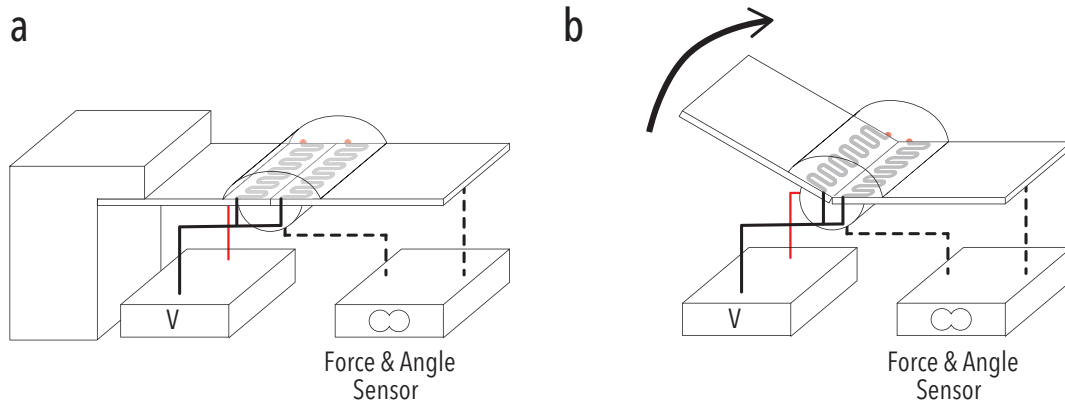
Figure 14: The experimental setup for moment measurement. a: The setup for the first experiment, where an actuator is kept horizontal. b: The setup for the second experiment, where the angle of an actuator is controlled (Figure reused from [P3]).

Figure 15 shows the result of the first experiment, which was post-processed by a low pass filter with a cut-off frequency of 0.2 Hz. As can be seen from Figure 15, the moment showed an exponential increase from 60 s to 115 s, while the liquid was evaporating. Also, when switched off, the moment steeply decreased approximately 3 times faster than its increase at the ON state.
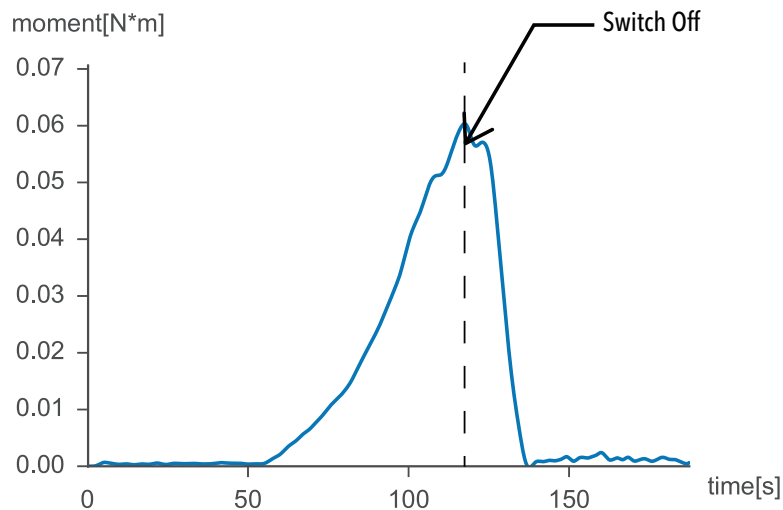
Figure 15: The experimental result of the moment at different times as $M(t)$. The results are post-processed by a low pass filter whose cut-off frequency of 0.2 Hz (Figure reused from [P3]).

Figure 16 shows the plot of the measured moment at different angles and different amounts of liquid along with its theoretical moment given by Equation 4. We observed that the activation (up) curves in
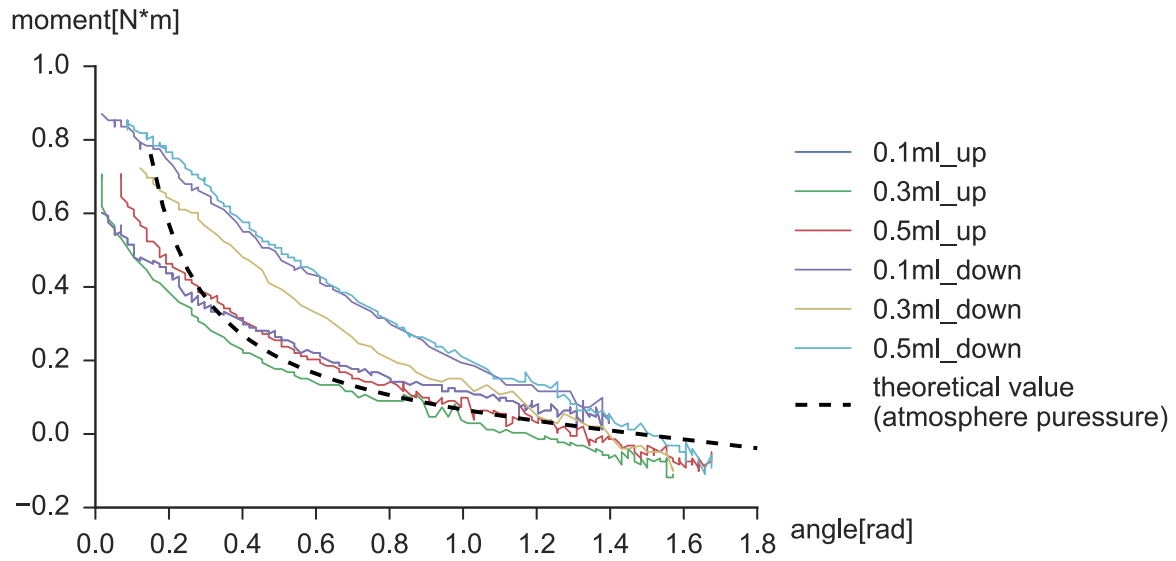
Figure 16: The experimental and theoretical values of the moment M at different angles θ. The outward and the return of the hysteresis is shown. Measured moments stay almost constant even if the amount of substance is different. This suggests as small as 0.04 ml is enough for theoretical actuation (Figure reused from [P3]).

the hysteresis correspond well with the theoretical curve, under the assumption that inside the pouch was kept in the atmospheric pressure. On the other hand, the deactivation curve did not fit well with the activation curve, which might be because of the hysteresis existing in the material property of the liquid. We also note that the moment value did not drastically change even though we used three different amounts of liquid, which is against the discussion done in Table **??**. We guess this was because the heat applied was much smaller than the amount of liquid inside the pouch; according to Equation **??**, the minimum amount of liquid needed for this pouch was 0.04 ml. For more precise analysis, we need to conduct experiments with a smaller amount of liquid.

3.5.4.2 T(t)

We also tested the heat conduction of the actuator. In this experiment, the shape of the pouch is an ellipse whose size is 25 mm x 15 mm, respectively. We attached two thermistors (SEMITEC 103-JT), one on the backside of the heater and the other on the front side of the pouch, to measure the temperature of the heater and the pouch. At the initial state, the temperature at both sides was at the room temperature of 27 °C.

Figure 17 shows the experimental result with the theoretical model overlaid. The solid lines show the experimental result, and the block lines represent theoretical model of heat temperature change with

appropriate parameters. We note that the measured temperature was lower than the theoretical value. This is because the thermistors were not embedded in the component but exposed to the atmosphere.
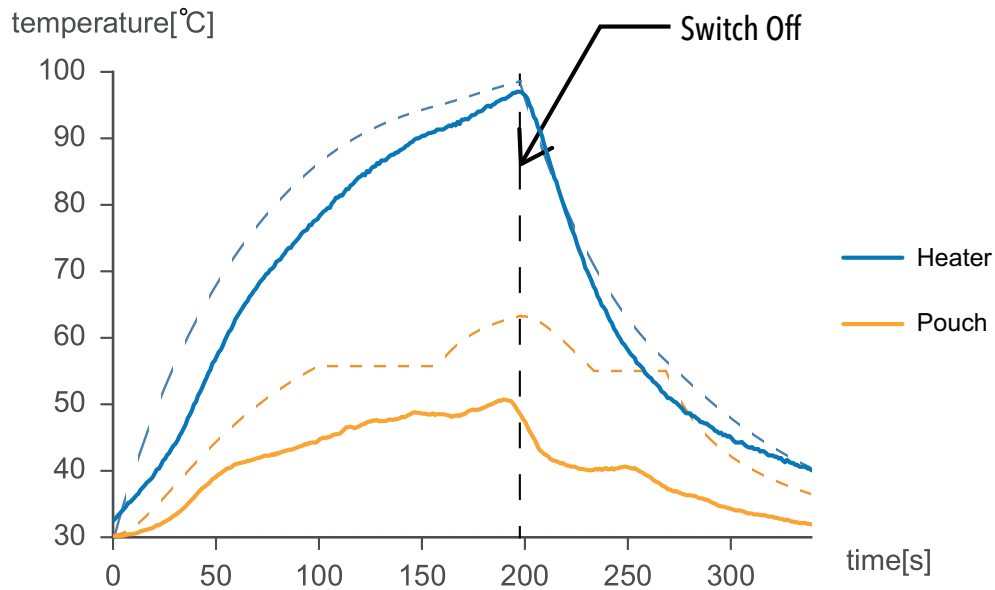
Figure 17: The experimental result of the temperature at different times as $T(t)$. The solid lines show the experimental result, and the block lines represent a theoretical model of heat temperature change with appropriate parameters (Figure reused from [P3]).

3.5.5 *Fabrication*

Figure 18 shows the fabrication procedure of an electric phase-change actuator. In this section, we describe each process in detail.

3.5.5.1 *Designing Components with Computer Aid*

First, we designed pouches and inkjet printable circuits. Both of them were designed by Adobe Illustrator in an above-mentioned way. More detail on designing the inkjet-printed circuit is written in [31][32].

3.5.5.2 *Printing Components*

The pouches and the conductive pattern were fabricated by heat drawing and inkjet printing, respectively. These processes usually finish within a few minutes. For the pouch fabrication, we use 0.05-mm-thick thermoplastic film and 0.076-mm-thick PTFE-coated glass fiber fabric as substrates, and a customized XY plotter as a printer. For the conductive pattern fabrication, we use silver nano-particle
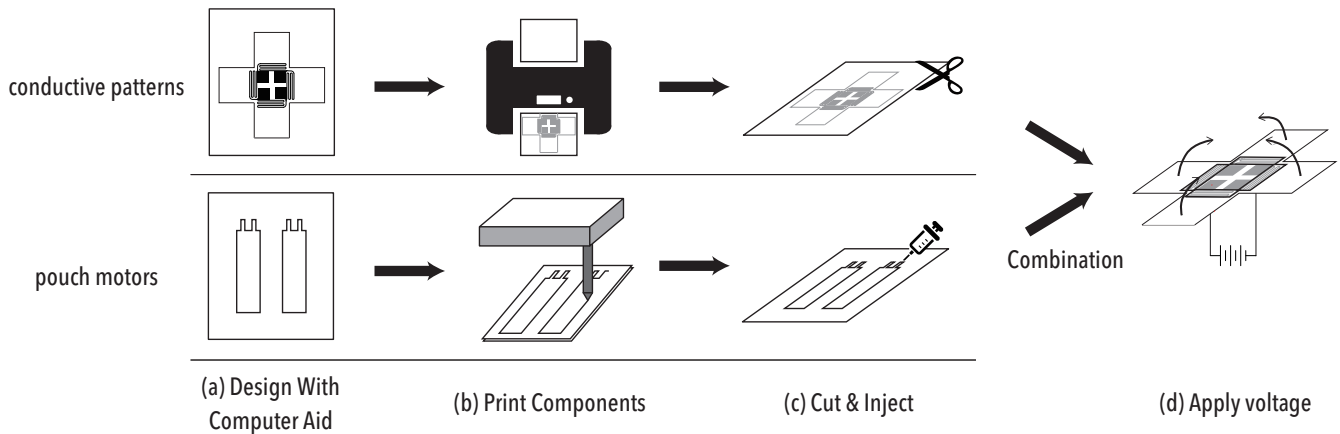
Figure 18: The fabrication process of an electric phase-change actuator. a: Design each component using a draw-
ing software such as Adobe Illustrator. The design of the heater with desirable size, resistance, and heat
distribution is automatically generated. Also, the generation of tool paths for the pouch is automated.
b: Both conductive patterns and pouch motors are printed within ten minutes in case of an A4-sized
paper. c: Printed components are manually cut or injected. d: After each component is assembled, The
final product is driven by an electric power source (Figure reused from [P3]).

ink NBSIJ-MU01 as ink, coated PET film NB-TP-3GU100 from Mitsubishi Paper Mill as a substrate, and
EPSON PX-045A as a printer. The sheet resistance value of the ink was approximately 0.2 Ω/sq.

3.5.5.3 *Manual Processing*

Next, a few numbers of manual processes are needed such as: cutting conductive substrates, injecting
liquid into pouches, and sealing injection holes at the edge of each pouch with heat-bonding. The entire
process usually finishes within around 20 minutes.

3.5.5.4 *Combination and Activation*

Finally, fabricated components were combined, using an off-the-shelf double-sided sticker. The final
product can be driven by an electric power source. The range of voltage and current we use was limited
to 3 - 15 V and 0 - 1 A, respectively.

3.5.5.5 *Time and Cost*

As described above, the whole process finishes within 30 minutes, except for the initial design process.
This is considered to be quite faster than previously proposed methods like soft-lithography, shape
deposition, embedded air tubes, and 3D-printed hydraulic actuators.

Now we estimate the cost for fabricating an electric phase-change actuator with A4-sized paper. Printing conductive patterns costs approximately $1 per sheet. And Printing a pouch typically costs less than $0.01 per sheet. Thus, the whole cost for the fabrication of one electric phase-change actuator is approximately $1. We also estimate the initial cost of fabrication devices. As one inkjet printer costs $50 and the XY plotter costs $300, the whole initial cost is approximately $350.

3.5.6 *Applications*

3.5.6.1 *Self-folding Box*

We developed a self-folding box as an example of transformation from 2D to 3D (Figure 19). The box was driven by 6.0 V of stabilized power supply. First, the whole structure was almost flat. Then when we turned on the power source, folding angles of hinges became around 90 degrees. After the power was turned off, the structure unfolded again into the flat shape.
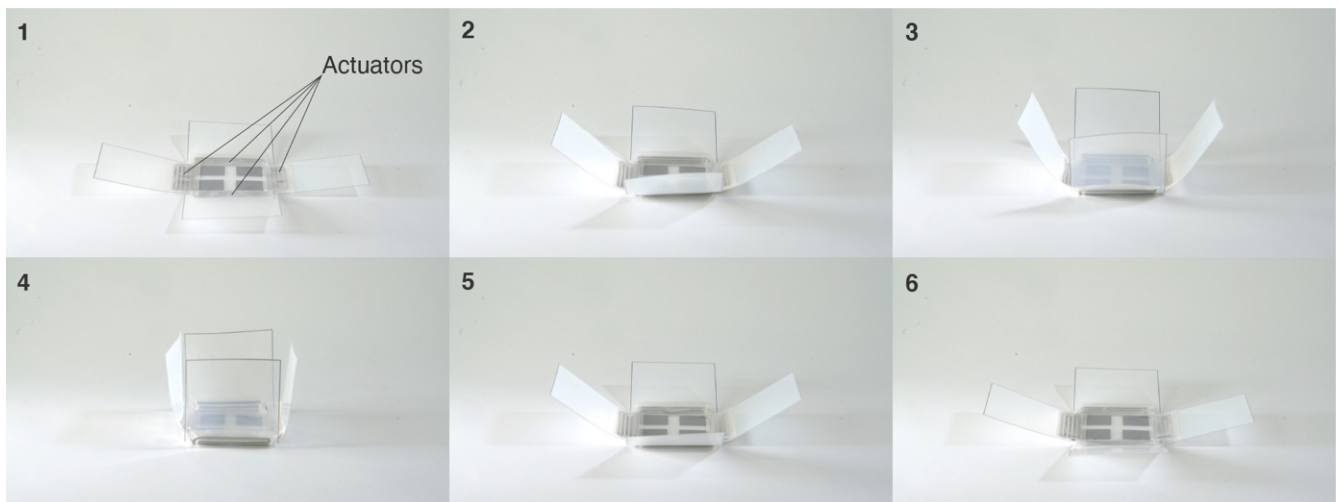
Figure 19: Self-folding box driven by electric phase-change actuators. (1-3) Activation. The unfolded surfaces of the structure get close when the voltage is applied to the heater pattern under the pouch. (4-6) After the current is shut down, the structure gets unfolded into almost flat shape again.

Although the structure shown here does not have the shape memory function, this application demonstrates that an electric phase-change actuator has the potential to be used in complex self-folding and autonomous assembly processes proposed in other groups [19][73][74].

3.5.6.2 *A gripper with Touch Sensor*

We also developed a three-fingered gripper with a touch sensor (Figure 20), to demonstrate the high affinity with additive electrical equipment. The ellipse-shaped actuators with the size of 15 mm x 25 mm

were equipped at the center of each finger, and they showed gripping motion when 6.0 V of stabilized power was applied to each heater. The touch sensor was fabricated on the same substrate with heaters and electric wiring in a single process.
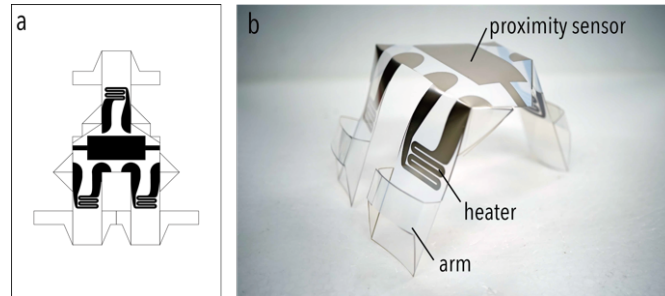
Figure 20: The three-fingered gripper. a: the net schematic. b: the constructed gripper (Figure reused from [P3]).

As shown in Figure 21, the gripper can close its arms when the heat is applied. We let the gripper hold a human arm (Figure 22). When activated, we observed that the gripper fitted along the human arm and sustained its own weight.
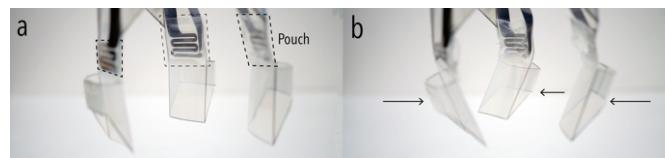
Figure 21: The gripper in motion before and after actuation (Figure reused from [P3]).
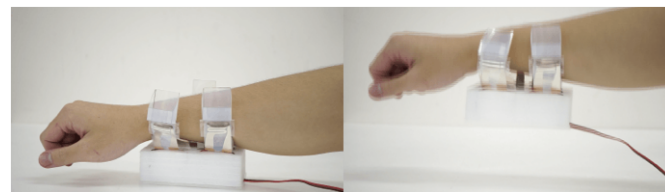
Figure 22: The gripper holding a human arm (Figure reused from [P3]).

Also, we measure the touch sensor's feasibility by iteratively hovering the arm onto the sensor (Figure 23). The touch sensor is composed of a rectangular wave generator and a conductive ink pad. When the arm approaches the sensor pad, the whole circuit makes a low pass filter, which distorts the input rectangular wave from the Arduino board. Then Arduino captures the output wave and calculates its time constant. Figure 23b demonstrates that the sensor recognizes the arm with a high S/N ratio.

3.5.6.3 *Soft interfaces as analogies of living things*

Figure 24 shows the butterfly robot and the flytrap robot. The butterfly robot in Figure 24A,B repeatedly flaps its wings. This example shows that the system can work safely on the fingertip, due to the lower
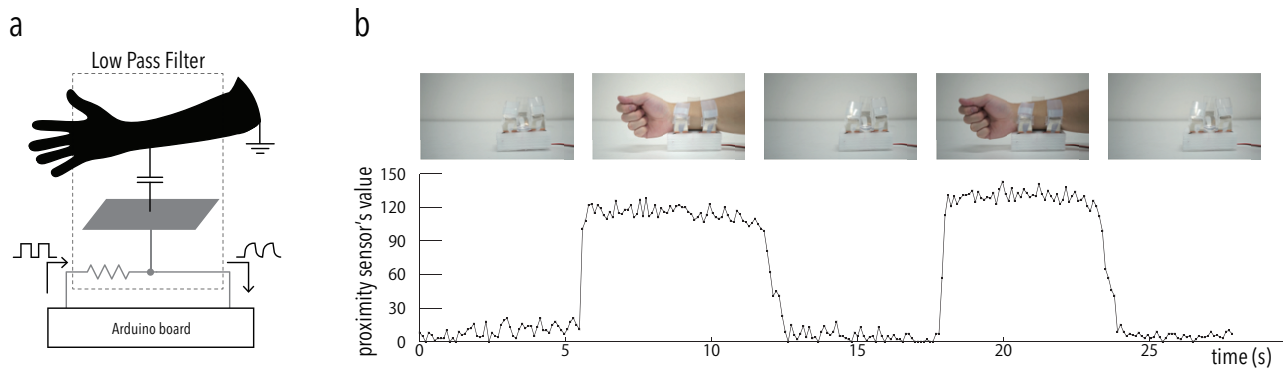
Figure 23: Proximity sensing capability of the gripper. a: Schematic of the touch sensor in a gripper. Gray lines and a pattern show conductive ink traces. When an object approaches the sensor pad, the whole circuit makes a low pass filter, which distorts the input signal from the Arduino board. b: Output of the touch sensor. When the arm approaches the gripper, the touch sensor successfully captures it and returns a distinctively high value (Figure reused from [P3]).

voltage, current, and temperature (approx. 5 V, 50 mA, 40 °C) by appropriately designing the sheet resistance of the printed electric heater. The butterfly robot shown in Figure 24C-E responds to human motion when the capacitive sensor printed on the surface detects the touch motion of the user by heating up the pouch to close the leaves. Through this example, we demonstrated the easy combination of wiring, sensors, and actuators to build an interactive object.

3.5.6.4 *Possible Improvements*

Although we demonstrated that phase-change phenomenon is a suitable actuation mechanism for rapid prototyping of robots with electrical wiring, there remains some issues to be addressed for more convenient use.

The first issue is that not all processes to fabricate an electric phase-change actuator are completely automated. So far the manual processes are needed in cutting the substrates, injecting low boiling point liquid into a pouch, and combining the pouch with the conductive patterns. All these processes are not so complex and can be automated with a laser-cutting machine, an automatic liquid injection device, and an XYZ stage.

Second, the actuation speed of an electric phase-change actuator is slow, compared with that of Pouch Motors and some other well reactive actuators. When trying to accelerate the motion while keeping the form factor of the electric phase-change actuator, we can increase the boiling point of the liquid compared to the environmental temperature.
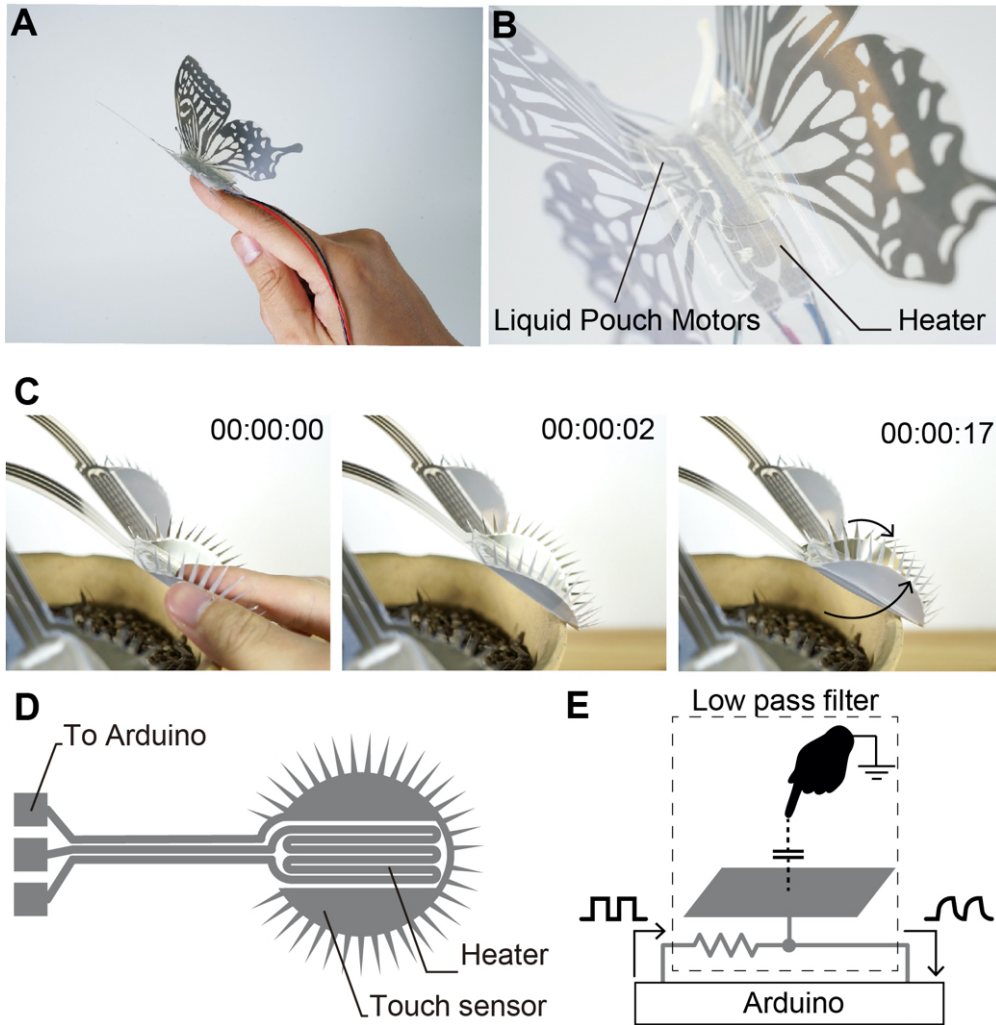
Figure 24: Soft interfaces as analogies of living things. A,B: the butterfly robot slowly flapping on a fingertip. The electric heater under the pouch was printed by silver ink along with decoration patterns. C-E: the flytrap robot. C: when the user touches the robot, it detects touch motion and responds by closing leaves. D: circuit design. E: the circuit diagram of capacitive touch sensing. The resistance of the circuit and the capacitance between the conductive pattern and the finger compose a 1-degree of low pass filter (Figure reused from [P1]).

Finally, we have to mention that the applications using electric phase-change actuators are all tethered to a stabilized power supply. But there is a possibility for these robots to be untethered, since the applications are driven by 6.0 V of power supply, which almost equals to the maximum output voltage of off-the-shelf light batteries. What is more, conductive ink patterns have the potential for adding a powering antenna to our actuator, which will open up the possibility of energy harvesting without battery replacement. This motivation of untethered actuation led to successive three applications described from the next section.

3.6 APPLICATION: PAPILION

3.7 APPLICATION: A LIVE UN LIVE

3.8 APPLICATION: LASER POUCH MOTORS

3.9 LIMITATIONS OF LIQUID POUCH MOTORS

Despite many merits, we demonstrated in previous sections, there are also some drawbacks when we use Liquid Pouch Motors. In this section, I will generally describe the intrinsic limitation of Liquid Pouch Motors.

3.9.1 *Controllability*

We only utilized the fully actuated or the fully rest states of Liquid Pouch Motors. This is due to the hard controllability of phase change; even if we try to measure the temperature to conduct a closed-loop feedback to achieve a half-way actuated state, the temperature when the phase change is on-going inside the pouch is always static at 34 °C. Thus the time-dependent open-loop feedback might be possible (*e.g.*, PWM of the heater) if we need to control the transition state of the actuator.

3.9.2 *Speed*

As already shown in previous sections, for example, the actuation speed of the 25 mm x 100 mm actuator is at the order of ten seconds. But there are three ways to achieve faster movement. The first solution is to make a smaller pouch, which will decrease the heat capacity of the actuator. Recently, Lu *et al.* have shown the fabrication technique to fabricate a small size of Liquid Pouch Motors, as a follow-up work of ours [46]. The second solution is to use a heat source with larger heat capacity. In our preliminary experiments, hot water in a mug or water vapor drove a 15 mm x 45 mm actuator within or at the order of seconds. The final solution is to increase the boiling point of the liquid compared to the environmental temperature, as we described in the section for electric phase-change actuators.

3.10 CONCLUSIONS

We extended pneumatically driven Pouch Motors and proposed Liquid Pouch Motors by filling them with low boiling point liquid. Liquid-to-gas phase change and its large volume expansion contributed to actuation in that the actuator as thin, flexible, lightweight as normal papers showed as large and powerful actuation as conventional pneumatic actuation constrained by the gas phase. For clarity, Figure **??** shows and compares the applications enabled by Liquid Pouch Motors.

Table 3: Four applications of Liquid Pouch Motors
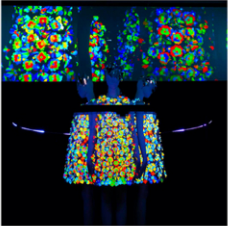
	Electric Phase-change Actuator	Papilion	A LIVE UN LIVE	Laser Pouch Motors
Energy source	Electric heater	Ambient heat	Body temperature	Laser
Tethered or untethered?	Tethered	**Untethered**	**Untethered**	**Untethered**
Selective actuation	**Possible**	Impossible	Impossible	**Possible**
Distance with human	–	Architecture	Wearable	Relatively far

4

SELF-HEALING UI

_____

4.1 INTRODUCTION − INTERFACES BEYOND PHASE BOUNDARIES

In the previous chapter, I introduced Liquid Pouch Motors, where clear liquid-to-gas phase change leads to a distinct shape change of the proposed actuator as a phase-switching interface. In this chapter, on the other hand, I will introduce the user interfaces "beyond phase boundaries of the material," that is, the "phase-transcendent interface" made from self-healing materials that work as if they are in the solid, solid-liquid (= elastomeric), and liquid states at the same time; by coordinating the suitable composite structure of the self-healing material and the mixed particles inside, it makes the interfaces (1) keep its shape as if it is solid, (2) transform as if it is elastomeric; and (3) heal at the local broken part as if it is liquid.

In this chapter, I will demonstrate two types of conductive and self-healing composite materials both made from carbon nanotubes and polyborosiloxane. In Section 4.2, I will describe the first project on a self-healing, elastomeric conductor (= SWCNTs aerogel-PBS) and its application that we newly synthesized and proposed in the context of materials science. From Section 4.3 to Section 4.13, we then extended the knowledge and experience of developing such materials and applications, and proposed the user interfaces made from self-healing materials beyond just healing (= MWCNTs dispersion-PBS). We explored the fabrication method of everyday devices with self-healing ability in the practical form factor and their design space leveraging such vague phase boundary of the material when compared to conventional shape-changing interfaces with limited use of a single phase, in the context of interaction. Note that Section 4.2 is one completed work in the context of materials science and thus long, but the main body of Self-healing is from Section 4.3, so those who are interested in the work for interaction can just skip Section 4.2. For reference, Table 4 compares two CNTs-PBS used in Section 4.2 and Section 4.3 – Section 4.13.

4.2 SWCNTS AEROGAL-PBS FOR MATERIALS SCIENCE

4.3 MWCNTS DISPERSION-PBS FOR INTERACTION

From lizard tails to starfish arms, from grafted trees to human skin, the regenerative and self-healing phenomena are ubiquitous in nature. Inspired by how natural self-healable systems can restore their mechanical integrity and functionality (*e.g.*, nervous system, nutrient canals) in an autonomous man-

Table 4: Comparison of two CNTs-PBS.

	SWCNTs aerogel-PBS (§ 4.2)	MWCNTs dispersion-PBS (§ 4.3-)
CNTs	Single-walled	Multi-walled
Goal	Materials science	Interaction
Structure	CNT first, then pour PBS	PBS first, then disperse CNT
Mechanical & electrical property	Higher	Lower
Takt time	~ weeks	~ days
Fabrication	Harder & more expensive	Easier & cheaper

ner, we proposed self-healing UI that mimics and exploits this unique healing property to design interface systems around us (*e.g.*, wearables, soft interface, digital fabrication, art). In human-computer interaction (HCI), shape-changing soft-bodied interfaces [3, 15, 69], radical atoms [27], deformable interfaces [6], and material-driven interfaces [68] are drawing increasing attention. This is due to the fact that shape change provides unique form, function, and interaction, represented by wearable sensors [30, 60, 87], deformable mobile devices [22], pneumatically actuated daily products [94], devices with haptic feedback [91], and interactive robotics [83].

However, such shape-changing interfaces proposed in the field of HCI are still limited in terms of material property. For example, although pin displays reconfigure the relative relationship of a number of pins, it does not mean "each pin can change into a liquid." Or, when the pneumatic shape-changing interfaces get broken, it is hard to fix them by sealing all the air leakage once the silicone liquid changes into the cured elastomer. In terms of device fabrication, we usually need glue (changing from liquid into solid) to paste multiple materials together. These kinds of limitations can be updated, if we have a material that is beyond the border of phases.

Although we have already developed the composite material of SWCNTs aerogel and PBS (shown in the previous section) when we started the project on interaction with a self-healing material, SWCNTs-PBS was unfortunately not suitable for building practical interfaces. The previous project of backfilling SWCNTs aerogel with PBS was mainly aiming at the novel material property, and the fabrication process of SWCNTs-PBS took weeks just to get a fingertip-sized composite. Thus for this project, in order to explore more on the interaction side, we changed the self-healing material into the one allowing faster, larger, and cheaper fabrication, from backfilling SWCNTs aerogel with PBS into dispersing MWCNTs into PBS.

In this paper, we present Self-healing UI, a soft-bodied material interface that follows these principles: (1) the devices can self-heal for repeated use; (2) the material affords a novel solution for device fabri-

cation that is able to fuse both conductive and non-conductive components; (3) the material sticks to a variety of soft materials such as fabric and silicone; (4) the interface is able to integrate both input sensing and output actuation. Furthermore, we exploited the self-healability of our material to demonstrate a novel design space of shape-changing interfaces.

The main contributions of this paper are as follows:

- Proposing a layered model for Self-healing UI, including stiffness-/conductivity- tunable self-healing polymers, as well as other common soft materials such as silicone and fabric.

- Developing a preparation and molding method of PBS and MWCNTs-PBS sheets by extending previous literature [92].

- Building a layer-by-layer stacking fabrication method that can achieve a continuous structure without additional gluing or bonding processes.

- Exemplifying the design space of Self-healing UI by incorporating its transformative, conformable, reconfigurable, healable, and fusible nature in proposed applications.

4.4 RELATED WORK

4.4.1 *Self-healing Materials*

4.4.1.1 *Basic principle and category studied in materials science*

Traditional polymers, which are typically crosslinked through irreversible covalent bonds, have been widely used in the modern industry. However, due to the strong bonding, these polymers lose their functionality after being damaged [76]. Hence, scientists and engineers developed several strategies to allow the system to restore its functionality.

Self-healing polymer is classified into four categories by these two factors, "extrinsic vs. intrinsic" and "autonomous vs. non-autonomous" properties. The self-healing mechanism explored first is extrinsic self-healing, represented by capsules within the polymer matrix [36, 90]. The damage will crack these small capsules, and the self-healing component will flow out and react to recover the operator area [36, 90]. However, these self-healing systems are not able to recover from the repeated damage due to the depletion of self-healing materials in the capsules.

In contrast, intrinsic self-healing polymers, with dynamic crosslinking bonds, have been developed to regain their properties repeatedly in different mechanisms [10, 40, 57, 67]. Some of them require non-autonomous external stimuli such as light, heat, and force which allow the self-healing procedure to be controllable [11]. On the contrary, other systems can self-heal autonomously without any external

stimuli. Many autonomous self-healing systems are made from hydrogels, which are mostly composed of water or organic solvents and therefore are widely used in biomedical materials [72]. However, they tend to involve degradation caused by evaporation of solvent [41, 44], which is not suitable for daily life applications.

Thus, in this paper, we focused on polyborosiloxane (PBS) as a candidate material for HCI, which retains intrinsic and autonomous self-healing property. It is also biocompatible and solvent-free, which leads to easy, safe fabrication and use and longer material lifetime [41, 44]. Multi-walled carbon nanotube (MWCNTs) were also introduced as the filler to impart conductivity to the polymer. Both PBS and MWCNTs-PBS are biocompatible under appropriate use (see Material Safety section for more discussion), and is suitable for daily life interface. Although conductive self-healing composites and flex sensors utilizing PBS were previously reported [17, 34, 92], their discussion was mainly limited to a few physical properties, and interface systems with a hybrid structure of conductor, insulator, and substrates have not been explored.

4.4.1.2 *Existing applications of self-healing phenomena*

Although it is still not pervasive, self-healing properties of materials are applied in several fields. As commercialized examples, we have access to self-healing coating for automobiles and displays. Self-healing concrete [28] for sustainable architecture and infrastructure is also readily available on the market. In the field of robotics, self-healing property of liquid (*e.g.,* oil, liquid metal) has been explored for soft actuators [1, 33, 78] and robust robots [50]. The most related example of self-healing phenomenon to digital fabrication or HCI might be fused deposition modeling (FDM) for 3D printing, in which thermoplastic fuses and sticks to the previous layer to build a continuous 3D object.

4.4.2 *Shape-changing Interfaces*

Shape-changing interfaces have already been intensively explored and reviewed [3, 15, 69]. Here, we classify previous studies about shape-changing interfaces by three phases of materials: solid, liquid, and solid-liquid, and explain the main types of shape change each phase affords.

4.4.2.1 *Solid shape-changing interfaces*

Solid shape-changing interfaces utilize dynamic mechanisms (*e.g.,* hinges, pistons) or the relative position of many stiff objects, which result in precise, fast, and reproducible motion. Above all, many researchers have recently focused on the latter strategy such as a 1D line and chain [54, 55], 2D pin dis-

plays [20, 56] and swarms [37], and dynamic 3D printing using magnetic blocks [75]. These examples all exploit the reconfigurable nature of physical elastic pixels or voxels.

4.4.2.2 *Liquid shape-changing interfaces*

Liquid shape-changing interfaces, on the other hand, mainly utilize the healing and fusing nature of two isolated portions of liquid into a single droplet. For example, Programmable blobs [82] uses magnetic fluid to demonstrate a liquid display that changes its shape depending on the magnetic field. LIME [45], Tangible Drops [71], and Programmable Droplets [80] control the shape, number, and position of liquid metal or aqueous solutions by an electric field. Despite its high degree of freedom in shape and potential for fusing interface, they are still hard to handle due to the viscose, fluidic nature.

4.4.2.3 *Solid-liquid shape-changing interfaces*

Solid-liquid materials [44] represented by silicone rubbers and dough retains viscoelastic property; by tuning their property, they can sustain its shape, while deforming dynamically. HCI researchers have developed many soft-bodied interfaces using these materials, such as pneumatic actuation interface [23, 64, 94], flexible, stretchable electronics [62, 89], and dough interfaces such as a conductive tack [65], sand [84], or a toy called Silly Putty [7]. They are able to transform and conform (while keeping their shapes) by the solid-liquid property of materials.

Our proposing Self-healing UI also falls into the solid-liquid shape-changing interface: the key difference to conventional solid-liquid interfaces is that our UI can heal and fuse like liquid, while achieving reconfigurability, transformability, and conformability that solid and solid-liquid interfaces offer. We will demonstrate each property by our proposing applications.

4.5 DESIGN CHOICES OF MATERIALS FOR HCI

As explained in Related Work, we used PBS [34, 41, 44] as a main self-healing material candidate for HCI for the following reasons:

1. *Intrinsic and autonomous self-healing ability* without any external stimuli (e.g., heat, light, additive materials causing chemical reactions) to avoid complex environmental setup.

2. *Controllable electrical and mechanical properties* depending on the applications. The property of PBS can be tuned by dispersing varying amounts of MWCNTs into the polymer to form MWCNTs-PBS composites.

3. *Robust material for long-term use* in a daily environment without time-dependent degradation.

4. *Simple and low-cost fabrication* with which researchers in the HCI field can leverage after training.

5. *Safety and compatibility* to human skin and conventional substrate (*e.g.*, acrylic, polydimethylsiloxane (PDMS), fabric).

Figure 25 shows that two separated PBS samples can quickly self-heal and recover its mechanical strength. In terms of its working mechanism, PBS is a room-temperature self-healing supramolecular polymer that is cross-linked through the dynamic bonds between boron and oxygen [34, 41, 44] (Figure 26). The boron atom in one PBS chain can form a dynamic bond with the oxygen atom from a nearby chain. However, PBS has a weak mechanical strength [34, 41, 44] and low conductivity. Therefore, MWCNTs were suggested as fillers that compose networks to tune its mechanical and electrical performance [90]; in the latter sections, we report performance evaluations of PBS and MWCNTs-PBS developed in our method.
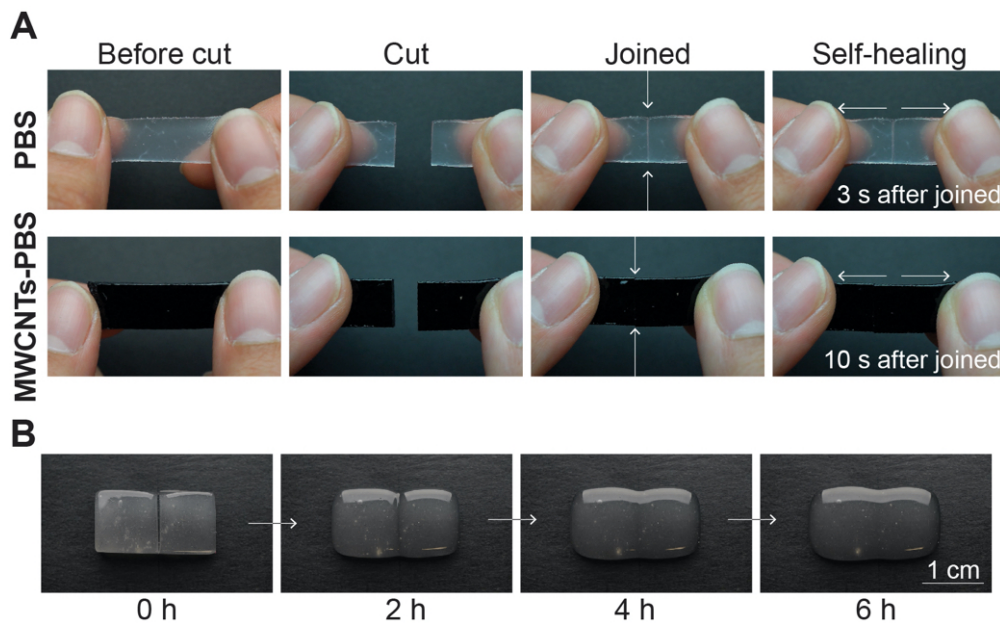
Figure 25: Self-healing process of PBS and MWCNTs-PBS. (A) The rapid healing process of PBS and MWCNTs-PBS. (B) The long-term healing process of PBS, where we observed the cut lines of samples disappearing over time (Figure reused from [P4]).

4.6 PREPARATION OF MATERIALS

In this section, we describe the preparation of PBS and MWCNTs-PBS. We note that MWCNTs are categorized into carcinogenic materials, we need to prepare the safety equipment and follow the procedure written here. All the preparation processes were done inside the fume hood along with appropriate disposal for wastes containing MWCNTs. Also, throughout the preparation, we wore disposable gloves
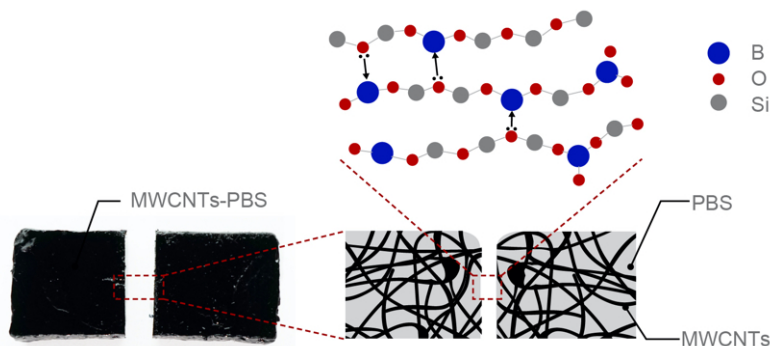
Figure 26: The working mechanism of MWCNTs-PBS. The dynamic bonds between boron and oxygen cause self-healing of the PBS matrix (Figure reused from [P4]).

and masks to avoid the direct contact and inhalation of MWCNTs. For more information on safety, see the latter section for material safety.

We have adopted conventional protocols from the literature [92] with additionally tailored procedures (sonication, doctor blading, and dilution explained below). Both PBS and MWCNTs-PBS were prepared on three criteria: large quantity preparation, the form factor of 2D thin sheets needed to stack them into 3D devices, and easy-to-follow material handling procedures, in order to fit in our layer-by-layer stacking fabrication strategy described later.

4.6.1 *Preparation of PBS Sheets*
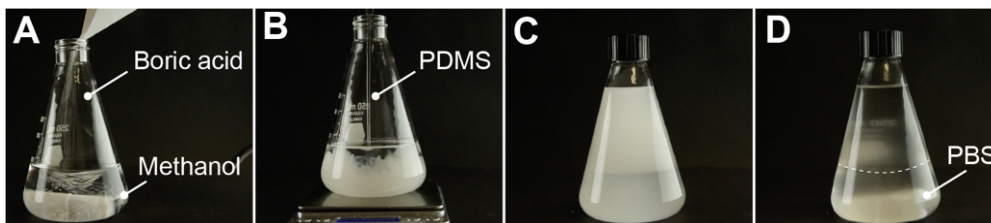
Figure 27: Preparation process of PBS (Figure reused from [P4]).

The boric acid-methanol solution was prepared by adding 1.0 g of boric acid (B6768; Sigma) into 10 mL of methanol and continuously mixed for 1 h with a magnetic stir (Figure 27A). Then 10 g of PDMS (silanol terminated, 35-45 cSt; Gelest) was added to the boric acid-methanol solution and vigorously mixed together for 3 h (Figure 27B,C). After that, the mixed solution was placed on a static table for 1 h until two separate liquid phases are clearly observed (Figure 27D). Uncured PBS was extracted from the bottom part using a transfer pipet. At this point, a small portion of silicone pigment (Silc-Pig; Smooth-on) can optionally be mixed with the solution. This solution was poured into a laser-cut acrylic mold coated with mold release spray (Food Grade Mold Release W0, CRC). The uncured PBS solution in the mold was then placed inside an oven at 60 °C for 24 h to fully cure.

4.6.2 *Preparation of MWCNTs-PBS Sheets*
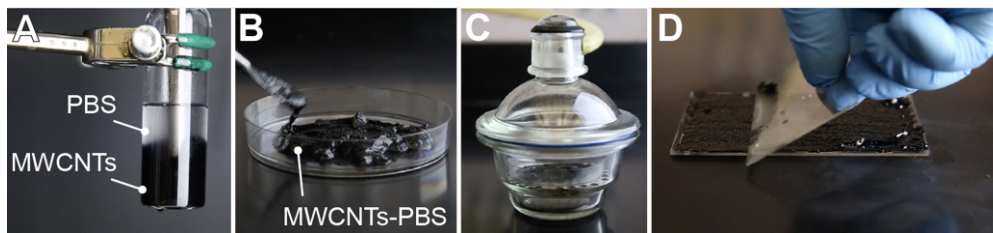
Figure 28: The preparation process of MWCNTs-PBS sheets (Figure reused from [P4]).

MWCNTs (Baytubes C 150 HP) were added into the uncured PBS solution and sonicated (Fisher Scientific Sonic Dismembrator Model 500) at an amplitude of 100 W for 1 h to de-bundle the MWCNTs (Figure 28A,B). The dispersion was vacuumed to remove extra methanol (Figure 28 C), poured into a mold, and transferred into an oven at 60 °C for 24 h to allow the sample to fully cure. Once cured, the sample becomes safe to use and cut with bare hands. During the molding process, we spread the surface of the MWCNTs evenly with a straight knife (Figure 28D, so-called doctor blading) to get a smooth shape of sheets. We newly adopted the sonication process to disperse MWCNTs more homogeneously than the conventional method [92], which led to higher conductivity of the material with a lower concentration of MWCNTs in PBS.

We note that uncured PBS can be stored at room temperature for over 1 month, while uncured MWCNTs-PBS dispersion must be used right after sonication to prevent aggregation and bundling of MWCNTs. If we use an old uncured MWCNTs-PBS dispersion sample, the sample needs a sonication process again. In addition, in order to prepare materials in large amounts and with precise MWCNTs fraction, we adjusted the conventional procedure by starting with the preparation of high-concentration MWCNTs-PBS and then subsequently dilute it with additional uncured PBS solution.

4.7 PERFORMANCE EVALUATION

We have conducted a detailed performance evaluation for both electrical and mechanical properties of PBS and MWCNTs-PBS, both before and after cut and joined. The data shown in this section are from 5 independent samples and measurements. The error bars shown are the maximum/minimum values of the samples. All the other plots show the mean value for each condition. The sample size was L: 12.5 mm, W: 6.10 mm, H: 1.32 mm on average. For electrical measurement, we covered both sides of each sample with silver epoxy (CP4922N-100; DuPont) and applied 2 probes to the silver parts to measure resistance. For mechanical measurement, we used a load measurement machine (Instron 5940).
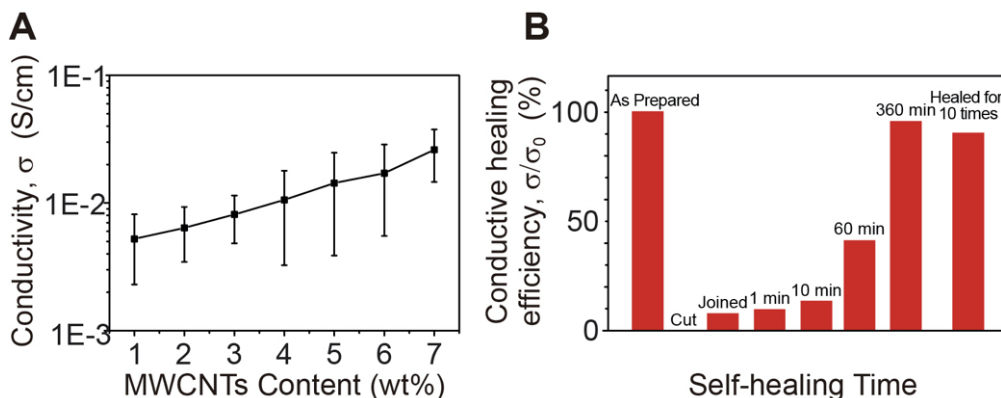
Figure 29: The electrical property of PBS and MWCNTs-PBS. (A) Conductivity vs weight fraction of MWCNTs in the samples. (B) Conductive healing efficiency depicting the time-dependent electrical self-healing property (Figure reused from [P4]).

4.7.1 Electrical Property of MWCNTs-PBS

In order to determine the suitable composition of MWCNTs-PBS for our devices, we measured electrical conductivity as a function of MWCNTs content. Figure 29A shows the conductivity of MWCNTs-PBS with different fractions of MWCNTs. Although the error bars overlap, we observed that the mean electrical conductivity showed a clear upward tendency with increasing MWCNTs content. The resultant conductivity was more than 10 times higher than the previous report when comparing 3wt% samples [92]. This higher conductivity can be attributed to the homogeneous network of MWCNTs inside PBS by the sonication process instead of mechanical stir [92]. To meet the electrical conductivity requirement for the devices, we used the MWCNTs content of 4wt% for all the other experiments and applications in this paper. We note that pure polymers like polydimethylsiloxane (PDMS), which is similar to PBS, have a conductivity ranging between 10^{-16} - 10^{-12} S/cm [49].

In addition, to investigate the electrical self-healing property, we cut and joined the composite. Conductive healing efficiency, defined as σ/σ_0, at different healing time was plotted in Figure 29B, where σ_0 is the electrical conductivity of the as-prepared samples and σ is the electrical conductivity at different self-healing times. We found that 10% of the electrical conductivity immediately recovered after we joined the two halves. Then, the electrical conductivity slowly recovered over time. After 6 h, 96% of electrical conductivity was recovered. We also tested electrical conductivity for the samples after 10 damaging-healing cycles to verify the repeated self-healing property. As shown in Figure 29B, approx. 90% of the electrical conductivity recovered after 10 damaging-healing cycles.
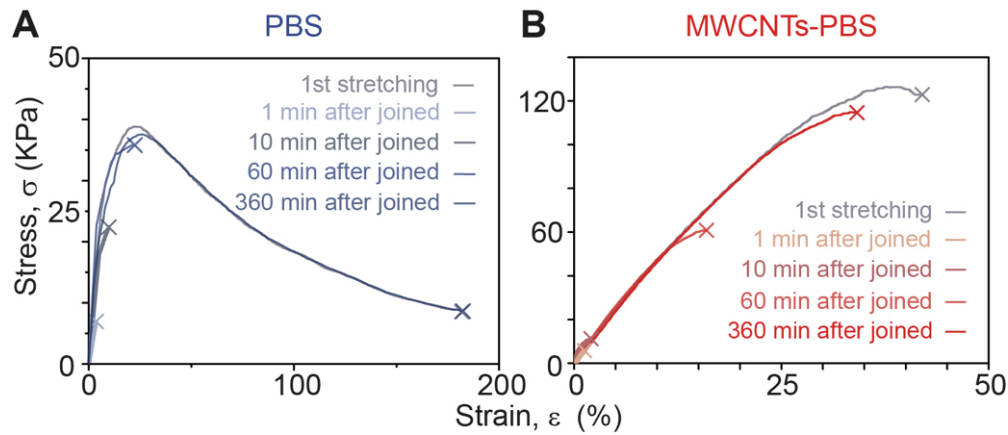
Figure 30: The mechanical property of (A) PBS and (B) MWCNTs-PBS. "×" mark means the sample at break (Figure reused from [P4]).

4.7.2 *Mechanical Property of PBS and MWCNTs-PBS*

To investigate the mechanical self-healing properties, we tested the tensile stress σ vs. strain ϵ over the range of ϵ = 0 - 200%. The mechanical properties of PBS and MWCNTs-PBS are shown in Figure 30A,B, respectively.

PBS showed the elastic region for ϵ < 5%. The sample reached the ultimate stress of 39 kPa at ϵ = 39%, but is able to be stretched to ϵ = 180% before a fracture occurred. To study mechanical self-healing, we cut the sample into halves and then joined them. We allowed the samples to self-heal for a certain amount of time before measuring the curve. As shown in Figure 30A, the ultimate elongation strain of PBS increased with more self-healing time, and after 6 h the samples exhibited an almost identical tendency as as-prepared samples.

The same measurements were performed on MWCNTs-PBS with 4wt% MWCNTs content. The elastic region of MWCNTs-PBS was extended to ϵ = 8%. Moreover, adding the MWCNTs filler makes the composite stronger, whose ultimate stress was enhanced to 120 kPa at strain ϵ = 40% as shown in Figure 30B. On the other hand, the addition of MWCNTs fillers slowed down the self-healing speed. As shown in Figure 30B, the composite did not fully restore its original mechanical property after 6 h.

4.8 SELF-HEALING UI AS A HYBRID MATERIAL SYSTEM

As we evaluated in the previous section, PBS and MWCNTs-PBS have pros and cons. Here, we propose a novel hybrid design that takes a middle way. We leveraged the fast healing and electrically insulating property of PBS, as well as the electrical conductivity and mechanical stiffness of MWCNTs-PBS to implement practical interface devices.

4.8.1 *Balance between PBS and MWCNTs-PBS*

Balance in self-healing speed. As explained in Figure 30, the self-healing speed of MWCNTs-PBS is slower despite its conductive property, while insulative PBS can heal faster. Thus, by combining PBS and MWCNTs-PBS, we can achieve fast mechanical healing while keeping conductivity.

Balance in stiffness. PBS changes its shape as time passes due to gravity (so-called a "creeping" effect shown in Figure 31), which is problematic for everyday use from the viewpoint of users. On the other hand, MWCNTs-PBS can hold its shape thanks to its sustainable network structure as shown in Figure 26. Thus, by exploiting MWCNTs-PBS as a substrate of PBS, the whole system can maintain its shape for more robust usage.
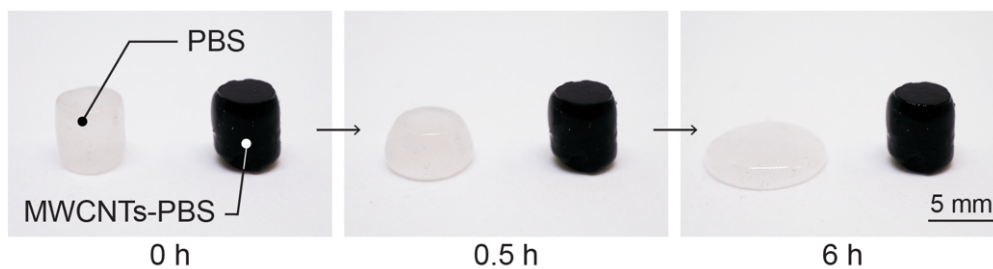
Figure 31: Creeping effect of PBS (Figure reused from [P4]).

4.8.2 *Functions of Each Layer*

Figure 32 shows an overview of our layer-by-layer stacking model. The whole structure is composed of three different types of layers: a substrate layer, one or multiple functional healing layers, and a covering layer.

The substrate layer. It works as elastic mechanical support (*e.g.*, Ecoflex 00-30 silicone (Smooth-on), PDMS (Sylgard 184; Dow Corning), and MWCNTs-PBS shown in Figure 33A,B,C) that restricts PBS layers from flowing and creeping over time. We note that PDMS and many other silicone elastomers are commonly used for HCI applications [62]. On the other hand, a composite of PBS and polyester fabric provides extra adhesion to the skin (Figure 33D). To achieve these substrates bonded with the functional layers, we poured uncured PBS solution on the cured PDMS and Ecoflex and put them in 60 °C oven for 24 h. MWCNTs-PBS was just joined together with PBS, and they fused into the continuous structure with their inherent self-healability. We made PBS-polyester fabric by first soaking fabric into uncured PBS solution, which was then vacuumed for approximately 30 min until no air bubbles were observed. This fabric composite was fully cured at 60 °C for 24 h.

The functional layer. It is composed of PBS, MWCNTs-PBS, miniaturized electronic components, connection wiring to the outer module, and some other functional layers (*e.g.*, color-changing composites).
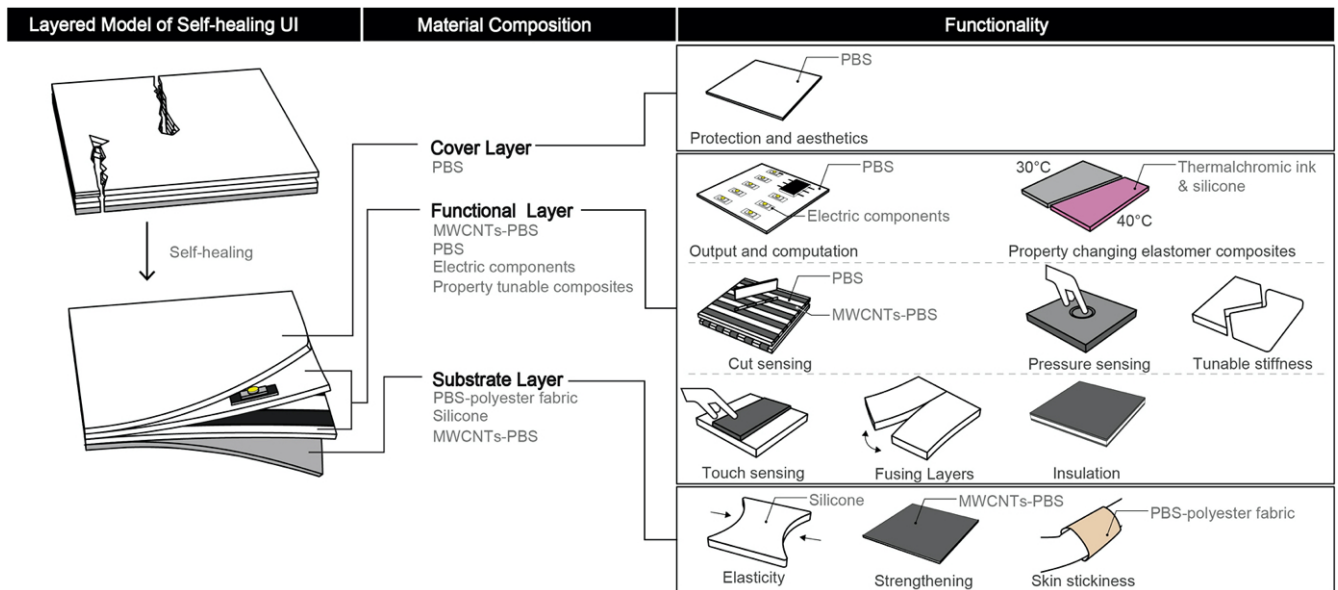
Figure 32: A layered Model of Self-healing UI. The substrate layer sustains the whole device to keep its shape and works as an interface to other materials or the human body. The functional layers work as a self-healing body, circuitry, sensors, or other functional media (*e.g.,* the color-changing layer). The cover layer is optionally used for the protection of the device and aesthetics (Figure reused from [P4]).

MWCNTs-PBS can work as sensors for pressure, touch, and cut. PBS in this layer has three major functions: effective self-healing medium, insulation components between conductive MWCNTs-PBS and other electronics, and integration matrix to embed other wires and components into one continuous body.

The covering layer. This layer is optionally used for the sake of protection, insulation, and aesthetics.

4.9 LAYER-BY-LAYER STACKING FABRICATION

Leveraging the self-healability of PBS, our fabrication process exhibits four advantages over conventional layer-stacking techniques: no need for adhesives between layers; no need for soldering between conductive wires and MWCNTs-PBS; the flexibility to stabilize electronic components between layers; the stable bonds between PBS and other silicone elastomers. In this section, we describe the fabrication process of Self-healing UI by stacking PBS, MWCNTs-PBS, and other components.

4.9.1 *Step 1: Fabrication of Each Layer*

First, PBS and MWCNTs-PBS sheets were removed from the molds carefully with tweezers. Then each material was cut by a CNC drag knife (12'x12' CNC Machine; Zen Toolworks, D2 drag knife; Donek) as
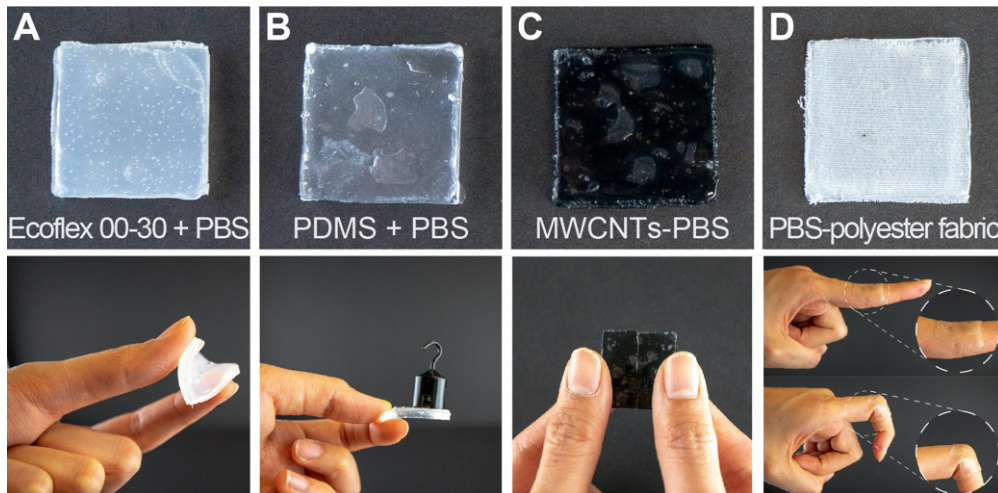
Figure 33: Options for the substrate layer. (A) Commercially available soft silicone (Ecoflex 00-30). (B) PDMS as a stiff substrate to hold the shape. (C) MWCNTs-PBS that better sustains the shape than pure PBS while achieving self-healability of the whole structure. (D) PBS-polyester fabric sticking and conforming to human skin (Figure reused from [P4]).
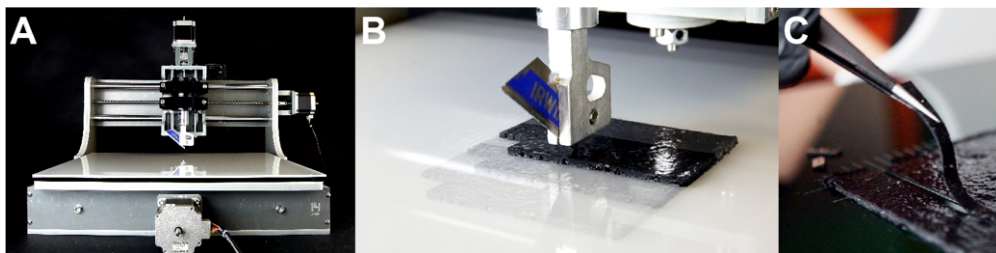
Figure 34: Cutting PBS and MWCNTs-PBS. (A) the materials were removed from the mold and cut by (B) a CNC drag knife or a die cutter into designated components. (C) Then each component was placed in order, and the whole structure automatically self-heals and fuses (Figure reused from [P4]).

shown in Figure 34 or a die cutter (made by laser cutting acrylic boards). After cutting each component, they were placed in order and fused together by their self-healing property.

4.9.2 *Step 2: Electrical Connection*

As shown in Figure 35, sandwiching the wire with self-healing material can work both for electrical and mechanical connection without glue. We demonstrated two methods of (1) placing additional MWCNTs-PBS material onto the wire and (2) cutting the middle part of MWCNTs-PBS and inserting the wire inside the gap. The former is easier for a smaller size of MWCNTs-PBS circuitry, while the latter is better in terms of aesthetics. We used multi-strand wire (36 AWG, UAA3607; Micron Meters), for maximizing the surface contact area on MWCNTs-PBS to stabilize the conductivity and minimizing the volume of the connection part to help MWCNTs-PBS self-heal faster.
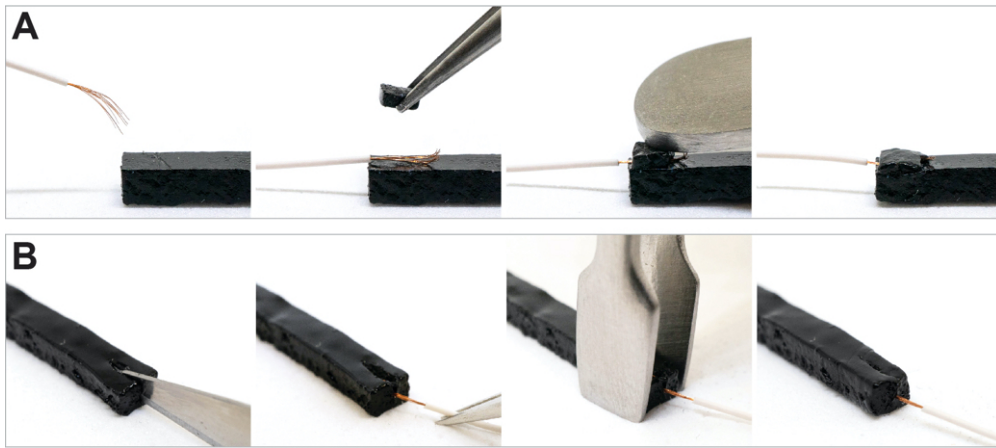
Figure 35: Two wiring methods for MWCNTs-PBS circuitry. (A) Placing additional MWCNTs-PBS piece with tweezers. (B) Cutting the middle part of the trace and insert the wire (Figure reused from [P4]).

4.9.3 *Step 3: Stacking Layers*
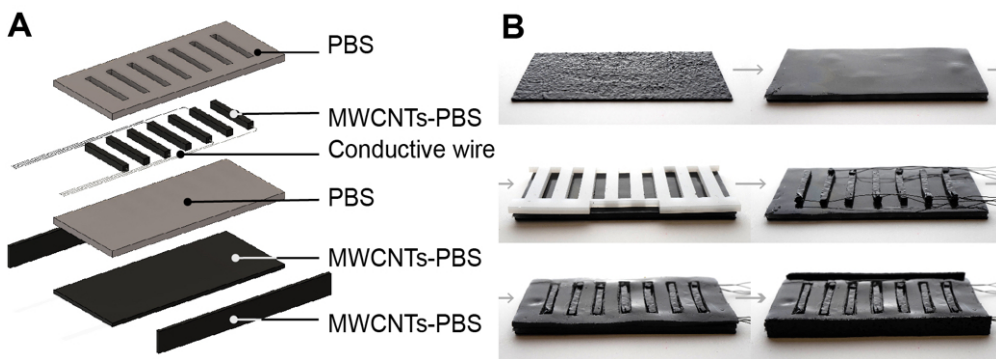
Figure 36: Stacking layers of Self-healing UI. (A) A layered model of a transformative soft controller. (B) Stacking layers in sequence. The device will self-heal and form one continuous body within 6 h. The white acrylic plate was used to guide the position of MWCNTs-PBS strips (Figure reused from [P4]).

Once the preparation of each layer and connection was done, Each layer and component was stacked in order as shown in Figure 36. We used a laser-cut acrylic board shown in Figure 36B to guide the position of MWCNTs-PBS strips.

4.10 SENSING PRIMITIVES

In this section we demonstrate three sensing primitives: touch sensing, pressure sensing, and cut sensing. Figure 37 and Figure 38 show the circuit diagram and the photos for each sensing method, respectively. We note that pressure sensing and cut sensing were performed with the same circuit diagram (Figure 37B). For implementation, we used Arduino Mega 2560 Rev 3 as a microcontroller.
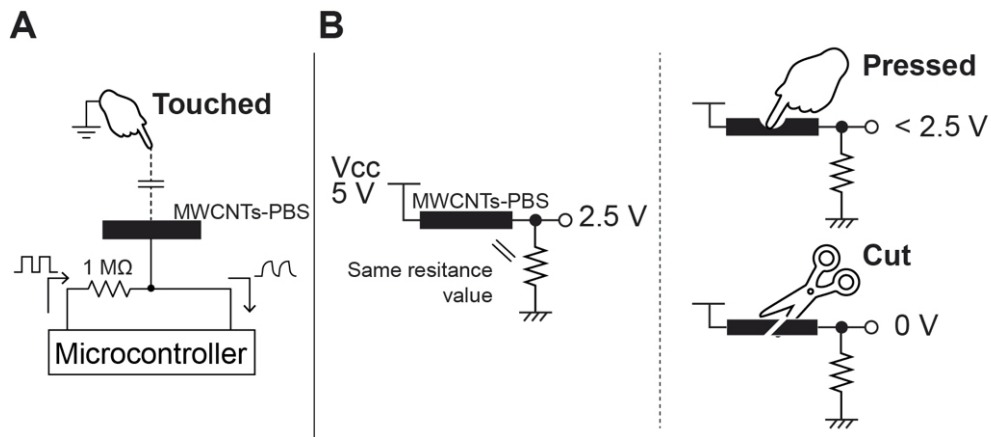
Figure 37: The sensing principle for (A) a touch sensor and (B) a pressure and cut sensor (Figure reused from [P4]).
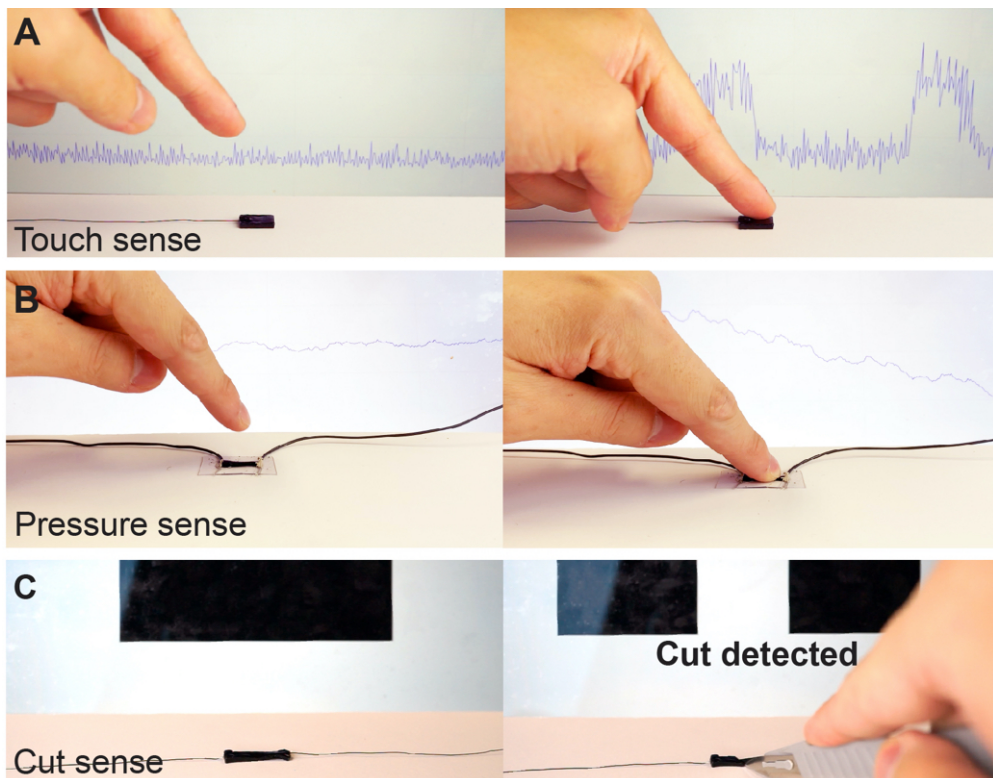
Figure 38: Photographs of sensing primitives. touch, pressure, and cut sensors are activated in front of the screen with their input values (Figure reused from [P4]).

4.10.1 *Touch Sensing*

Touch sensing was implemented in the same way as a conventional touch sensor made of a bulk metal conductor. Depending on the distance between the human body and MWCNTs-PBS, the capacitance value (shown with a dashed line in Figure 37A) changes, resulting in the configuration of the low pass filter. We used the Capacitive Sensing Library of Arduino.

4.10.2 *Pressure and Cut Sensing*

Each end of MWCNTs-PBS was connected to V_{cc} (= 5 V) and a digital pin reading the voltage value. When we apply pressure to the MWCNTs-PBS, it deforms to increase its resistance value. This change in resistance can be read by the digital pin as a decreased voltage. The same mechanism as pressure sensing can be applied to cut sensing. If MWCNTs-PBS is cut into pieces, the voltage value read from the digital pin goes to 0 V, which is clearly detectable. Although this sensing mechanism is as simple as a tact switch, the self-healing property of MWCNTs-PBS allows detecting cuts repeatedly if we make a mechanical connection of each piece, which is a unique property for this sensing method.

4.11 APPLICATIONS
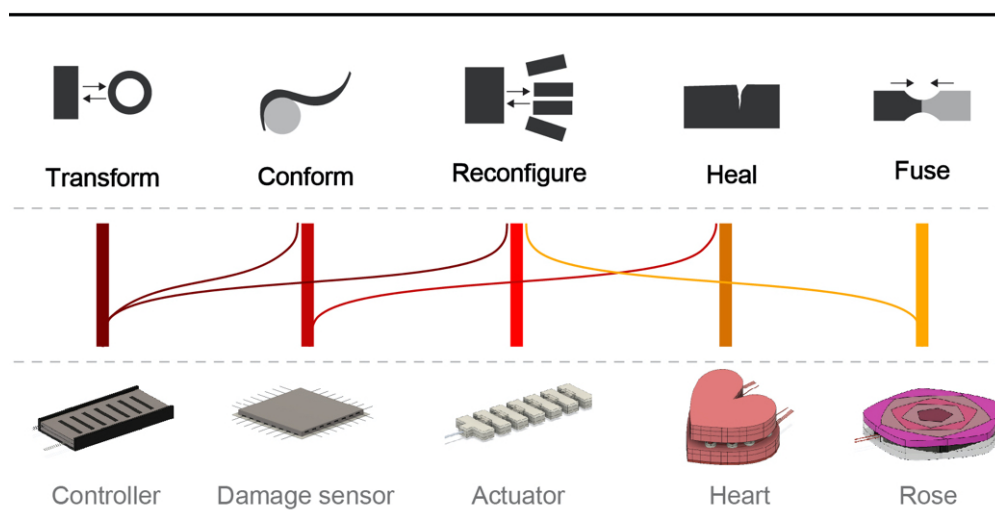
Figure 39: The design space of Self-healing UI (Figure reused from [P4]).

In this section, we explored the design space of the Self-healing UI through five demonstration artifacts. As shown in Figure 39, we can distinguish the functionality of soft, self-healing materials into five: (1) dynamic transformation of shape; (2) Conformable applications of UIs to other objects; (3) Reconfiguration of the number and the function of devices; (4) Healability of the damaged or broken part; and (5) fusing nature of two different modules. Each of these five spaces is mainly related to five applications

we will demonstrate (thick line in Figure 39), but some of them have overlapping features depicted as a thin curved line in Figure 39.

4.11.1 *Transformative Soft Controller*
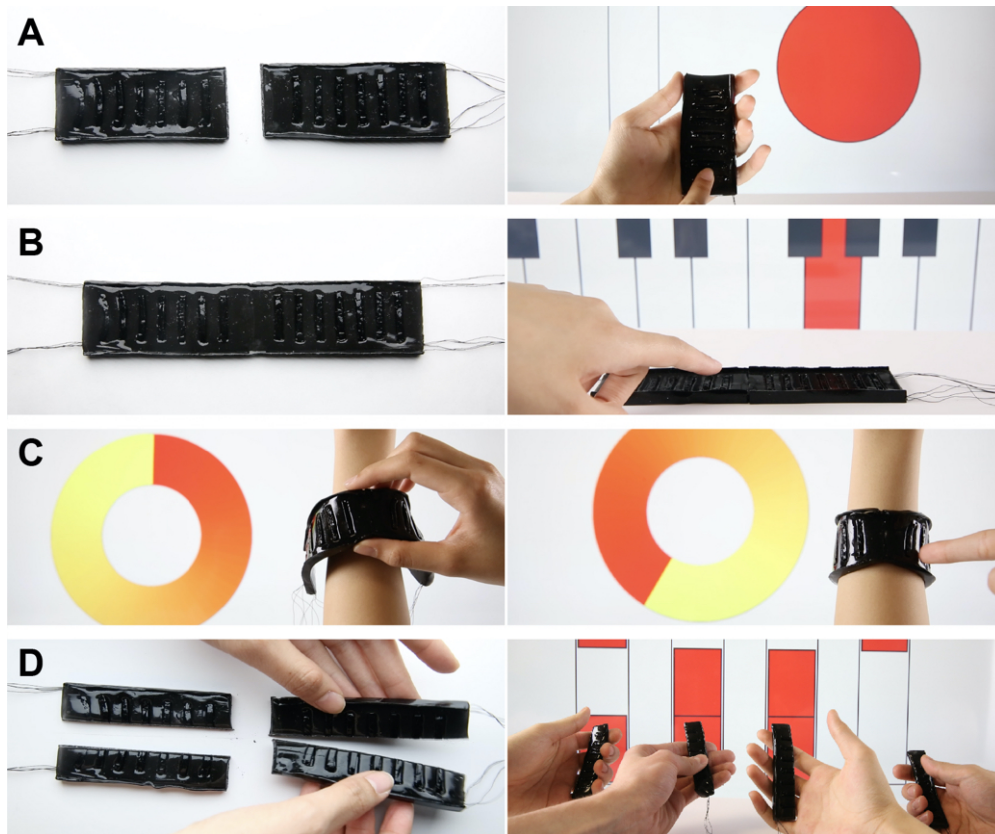
Figure 40: The transformative soft controller can change its shape and reconfigure the number and the function of the device as user needs (Figure reused from [P4]).

We envisioned a controller device that can dynamically change its shape and number of modules depending on the different ways we expect to it. Figure 36 shows the layered structure of the proposed controller; one of the MWCNTs-PBS strips is a pressure/cut sensor and all the other strips are touch sensors. Wiring was connected to Arduino. A series of touch sensors were used to detect both a single touch and the sliding motion.

Figure 40 shows four use scenarios of this controller. First, a single controller detects a finger press motion in Figure 40A (the normal mode). Then two controllers were joined to form long touch buttons and worked as a piano keyboard in Figure 40B (the long mode). Next, two connected controllers wrapped around the user's wrist, working as a wrist band slider device in Figure 40C (the wrist band mode). When three friends came to play a video game, the controller was cut into four pieces and worked as

half-sized gaming devices with three touch sensors for each in Figure 40D (the cut mode). After use, the four pieces can be joined into the original two controllers for 6 h.

4.11.2 *Conformable Damage Sensor*
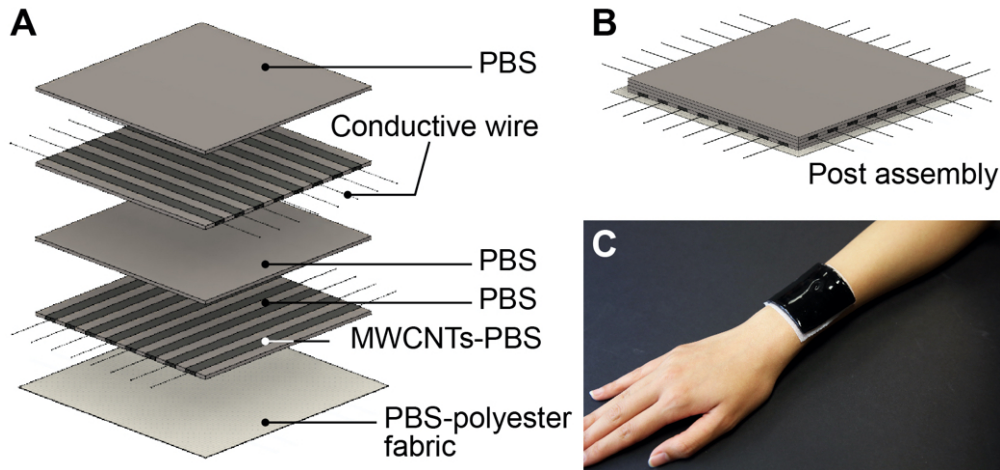
Figure 41: Overview of the conformable damage sensor. (A, B) A layered model of 8 × 8 damage sensor pad. (C) The soft sensor pad sticks and conforms to skin. This photo was taken without wiring to the sensor for clarity (Figure reused from [P4]).

We prototyped a self-healing damage sensor matrix as a second skin. The layered model of the damage sensor is shown in Figure 41A,B. The first (substrate) layer was made by PBS-polyester fabric which can stick to human skin (Figure 41C), In the second and the fourth layer, MWCNTs-PBS cut sensors were distributed in series, composing an 8 × 8 cut sensor matrix. The third PBS layer was added for insulation between two conductive layers.

Figure 42A shows a demonstration of how it works. First, when we made a single cut at one node of the matrix, the red dot showed up on the screen and visualized the damaged point. Next, we made another cut on the damage sensor matrix, and then the red circle on the screen got bigger, showing the region of two cuts. We again cut the third node, and the circle got bigger again. Figure 42B shows almost the same situation, but in this case, three cuts are on the same line. Then the screen showed a more precise position of damages. We note that the damages in Figure 42A were expressed as a big circle, not multiple points, because we suffered from a "ghosting effect" of the sensor matrix, which will be discussed later.
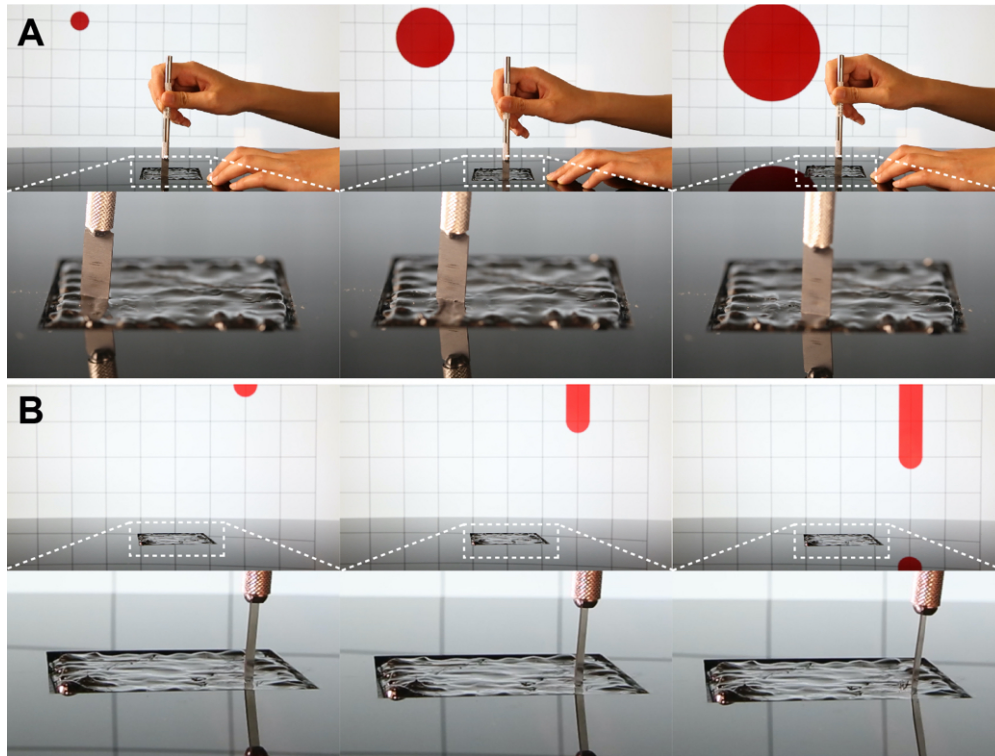
Figure 42: Demonstration of the damage sensor matrix on the table. (A) Three diagonal cuts induced a damaged area bigger in sequence. (B) Three linear cuts made the red line on the screen longer, implying the cut gets longer (Figure reused from [P4].

4.11.3 *Reconfigurable Pneumatic Soft Actuator*

Conventional pneumatic soft actuators were subject to the small damage; we propose a cuttable and thereby reconfigurable version of such actuators with PBS. Figure 43 shows the layered model and the photo of the proposed pneumatic actuator. The top and the bottom parts of the pneumatic channel were made from two different silicone Ecoflex 00-30 and Dragon Skin 00-30 (Smooth-On) with different stiffness, which led to anisotropic bending motion when we supply air. We coated each node of the actuator with PBS, which keeps the pneumatic channel airtight ever after cut and joined.

Originally, the actuator bent into a "C" curve (Figure 44A). After cutting one node of the actuator and attaching the cut piece upside down, however, the actuator formed an "S" curve (Figure 44B). When we shortened the length of the actuator and attached the end piece back, a shorter version of the "C" curve still worked in the same way as the longer one (Figure 44C).
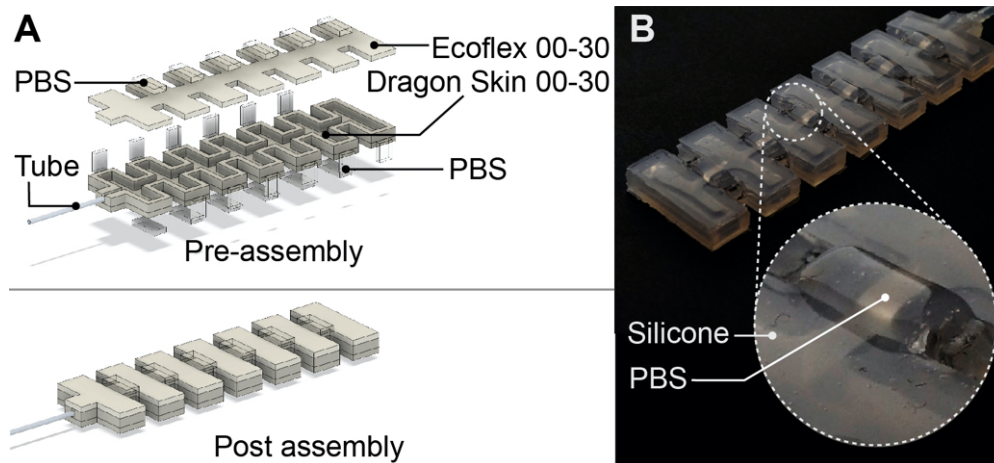
Figure 43: Overview of the reconfigurable soft actuator. (A) A layered model of the reconfigurable soft actuator. (B) PBS wraps around and covers each node (Figure reused from [P4]).
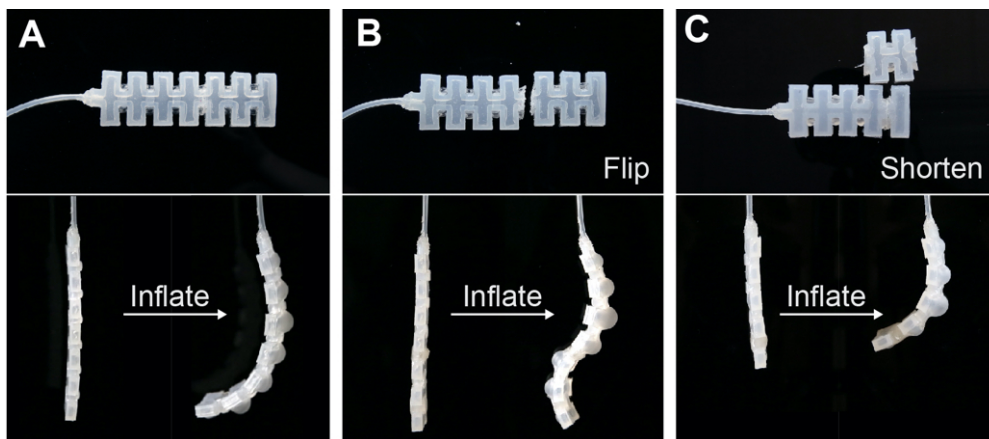
Figure 44: The photos of different configurations and functions of the actuator.

4.11.4 *Healing Heart*

We mimicked the heart- warming/breaking moment with our self-healing materials. Figure 45 shows the layered model of the self-healing heart and its assembling procedure. We embedded LED components and MWCNTs-PBS cut sensor inside. When the cut sensor detects the mechanical and electrical connection, LEDs are lit up as feedback. The actual workflow is shown in Figure 46. First, two users joined the heart, and the LEDs reacted to the physical and mental connection (Figure 46A,B). Over time, the gap between the two pieces gradually got vague and disappeared in 6 h (Figure 46C). Finally, the shape of the heart became continuous in Figure 46D.
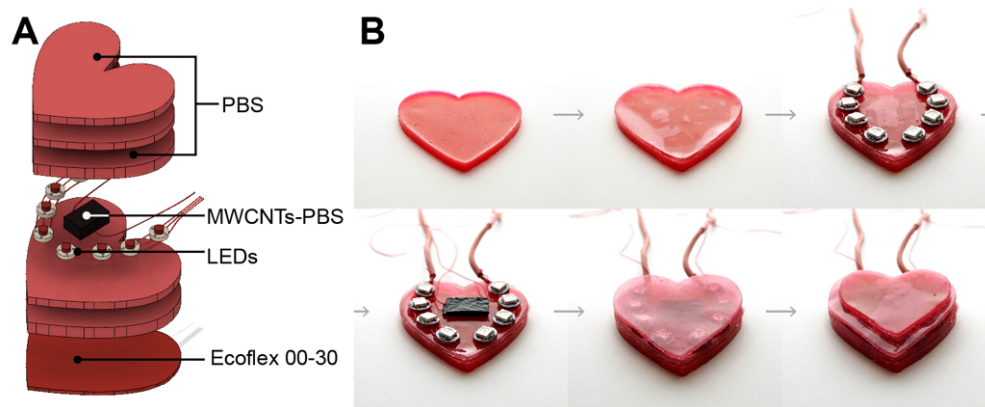
Figure 45: Overview of the healing heart. (A) A layered model of the healing heart. (B) Assembly process of the heart (Figure reused from [P4]).

4.11.5 *Fusing Modular Rose Puzzle*

We utilized the fusing property of different modules, and made a puzzle with a rose shape. As shown in Figure 47A, it is basically composed of PBS pieces with different colors, but only the outer pieces are made of Ecoflex mixed with thermochromic ink, MWCNTs-PBS conductor, and PDMS. This outer layer works both as (1) a mechanical constraint that prohibits the inner PBS pieces from flowing out and (2) an electrical heater with logic. When users finished the assembly shown in Figure 47B-F, MWCNTs-PBS in the outer pieces were electrically connected and heated up by Joule heat, which turned the black color of the thermochromic layer into pink (Figure 48A,B). Moreover, as time passed, each piece fused into one smooth and continuous structure as shown in Figure 48C,D.
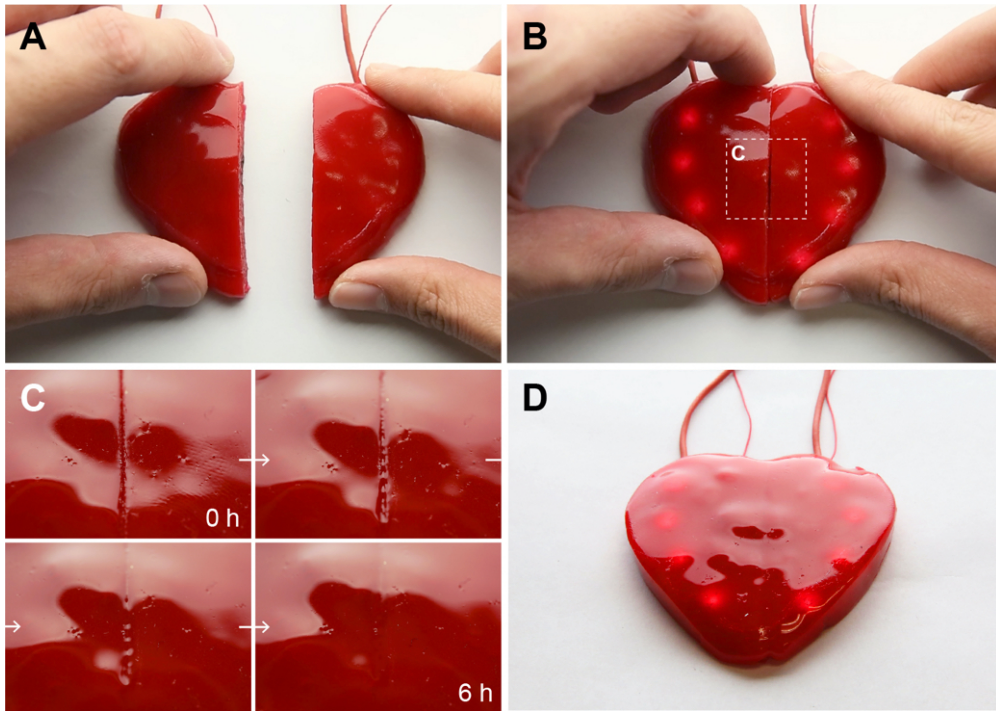
Figure 46: Working process of the healing heart. (A,B) The device can sense when the two halves are joined. (C,D) The heart can stick together after a few seconds and self-heals completely in 6 h (Figure reused from [P4]).
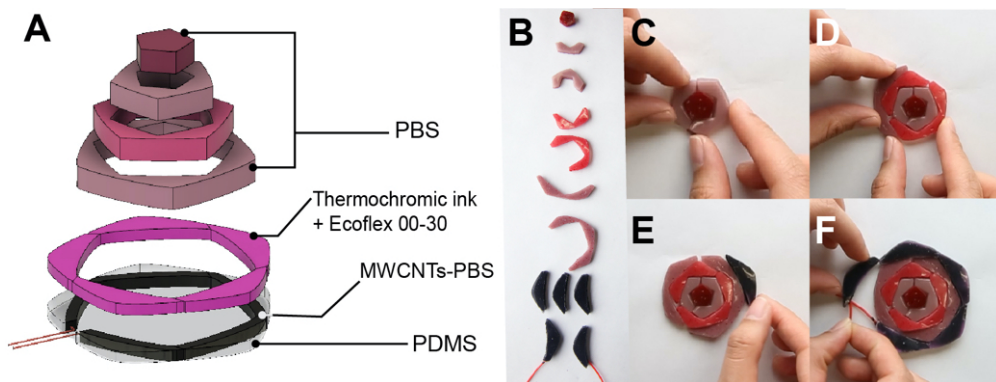
Figure 47: Overview of the fusing rose puzzle. (A) A layered model of the fusing rose puzzle. (B-F) The assembly process (Figure reused from [P4]).
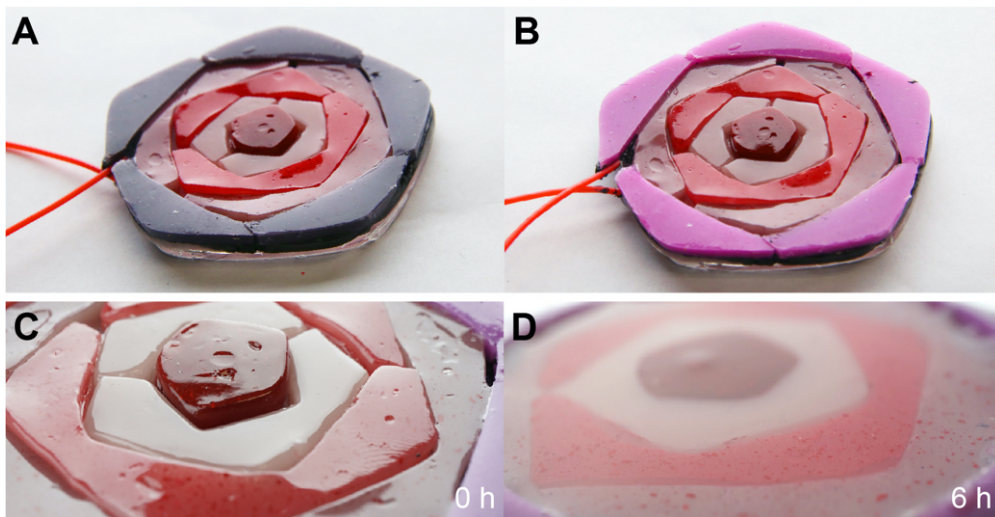
Figure 48: Working process of the fusing rose puzzle. (A,B) Right after joined, the thermochromic layer in the outer pieces was activated by the MWCNTs-PBS heater below. (C,D) In 6 h, the puzzle fused into a unibody (Figure reused from [P4]).

4.12   MATERIAL SAFETY IN PREPARATION AND USE

We put this discussion section in order to inform of appropriate knowledge on the danger our materials potentially have. In summary, the use of Self-healing UI is skin-compatible at room temperature, and users can handle and cut it with bare hands as demonstrated below. However, the preparation process clearly involves manipulation of dangerous substances and this should be done by those who took the proper training under a suitable environment.

4.12.1   *Safety of MWCNTs*

The main safety concern for MWCNTs use is inhalation, which may bring them in contact with the cardiovascular system; a prior study suggests the maximum exposure of Baytubes MWCNTs, which we used in our study, to be ~ 0.05 mg/m^3 inside the lungs [66].

However, we observed that the MWCNTs powder used in our fabrication process forms small bundles of diameter ~ 1 mm and thus are too heavy to become airborne. In addition, the strong interactions between MWCNTs and encapsulating PBS polymer matrix [16, 61] further prevent MWCNT bundles from releasing into the air even during cutting or tearing (see Figure S1 (e) in [61]). Thus our UIs do not expose the underlying cells to MWCNTs through skin contact. MWCNTs have already been used in consumer products including car tires, ship hulls, and water filters, showing that MWCNTs can be safely handled [18].

4.12.2   *Safety of PBS*

We also used PBS, which is made by reacting PDMS with boric acid. PDMS is used in biomedical applications due to its bio-inertness [5, 51]. Boric acid is used in contact cleaning solutions, displaying low cytotoxicity [38]. PBS has even been used as a toy called Silly Putty [44].

4.12.3   *Extreme Heat Applied to MWCNTs-PBS*

Although MWCNTs-PBS after preparation is safe for use, we should avoid applying heat over a few hundred degrees Celsius to it. The extreme heat could not only ruin the self-healing property of PBS but also burn the PBS shell, making MWCNTs exposed to the air; this is the reason why we used the automated cutting process with a drag knife, not laser cutting in which laser irradiation can cause overheating.

4.13 LIMITATIONS AND FUTURE WORK

4.13.1 *Ease of Fabrication*

As explained above, our current fabrication method is based on molding, automated cutting, and stacking layers, which is time-consuming and restricted in terms of its design freedom, while laser cutting should be avoided. As an alternative way of fabrication, we expect a 3D printing process of PBS and MWCNTs-PBS can potentially replace the whole procedure as one of the future works.

4.13.2 *Different Material Choices for Specific Use*

While MWCNTs-PBS is easy to handle due to its elastic nature, PBS tends to be troublesome when we try to make a thin film (approx. < 1 mm) with our current molding process. When we apply force to the thin PBS sheet to peel it off, the sheet can easily deform and sometimes result in fractured shape. Adding an appropriate amount of insulative particles into PBS and forming an insulative composite of PBS could help us enlarge the design freedom as well as make the process easier. The other option is to use a stiff self-healing material. Recently, intrinsic, autonomous, and mechanically robust self-healing material was reported [93], which can be useful if we do not need the soft property of self-healing materials.

Also, our current method of pressure sensing has room for improvement. Due to the aspect ratio of MWCNTs particles, the resistance change responding to the pressure deformation is not significant, which causes a low S/N ratio. It may be effective to replace the conductive material into graphite micro sheet that has more surface area than MWCNTs and will react more drastically to the deformation [7].

4.13.3 *Electrical Disconnection due to Creeping of PBS*

As shown in Figure 31, PBS starts to creep and flow out if there is no constraint. In the prototype of the self-healing controller, we observed that wiring was pulled off by surrounding PBS and disconnected from the MWCNTs-PBS sensors. In order to prevent this issue, we need to either (1) anchor the wire to non-flowing material such as Ecoflex and MWCNTs-PBS or (2) constrain the PBS structure with the surrounding structure.

4.13.4 *Conclusions*

In this paper, we proposed Self-healing UI, a soft-bodied interface that can intrinsically self-heal its mechanical and electrical damages without external stimuli or glue. We proposed and implemented the hybrid devices of PBS, MWCNTs-PBS, and other components fabricated by the layer-by-layer structure.

We also demonstrated the unique design space of self-healing materials through five applications. We strongly believe our Self-healing UI will enrich the field of HCI, as a new embodiment of material-driven shape-changing interfaces.

<div style="text-align: right; font-size: 3em;">5</div>

CONCLUSIONS

5.1 SUMMARY

In this thesis, I proposed the vision of human-material interaction (Figure 10) in which the material directly interacts with humans, mediated via mechanical, electrical, chemical and rheological properties of the materials, instead of human-computer interaction in which humans and computers interact with each other via several types of user interfaces. Because the material composing daily objects and environments around us can directly work as interaction, human-material interaction corresponds with the idea of ubiquitous computing in which the computer interfaces are weaved into objects and becomes indistinguishable.

As the embodiments of such human-material interaction, I focused on leveraging multiple phases of materials as a new space for interaction design, and proposed two interfaces, (1) phase-switching interfaces and (2) phase-transcendent interfaces through the implementation of Liquid Pouch Motors and Self-healing UI, respectively. These two types of interfaces dealt with and made use of solid, solid-liquid, liquid, and gas phases of the materials. We also demonstrated applications coordinating with our daily objects and environments of paper, architecture, clothe, and shape-changing devices that human-material interaction is suitable for.

Figure 49 and Figure 50 revisit the summarized contribution of this thesis, human-material interaction and phase-changing interfaces.

Here are the research questions I raised in the first section 1.1 and the summarized answers to them:

1. What is human-material interaction (HMI)? What is the relationship between HCI and HMI? How can we leverage human-material interaction?

   – Based on the recent trend of more physical interfaces prevailing, I defined human-material interaction as the interaction between humans and objects mediated by the physical properties of materials that compose the objects. The interface function is encoded in the material properties by means of computational fabrication and/or functional materials in a tunable way (Section 2.1.1 and Section 2.1.2).
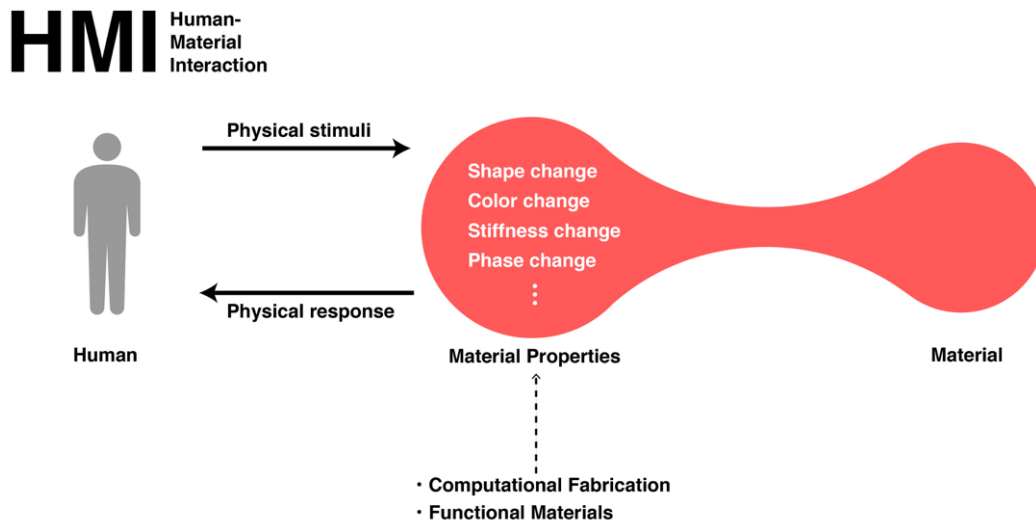
Figure 49: Human-material interaction (reprint of Figure 10). The material properties work as an input/output function between humans and the materials, both of which are in the physical world. In this relationship, the materials and their properties are strongly connected with each other. We can customize the function of materials' intrinsic properties by computational fabrication and/or functional materials.
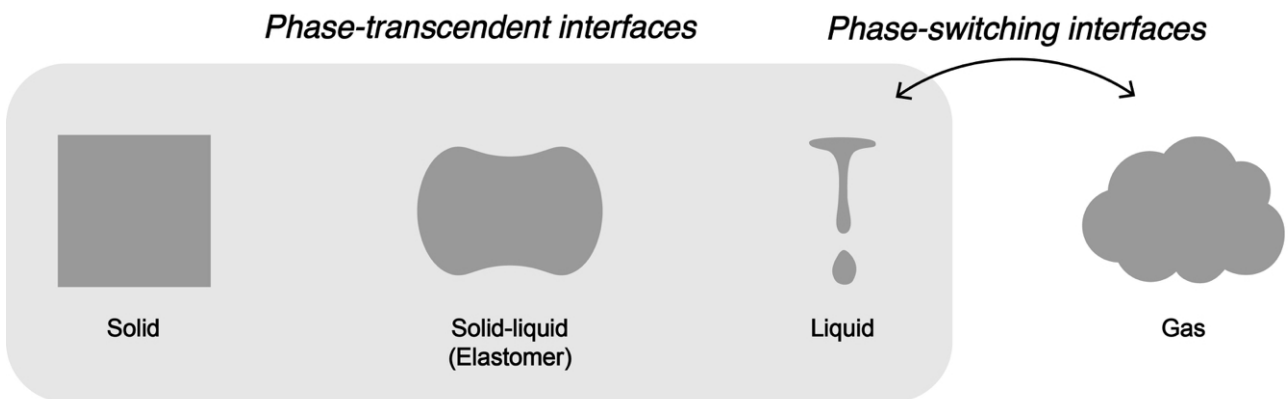
Figure 50: Summary of contribution in this thesis (reprint of Figure 7). Two types of interfaces were proposed that range from solid, solid-liquid, liquid, and gas all of which are the material phases we usually observe in our lives: (1) Phase-changing interfaces that switch the phases on demand, through the project Liquid Pouch Motors and (2) Phase-covering interfaces that work as if they are in multiple phases at the same time, through the project Self-healing UI.

– I introduced several recent example projects that can be categorized into human-material interaction, and sorted them out depending on the tunable physical properties they allow for (Section 2.1.3 and Section 2.1.4).

– By comparing human-material interaction with existing human-computing interaction, I clarified that human-material interaction has a unique niche in interaction with daily objects and environments (Section 2.1.5).

2. As one embodiment of HMI, what are phase-changing interfaces? How can we fabricate and make use of phase-changing interfaces?

– I proposed two mechanisms of phase-changing interfaces: (1) phase-switching interfaces that can toggle between two (or potentially more) phases and leveraged benefits of each phases; (2) phase-transcendent interfaces that work as if they are in the multiple phases at the same time (*e.g.,* basically solid, but as flexible as elastomer and as healable as liquid at the interface of damage).

– Fabrication of Liquid Pouch Motors: liquid injection into the pouch has already been done by many manufacturers (just like filling soy sauce into the plastic pouch), leading to easy and scalable fabrication. On the other hand, the amount of liquid inside the pouch is extremely small thanks to the large volume expansion ratio of phase change, leading to affordable fabrication.

– Fabrication of Self-healing UI: the molding and stacking processes are suitable for self-healing materials that are intrinsically hard to keep their shape through additive manufacturing like 3D printing. On the other hand, the self-healability of the materials allows stacking fabrication to finish without any gluing process.

– Interaction of Liquid Pouch Motors: by leveraging the large volume expansion of liquid-to-gas phase change, the actuator allows both the strong actuation and large strain like pneumatic actuators, while thin, flexible, and lightweight nature achieves the actuators without tethering pumps or tubes.

– Interaction Self-healing UI: by leveraging multiple phases of self-healing materials, we can potentially build conventionally contradicting function of, for example, keeping shape but conform and heal.

5.2 DISCUSSION

Although I explained about the pros and the cons of human-material interaction and phase-changing interfaces throughout this thesis, there are still two fundamental topics for discussion.

5.2.1 *Does a Foldable Chair Fall into Human-material Interaction?*

In Section 2.1.1, I defined human-material interaction as the interaction between humans and objects mediated by the physical properties of materials that compose the objects. Under this definition, one might wonder if a foldable chair can also be categorized within human-material interaction, for instance; it is an object and works as a mechanical structure even without connecting to the computer.

In my idea, the foldable chair does not fall into the category of human-material interaction. The reason is that the mechanical function of the foldable chair is usually enabled by the mechanical hinge attached to the chair, not by the raw material of the chair (*e.g.*, wood). The benefit of human-material interaction is that the interfaces can be indistinguishable with non-functional objects around us. In this regard, the physical properties added by some other components are not considered the material property.

Having said so, drawing a clear border of what is HMI and what is still hard and I believe we should leave the border vague so far. For example, Metamaterial Mechanisms [26] utilized the mechanical metamaterial structure, but in what scale is this called a metamaterial and in what scale not? If the scale of each meta structure is bigger enough, it should be called a collection of beams, not metamaterials. Thus, the definition of "material" also depends on the scale factor from the viewpoint of humans. Based on the discussion here, I conclude that "the invisibility" of entities rendering the physical components is one of the most important factors for HMI. *Vice versa*, if it is literally invisible, computers can also be defined as materials.

5.2.2 *Speed of Human-material Interaction*

As I mentioned in the case of liquid-to-gas phase change in Section 3.9.2, the speed of human-material interaction can be an issue depending on the properties (*c.f.*, PBS also needs 6 hours to fully heal). In other examples, thermochromic and photochromic inks need long resting time to deactivate them.

In general, the digital interfaces have much more degree of freedom and reaction speed than the physical interfaces. Although I said that human-material interaction is suitable for ambient interaction, it also means that the material interaction is limited by the slower speed of the physical world.

5.3 OPEN QUESTIONS

At the same time as the discussion above, there are four open questions that can potentially lead my projects to the next steps.

5.3.1 *Autonomous Life-form Interfaces*

As I showed in Table 2, human-material interaction has an intrinsic and thus autonomous nature; the system does not necessarily require extrinsic instruction from the computer. Therefore, if we appropriately collect a series of functional materials that can act as a biological system (*e.g.,* muscles for actuation, nerves for communication, sensory perception for sensing, skins for a healable body, and so on),

It would be interesting if we can achieve the objects like life-form that can eat, talk, perceive, and move around at their discretion. If such life-form interfaces prevail around our environment, will they be just a noisy toy or can they be calm enough to be harmonized with humans and environments?

5.3.2 *Environment-material Interaction*

In this thesis, I defined human-material interaction as a relationship between humans versus materials. But as we saw in the application of Papilion (Section 3.6) and A LIVE UN LIVE (Section 3.7), the materials can also interact with environmental stimuli.

Perhaps for the future research projects related to human-material interaction or ubiquitous computing, it might be beneficial to assume interaction among three entities of humans, objects, and environments, rather than the binary relationship of humans and objects.

5.3.3 *Dependency of Materials and their Properties*

In human-material interaction, the physical properties of the materials act as the interfaces of human-computer interaction. But this also leads to the strong dependency between the interfaces and the object. This situation can be problematic when there is a mismatch between the functional material used for interaction and the material the designer actually hopes to use.

Also, even if there luckily exists some good material that meets both interaction and the designers' needs, it is currently almost impossible for the designers to find and synthesize it. For many people other than materials scientists more to explore HMI, we might need a kind of "material swatches for interaction," which is still an open question.

5.3.4 *Integration of Computing*

Although human-material interaction does not necessarily require computing components, it does not mean that computing *should not* be integrated into it. The long history of computer science developed

many practical benefits from the network theory, communication, machine learning for analysis, language, or vision, and data processing. So imparting computing capability to human-material interaction will also allow for other design freedom.

The easiest way to impart computing to material interfaces is just to embed small microcontrollers with wireless communication, but the problem is that such electrical devices are incompatible with novel materials. For example, microcontrollers and wiring do not self-heal. The difference in stiffness can also cause mechanical failure. Therefore, we need to use as small computing components as possible so far.

I am currently envisioning what if we mix the huge numbers of tiny (and almost invisible) computing modules as a composite of the material interfaces and let them locally communicate and sense, and looking for the way to achieve or prototype this vision in a realistic manner to go to the next step of "intellectual materials."

5.4   CONCLUDING REMARKS

When I started my undergraduate research, I did not expect I would approach my hands to soft robotics or even to materials science and write a doctoral thesis on the topic that are little to do with "pure" information science. But going into the bush and encountering the unknown every time I started a new project was always very exciting to me.

When we published Self-healing UI to UIST, the committee asked us to put the safety caution in the beginning and at the end of the video as well as the top right of the manuscript surrounded by a bold (specifically 2 mm wide) frame, which was (as long as I know) the very first and unusual thing for UIST. As I grew up, so the conference and committee have to change to cope with emerging technologies.

For the future, I hope to be a person to influence others by my idea, and also hope to remain a person easily influenced by such new technologies.

APPENDIX

A.1 MODELING TIME RESPONSE FOR ELECTRIC PHASE-CHANGE ACTUATORS

In this appendix section, I would like to detail the mathematical modeling of time response for electric phase-change actuators, because time-dependent analysis includes relatively complicated equations; those who are only interested in the result do not need to read this section.

According to Equation 7, known as Newton's law of cooling, the heat conduction $\frac{dQ}{dt}$ [W] is proportional to the difference of temperature between adjacent substances, $T_x - T_r$ [K], where h is a constant called heat transfer coefficient, which depends on the combination of two substances.

$$-\frac{dQ}{dt} = h(T_x - T_r) \tag{7}$$

We assume that the heat transfer occurs only among a heater, a pouch, and the air. Also, we regard following parameters as constant in this analysis: heat transfer coefficients $h = \alpha, \beta, \gamma$ between each two sections (shown in Figure 51), the generated heat at the heater q [W], the temperature of the air T_a [K], and the boiling point of liquid T_b [K].
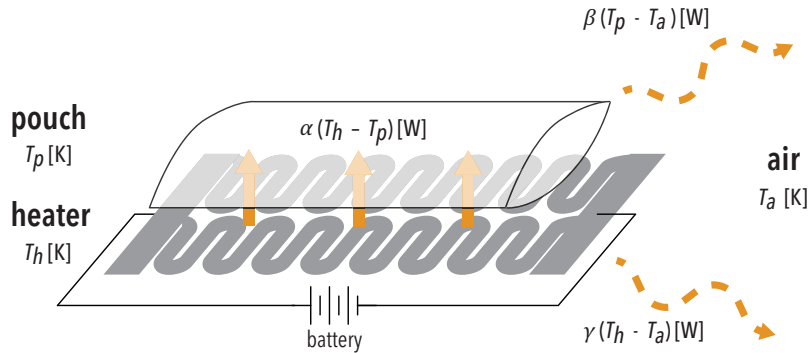
Figure 51: The heat conduction model of an electric phase-change actuator (Figure reused from [P3]).

Let the amount of extra thermal energy of a heater and a pouch be Q_h, Q_p [J] respectively. Also, let each temperature of a heater, a pouch, and the air, be T_h, T_p, T_a [K] respectively.

Then, these two equations are derived at the places of a heater and a pouch.

$$\frac{dQ_h}{dt} = q - \alpha(T_h - T_p) - \gamma(T_h - T_a) \tag{8}$$

$$\frac{dQ_p}{dt} = \alpha(T_h - T_p) - \beta(T_p - T_a) \tag{9}$$

Next, we evaluate T_h and T_p. As for the heater, T_h is proportional to Q_h. As for the pouch, however, T_p is not always proportional to Q_p, since evaporation heat of organic solvent Q_v is lost when liquid changes into gas. Thus, letting specific heat capacities of the heater and the pouch be C_h and C_p respectively, T_h and T_p can be expressed as

$$T_h \quad = \quad T_a + \frac{Q_h}{C_h} \tag{10}$$

$$T_p \quad = \quad \begin{cases} T_a + \frac{Q_p}{C_p} & (Q_p < a) & \text{(i)} \\ T_b & (a < Q_p < b) & \text{(ii)} \\ T_a + \frac{Q_p - Q_v}{C_p} & (b < Q_p) & \text{(iii)} \end{cases}$$

$$a \quad = \quad C_p(T_b - T_a)$$

$$b \quad = \quad C_p(T_b - T_a) + Q_v \tag{11}$$

We note that Equation 11 corresponds to three states of (i) before, (ii) during, and (iii) after evaporation. Therefore, we obtain the differential equation of each state from Equation 8, 9, 10, 11).

(i) Before evaporation starts, or (iii) after evaporation completes, T_h and T_p change as follows.

$$\frac{dT_h}{dt} \quad = \quad \frac{1}{C_h}\frac{dQ_h}{dt} = \frac{1}{C_h}\{q - \alpha(T_h - T_p) - \gamma(T_h - T_a)\} \tag{12}$$

$$\frac{dT_p}{dt} \quad = \quad \frac{1}{C_p}\frac{dQ_p}{dt} = \frac{1}{C_p}\{\alpha(T_h - T_p) - \beta(T_p - T_a)\} \tag{13}$$

Equation 12 and Equation 13 can numerically be solved, once the parameters (q, C_h, C_p, α, β, γ) are given by experimental results,

(ii) During evaporation, on the other hand, T_p stays constant at T_b. Thus the time response of temperature at the heater T_h can analytically be calculated as follows, where k is a constant decided by the boundary condition of T_h. If k is negative, T_h becomes monotonically decreasing function, so evaporation never occurs.

$$\frac{dT_h}{dt} \quad = \quad -\frac{\alpha + \gamma}{C_h}T_h + \frac{q + \alpha T_b + \gamma T_a}{C_h}$$

$$T_h(t) \quad = \quad -ke^{-\frac{\alpha+\gamma}{C_h}t} + \frac{q + \alpha T_b + \gamma T_a}{\alpha + \gamma} \tag{14}$$

$$k \quad = \quad \frac{q - \gamma(T_b - T_a)}{\alpha + \gamma}$$

From Equation 14, we can also calculate the value of Q_p during evaporation. From Equation 9 and Equation 14, the temporal change of Q_p can be expressed as follows, where a_1 and a_2 are constants which can be determined by Equation 15.

$$\frac{dQ_p}{dt} = \alpha T_h(t) - (\alpha + \beta)T_b + \beta T_a \tag{15}$$

$$= -c_1 e^{-\frac{\alpha+\gamma}{C_h}t} + c_2 \tag{16}$$

$$c_1 = k\alpha$$

$$c_2 = \frac{\alpha}{\alpha+\gamma}q - \frac{\alpha\beta + \beta\gamma + \gamma\alpha}{\alpha+\gamma}(T_b - T_a)$$

Equation 16 indicates that if $a_2 < 0$, namely if $q < \frac{\alpha\beta+\beta\gamma+\gamma\alpha}{\alpha}(T_b - T_a)$, the change in Q_p becomes negative and actuation never occurs.

Next, we induce the time response of the amount of evaporating solvent and the moment below. Equation 16 is reduced to be Equation 17, in which the value of Q_p at the time when the solvent starts to evaporate, Q_{ini}, is introduced.

$$Q_p(t) = c_2 t + \frac{c_1 C_h}{\alpha+\gamma}e^{-\frac{\alpha+\gamma}{C_h}t} - \frac{c_1 C_h}{\alpha+\gamma} + Q_{ini} \tag{17}$$

Letting all the amount of substance of the solvent be N [mol], we can obtain the amount of substance of evaporating solvent $n(t)$ [mol], since it is proportional to the Q_p during evaporation.

$$n(t) = \frac{Q_p(t) - Q_{ini}}{Q_v}N \tag{18}$$

$$= \frac{N}{Q_v}\left(a_2 t + \frac{c_1 C_h}{\alpha+\gamma}e^{-\frac{\alpha+\gamma}{C_h}t} - \frac{c_1 C_h}{\alpha+\gamma}\right) \tag{19}$$

Substituting $n(t)$ in Equation 19 and $T_p = T_b$ in Equation 11 into n in Equation 4, we can obtain time response of the moment (ii) during evaporation.

$$M(\theta, t) = RT_b n(t)\frac{\cos\theta(\sin\theta - \theta\cos\theta)}{\theta(\theta - \cos\theta\sin\theta)} \tag{20}$$

$$= \frac{NRT_b}{Q_v}F(\theta)G(t) \tag{21}$$

where

$$F(\theta) = \frac{\cos\theta(\sin\theta - \theta\cos\theta)}{\theta(\theta - \cos\theta\sin\theta)}$$

$$G(t) = c_2 t + \frac{c_1 C_h}{\alpha+\gamma}e^{-\frac{\alpha+\gamma}{C_h}t} - \frac{c_1 C_h}{\alpha+\gamma}$$

A.2 DETAILED PREPARATION PROCESS OF SWCNTS AEROGEL

REFERENCE

[1] E Acome, SK Mitchell, TG Morrissey, MB Emmett, C Benjamin, M King, M Radakovitz, and C Keplinger. "Hydraulically amplified self-healing electrostatic actuators with muscle-like performance." In: *Science* 359.6371 (2018), pp. 61–65.

[2] Tetsuya Akagi, Shujiro Dohta, Shinsaku Fujimoto, Yasuyuki Tsuji, and Yuto Fujiwara. "Development of flexible thin actuator driven by low boiling point liquid." In: *Int. J. Mater. Sci. Eng* 3.1 (2015), pp. 55–58.

[3] Jason Alexander, Anne Roudaut, Jürgen Steimle, Kasper Hornbæk, Miguel Bruns Alonso, Sean Follmer, and Timothy Merritt. "Grand Challenges in Shape-Changing Interface Research." In: *Proceedings of the 2018 CHI Conference on Human Factors in Computing Systems*. CHI '18. Montreal QC, Canada: ACM, 2018, 299:1–299:14. ISBN: 978-1-4503-5620-6. DOI: 10.1145/3173574.3173873. URL: http://doi.acm.org/10.1145/3173574.3173873.

[4] Byoungkwon An et al. "Thermorph: Democratizing 4D Printing of Self-Folding Materials and Interfaces." In: *Proceedings of the 2018 CHI Conference on Human Factors in Computing Systems*. CHI '18. Montreal QC, Canada: Association for Computing Machinery, 2018. ISBN: 9781450356206. DOI: 10.1145/3173574.3173834. URL: https://doi.org/10.1145/3173574.3173834.

[5] G. Bartalena, Y. Loosli, T. Zambelli, and J. G. Snedeker. "Biomaterial surface modifications can dominate cell-substrate mechanics: the impact of PDMS plasma treatment on a quantitative assay of cell stiffness." In: *Soft Matter* 8 (3 2012), pp. 673–681. DOI: 10.1039/C1SM06250F. URL: http://dx.doi.org/10.1039/C1SM06250F.

[6] Alberto Boem and Giovanni Maria Troiano. "Non-Rigid HCI: A Review of Deformable Interfaces and Input." In: *Proceedings of the 2019 on Designing Interactive Systems Conference*. DIS '19. San Diego, CA, USA: ACM, 2019, pp. 885–906. ISBN: 978-1-4503-5850-7. DOI: 10.1145/3322276.3322347. URL: http://doi.acm.org/10.1145/3322276.3322347.

[7] Conor S. Boland et al. "Sensitive electromechanical sensors using viscoelastic graphene-polymer nanocomposites." In: *Science* 354.6317 (2016), pp. 1257–1260. ISSN: 0036-8075. DOI: 10.1126/science.aag2879. eprint: https://science.sciencemag.org/content/354/6317/1257.full.pdf. URL: https://science.sciencemag.org/content/354/6317/1257.

[8] Leonardo Amerigo Bonanni, Hiroshi Ishii, Austin Lee, Paula Aguilera, and Williams Jonathan. *Perfect Red*. https://tangible.media.mit.edu/project/perfect-red/. Accessed: July 1, 2019. 2012.

[9] Eric Brown, Nicholas Rodenberg, John Amend, Annan Mozeika, Erik Steltz, Mitchell R Zakin, Hod Lipson, and Heinrich M Jaeger. "Universal robotic gripper based on the jamming of granular material." In: *Proceedings of the National Academy of Sciences* 107.44 (2010), pp. 18809–18814.

[10] Stefano Burattini, Barnaby W. Greenland, Daniel Hermida Merino, Wengui Weng, Jonathan Seppala, Howard M. Colquhoun, Wayne Hayes, Michael E. Mackay, Ian W. Hamley, and Stuart J. Rowan. "A Healable Supramolecular Polymer Blend Based on Aromatic π-π Stacking and Hydrogen-Bonding Interactions." In: *Journal of the American Chemical Society* 132.34 (2010), pp. 12051–12058. DOI: 10.1021/ja104446r. eprint: https://doi.org/10.1021/ja104446r. URL: https://doi.org/10.1021/ja104446r.

[11] Mark Burnworth, Liming Tang, Justin R Kumpfer, Andrew J Duncan, Frederick L Beyer, Gina L Fiore, Stuart J Rowan, and Christoph Weder. "Optically healable supramolecular polymers." In: *Nature* 472.7343 (2011), p. 334. DOI: 10.1038/nature09963.

[12] Jorge G Cham, Sean A Bailey, Jonathan E Clark, Robert J Full, and Mark R Cutkosky. "Fast and robust: Hexapedal robots via shape deposition manufacturing." In: *The International Journal of Robotics Research* 21.10-11 (2002), pp. 869–882.

[13] Zekun Chang et al. "Kirigami Haptic Swatches: Design Methods for Cut-and-Fold Haptic Feedback Mechanisms." In: *Proceedings of the 2020 CHI Conference on Human Factors in Computing Systems*. CHI '20. Honolulu, HI, US: Association for Computing Machinery, 2020. ISBN: 9781450367080. DOI: 10.1145/3313831.3376655. URL: http://dx.doi.org/10.1145/3313831.3376655.

[14] Ching-Ping Chou and Blake Hannaford. "Measurement and modeling of McKibben pneumatic artificial muscles." In: *IEEE Transactions on robotics and automation* 12.1 (1996), pp. 90–102.

[15] Marcelo Coelho and Jamie Zigelbaum. "Shape-changing Interfaces." In: *Personal Ubiquitous Comput.* 15.2 (Feb. 2011), pp. 161–173. ISSN: 1617-4909. DOI: 10.1007/s00779-010-0311-y. URL: http://dx.doi.org/10.1007/s00779-010-0311-y.

[16] Jonathan N. Coleman, Umar Khan, Werner J. Blau, and Yurii K. Gun'ko. "Small but strong: A review of the mechanical properties of carbon nanotube-polymer composites." In: *Carbon* 44.9 (2006), pp. 1624 –1652. ISSN: 0008-6223. DOI: 10.1016/j.carbon.2006.02.038. URL: http://www.sciencedirect.com/science/article/pii/S0008622306001229.

[17] Eleonora D'Elia, Suelen Barg, Na Ni, Victoria G. Rocha, and Eduardo Saiz. "Self-Healing Graphene-Based Composites with Sensing Capabilities." In: *Advanced Materials* 27.32 (2015), pp. 4788–4794. DOI: 10.1002/adma.201501653. eprint: https://onlinelibrary.wiley.com/doi/pdf/10.1002/adma.201501653. URL: https://onlinelibrary.wiley.com/doi/abs/10.1002/adma.201501653.

[18] Michael F. L. De Volder, Sameh H. Tawfick, Ray H. Baughman, and A. John Hart. "Carbon Nanotubes: Present and Future Commercial Applications." In: *Science* 339.6119 (2013), pp. 535–539. ISSN: 0036-8075. DOI: 10.1126/science.1222453. eprint: https://science.sciencemag.org/

content/339/6119/535.full.pdf. URL: https://science.sciencemag.org/content/339/6119/535.

[19]   S Felton, M Tolley, E Demaine, D Rus, and R Wood. "A method for building self-folding machines." In: *Science* 345.6197 (2014), pp. 644–646.

[20]   Sean Follmer, Daniel Leithinger, Alex Olwal, Akimitsu Hogge, and Hiroshi Ishii. "inFORM: dynamic physical affordances and constraints through shape and object actuation." In: *Proceedings of the 26th Annual Symposium on User Interface Software and Technology*. UIST '13. St. Andrews, United Kingdom: ACM, 2013, pp. 417–426. DOI: 10.1145/2501988.2502032.

[21]   Michael Goldfarb, Eric J Barth, Michael A Gogola, and Joseph A Wehrmeyer. "Design and energetic characterization of a liquid-propellant-powered actuator for self-powered robots." In: *IEEE/ASME transactions on mechatronics* 8.2 (2003), pp. 254–262.

[22]   Antonio Gomes, Andrea Nesbitt, and Roel Vertegaal. "MorePhone: A Study of Actuated Shape Deformations for Flexible Thin-film Smartphone Notifications." In: *Proceedings of the SIGCHI Conference on Human Factors in Computing Systems*. CHI '13. Paris, France: ACM, 2013, pp. 583–592. ISBN: 978-1-4503-1899-0. DOI: 10.1145/2470654.2470737. URL: http://doi.acm.org/10.1145/2470654.2470737.

[23]   Chris Harrison and Scott E. Hudson. "Providing Dynamically Changeable Physical Buttons on a Visual Display." In: *Proceedings of the SIGCHI Conference on Human Factors in Computing Systems*. CHI '09. Boston, MA, USA: ACM, 2009, pp. 299–308. ISBN: 978-1-60558-246-7. DOI: 10.1145/1518701.1518749. URL: http://doi.acm.org/10.1145/1518701.1518749.

[24]   Jeremy M. Heiner, Scott E. Hudson, and Kenichiro Tanaka. "The Information Percolator: Ambient Information Display in a Decorative Object." In: *Proceedings of the 12th Annual ACM Symposium on User Interface Software and Technology*. UIST '99. Asheville, North Carolina, USA: Association for Computing Machinery, 1999, 141–148. ISBN: 1581130759. DOI: 10.1145/320719.322595. URL: https://doi.org/10.1145/320719.322595.

[25]   Takayuki Hirai, Satoshi Nakamaru, Yoshihiro Kawahara, and Yasuaki Kakehi. "XSlate: A Stiffness-Controlled Surface for Shape-Changing Interfaces." In: *Extended Abstracts of the 2018 CHI Conference on Human Factors in Computing Systems*. CHI EA '18. Montreal QC, Canada: Association for Computing Machinery, 2018. ISBN: 9781450356213. DOI: 10.1145/3170427.3186496. URL: https://doi.org/10.1145/3170427.3186496.

[26]   Alexandra Ion, Johannes Frohnhofen, Ludwig Wall, Robert Kovacs, Mirela Alistar, Jack Lindsay, Pedro Lopes, Hsiang-Ting Chen, and Patrick Baudisch. "Metamaterial Mechanisms." In: *Proceedings of the 29th Annual Symposium on User Interface Software and Technology*. UIST '16. Tokyo, Japan: Association for Computing Machinery, 2016, 529–539. ISBN: 9781450341899. DOI: 10.1145/2984511.2984540. URL: https://doi.org/10.1145/2984511.2984540.

[27] Hiroshi Ishii, Dávid Lakatos, Leonardo Bonanni, and Jean-Baptiste Labrune. "Radical Atoms: Beyond Tangible Bits, Toward Transformable Materials." In: *interactions* 19.1 (Jan. 2012), pp. 38–51. ISSN: 1072-5520. DOI: 10.1145/2065327.2065337. URL: http://doi.acm.org/10.1145/2065327.2065337.

[28] Henk M. Jonkers. "Self Healing Concrete: A Biological Approach." In: *Self Healing Materials: An Alternative Approach to 20 Centuries of Materials Science*. Ed. by Sybrand van der Zwaag. Dordrecht: Springer Netherlands, 2007, pp. 195–204. ISBN: 978-1-4020-6250-6. DOI: 10.1007/978-1-4020-6250-6_9. URL: https://doi.org/10.1007/978-1-4020-6250-6_9.

[29] Viirj Kan, Emma Vargo, Noa Machover, Hiroshi Ishii, Serena Pan, Weixuan Chen, and Yasuaki Kakehi. "Organic Primitives: Synthesis and Design of PH-Reactive Materials Using Molecular I/O for Sensing, Actuation, and Interaction." In: *Proceedings of the 2017 CHI Conference on Human Factors in Computing Systems*. CHI '17. Denver, Colorado, USA: Association for Computing Machinery, 2017, 989–1000. ISBN: 9781450346559. DOI: 10.1145/3025453.3025952. URL: https://doi.org/10.1145/3025453.3025952.

[30] Hsin-Liu (Cindy) Kao, Christian Holz, Asta Roseway, Andres Calvo, and Chris Schmandt. "DuoSkin: Rapidly Prototyping On-skin User Interfaces Using Skin-friendly Materials." In: *Proceedings of the 2016 ACM International Symposium on Wearable Computers*. ISWC '16. Heidelberg, Germany: ACM, 2016, pp. 16–23. ISBN: 978-1-4503-4460-9. DOI: 10.1145/2971763.2971777. URL: http://doi.acm.org/10.1145/2971763.2971777.

[31] Yoshihiro Kawahara, Steve Hodges, Benjamin S Cook, Cheng Zhang, and Gregory D Abowd. "Instant inkjet circuits: lab-based inkjet printing to support rapid prototyping of UbiComp devices." In: *Proceedings of the 2013 ACM international joint conference on Pervasive and ubiquitous computing*. ACM. 2013, pp. 363–372.

[32] Yoshihiro Kawahara, Steve Hodges, Nan-Wei Gong, Simon Olberding, and Jürgen Steimle. "Building functional prototypes using conductive inkjet printing." In: *IEEE Pervasive Computing* 13.3 (2014), pp. 30–38.

[33] Nicholas Kellaris, Vidyacharan Gopaluni Venkata, Garrett M Smith, Shane K Mitchell, and Christoph Keplinger. "Peano-HASEL actuators: Muscle-mimetic, electrohydraulic transducers that linearly contract on activation." In: *Science Robotics* 3.14 (2018), eaar3276.

[34] Michael. Keller, Scott White, and Nancy Sottos. "A Self-Healing Poly(Dimethyl Siloxane) Elastomer." In: *Advanced Functional Materials* 17.14 (2007), pp. 2399–2404. DOI: 10.1002/adfm.200700086. eprint: https://onlinelibrary.wiley.com/doi/pdf/10.1002/adfm.200700086. URL: https://onlinelibrary.wiley.com/doi/abs/10.1002/adfm.200700086.

[35] Kwang J Kim and Satoshi Tadokoro. "Electroactive polymers for robotic applications." In: *Artificial Muscles and Sensors (291 p.), Springer: London, United Kingdom* (2007).

[36] GW Lai, SJ Chang, JT Lee, H Liu, and CC Li. "Conductive microcapsules for self-healing electric circuits." In: *RSC Advances* 5.126 (2015), pp. 104145–104148. DOI: 10.1039/C5RA22021A.

[37] Mathieu Le Goc, Lawrence H. Kim, Ali Parsaei, Jean-Daniel Fekete, Pierre Dragicevic, and Sean Follmer. "Zooids: Building Blocks for Swarm User Interfaces." In: *Proceedings of the 29th Annual Symposium on User Interface Software and Technology*. UIST '16. Tokyo, Japan: ACM, 2016, pp. 97–109. ISBN: 978-1-4503-4189-9. DOI: 10.1145/2984511.2984547. URL: http://doi.acm.org/10.1145/2984511.2984547.

[38] David M. Lehmann, Megan E. Cavet, and Mary E. Richardson. "Nonclinical safety evaluation of boric acid and a novel borate-buffered contact lens multi-purpose solution, Biotrue™ multi-purpose solution." In: *Contact Lens and Anterior Eye* 33 (2010), S24 –S32. ISSN: 1367-0484. DOI: 10.1016/j.clae.2010.06.010. URL: http://www.sciencedirect.com/science/article/pii/S136704841000127X.

[39] Daniel Leithinger, Sean Follmer, Alex Olwal, Samuel Luescher, Akimitsu Hogge, Jinha Lee, and Hiroshi Ishii. "Sublimate: State-Changing Virtual and Physical Rendering to Augment Interaction with Shape Displays." In: *Proceedings of the SIGCHI Conference on Human Factors in Computing Systems*. CHI '13. Paris, France: Association for Computing Machinery, 2013, 1441–1450. ISBN: 9781450318990. DOI: 10.1145/2470654.2466191. URL: https://doi.org/10.1145/2470654.2466191.

[40] Cheng-Hui Li, Chao Wang, Christoph Keplinger, Jing-Lin Zuo, Lihua Jin, Yang Sun, Peng Zheng, Yi Cao, Franziska Lissel, Christian Linder, et al. "A highly stretchable autonomous self-healing elastomer." In: *Nature chemistry* 8.6 (2016), p. 618. DOI: 10.1038/nchem.2492.

[41] Xufeng Li, Dian Zhang, Kewei Xiang, and Guangsu Huang. "Synthesis of polyborosiloxane and its reversible physical crosslinks." In: *Rsc Advances* 4.62 (2014), pp. 32894–32901. DOI: 10.1039/C4RA01877J.

[42] David Lindlbauer, Joerg Mueller, and Marc Alexa. "Changing the Appearance of Physical Interfaces Through Controlled Transparency." In: *Proceedings of the 29th Annual Symposium on User Interface Software and Technology*. UIST '16. Tokyo, Japan: Association for Computing Machinery, 2016, 425–435. ISBN: 9781450341899. DOI: 10.1145/2984511.2984556. URL: https://doi.org/10.1145/2984511.2984556.

[43] Yanju Liu, Haibao Lv, Xin Lan, Jinsong Leng, and Shanyi Du. "Review of electro-active shape-memory polymer composite." In: *Composites Science and Technology* 69.13 (2009), pp. 2064–2068.

[44] Zhen Liu, Stephen J. Picken, and Nicolaas A. M. Besseling. "Polyborosiloxanes (PBSs), Synthetic Kinetics, and Characterization." In: *Macromolecules* 47.14 (2014), pp. 4531–4537. DOI: 10.1021/ma500632f. eprint: https://doi.org/10.1021/ma500632f. URL: https://doi.org/10.1021/ma500632f.

[45] Qiuyu Lu, Chengpeng Mao, Liyuan Wang, and Haipeng Mi. "LIME: LIquid MEtal Interfaces for Non-Rigid Interaction." In: *Proceedings of the 29th Annual Symposium on User Interface Software and Technology*. UIST '16. Tokyo, Japan: ACM, 2016, pp. 449–452. ISBN: 978-1-4503-4189-9. DOI: 10.1145/2984511.2984562. URL: http://doi.acm.org/10.1145/2984511.2984562.

[46] Qiuyu Lu, Jifei Ou, João Wilbert, André Haben, Haipeng Mi, and Hiroshi Ishii. "milliMorph – Fluid-Driven Thin Film Shape-Change Materials for Interaction Design." In: *Proceedings of the 32Nd Annual ACM Symposium on User Interface Software and Technology*. UIST '19. New Orleans, LA, USA: ACM, 2019, pp. 663–672. ISBN: 978-1-4503-6816-2. DOI: 10.1145/3332165.3347956. URL: http://doi.acm.org/10.1145/3332165.3347956.

[47] Robert MacCurdy, Robert Katzschmann, Youbin Kim, and Daniela Rus. "Printable Hydraulics: A Method for Fabricating Robots by 3D Co-Printing Solids and Liquids." In: *arXiv preprint arXiv:1512.03744* (2015).

[48] Andrew D Marchese, Robert K Katzschmann, and Daniela Rus. "A recipe for soft fluidic elastomer robots." In: *Soft Robotics* 2.1 (2015), pp. 7–25.

[49] James E Mark. *Polymer data handbook*. Oxford university press, 2009.

[50] Eric J Markvicka, Michael D Bartlett, Xiaonan Huang, and Carmel Majidi. "An autonomously electrically self-healing liquid metal–elastomer composite for robust soft-matter robotics and electronics." In: *Nature materials* 17.7 (2018), p. 618. DOI: 10.1038/s41563-018-0084-7.

[51] Alvaro Mata, Aaron J. Fleischman, and Shuvo Roy. "Characterization of Polydimethylsiloxane (PDMS) Properties for Biomedical Micro/Nanosystems." In: *Biomedical Microdevices* 7.4 (2005), pp. 281–293. ISSN: 1572-8781. DOI: 10.1007/s10544-005-6070-2. URL: https://doi.org/10.1007/s10544-005-6070-2.

[52] Hiroki Matsuoka, Koichi Suzumori, and Takefumi Kanda. "Development of a gas/liquid phase change actuator for high temperatures." In: *ROBOMECH Journal* 3.1 (2016), p. 1.

[53] Viktor Miruchna, Robert Walter, David Lindlbauer, Maren Lehmann, Regine von Klitzing, and Jorg Muller. "GelTouch: Localized Tactile Feedback Through Thin, Programmable Gel." In: *Proceedings of the 28th Annual ACM Symposium on User Interface Software and Technology*. UIST '15. Charlotte, NC, USA: Association for Computing Machinery, 2015, 3–10. ISBN: 9781450337793. DOI: 10.1145/2807442.2807487. URL: https://doi.org/10.1145/2807442.2807487.

[54] Ken Nakagaki, Sean Follmer, and Hiroshi Ishii. "LineFORM: Actuated Curve Interfaces for Display, Interaction, and Constraint." In: *Proceedings of the 28th Annual ACM Symposium on User Interface Software & Technology*. UIST '15. Charlotte, NC, USA: ACM, 2015, pp. 333–339. ISBN: 978-1-4503-3779-3. DOI: 10.1145/2807442.2807452. URL: http://doi.acm.org/10.1145/2807442.2807452.

[55] Ken Nakagaki, Artem Dementyev, Sean Follmer, Joseph A. Paradiso, and Hiroshi Ishii. "Chain-FORM: A Linear Integrated Modular Hardware System for Shape Changing Interfaces." In: *Proceedings of the 29th Annual Symposium on User Interface Software and Technology*. UIST '16. Tokyo, Japan: ACM, 2016, pp. 87–96. ISBN: 978-1-4503-4189-9. DOI: 10.1145/2984511.2984587. URL: http://doi.acm.org/10.1145/2984511.2984587.

[56] Ken Nakagaki, Luke Vink, Jared Counts, Daniel Windham, Daniel Leithinger, Sean Follmer, and Hiroshi Ishii. "Materiable: Rendering Dynamic Material Properties in Response to Direct Physical Touch with Shape Changing Interfaces." In: *Proceedings of the 2016 CHI Conference on Human Factors in Computing Systems*. CHI '16. San Jose, California, USA: ACM, 2016, pp. 2764–2772. ISBN: 978-1-4503-3362-7. DOI: 10.1145/2858036.2858104. URL: http://doi.acm.org/10.1145/2858036.2858104.

[57] Masaki Nakahata, Yoshinori Takashima, Hiroyasu Yamaguchi, and Akira Harada. "Redox-responsive self-healing materials formed from host–guest polymers." In: *Nature communications* 2 (2011), p. 511. DOI: 10.1038/ncomms1521.

[58] Ryuma Niiyama, Daniela Rus, and Sangbae Kim. "Pouch motors: Printable/inflatable soft actuators for robotics." In: *Robotics and Automation (ICRA), 2014 IEEE International Conference on*. IEEE. 2014, pp. 6332–6337.

[59] Ryuma Niiyama, Xu Sun, Cynthia Sung, Byoungkwon An, Daniela Rus, and Sangbae Kim. "Pouch motors: Printable soft actuators integrated with computational design." In: *Soft Robotics* 2.2 (2015), pp. 59–70.

[60] Aditya Shekhar Nittala, Anusha Withana, Narjes Pourjafarian, and Jürgen Steimle. "Multi-Touch Skin: A Thin and Flexible Multi-Touch Sensor for On-Skin Input." In: *Proceedings of the 2018 CHI Conference on Human Factors in Computing Systems*. CHI '18. Montreal QC, Canada: ACM, 2018, 33:1–33:12. ISBN: 978-1-4503-5620-6. DOI: 10.1145/3173574.3173607. URL: http://doi.acm.org/10.1145/3173574.3173607.

[61] Youngseok Oh and Mohammad F. Islam. "Preformed Nanoporous Carbon Nanotube Scaffold-Based Multifunctional Polymer Composites." In: *ACS Nano* 9.4 (2015), pp. 4103–4110. DOI: 10.1021/acsnano.5b00170. eprint: https://doi.org/10.1021/acsnano.5b00170. URL: https://doi.org/10.1021/acsnano.5b00170.

[62] Simon Olberding, Michael Wessely, and Jürgen Steimle. "PrintScreen: Fabricating Highly Customizable Thin-film Touch-displays." In: *Proceedings of the 27th Annual ACM Symposium on User Interface Software and Technology*. UIST '14. Honolulu, Hawaii, USA: ACM, 2014, pp. 281–290. ISBN: 978-1-4503-3069-5. DOI: 10.1145/2642918.2647413. URL: http://doi.acm.org/10.1145/2642918.2647413.

[63] Cagdas D Onal, Xin Chen, George M Whitesides, and Daniela Rus. "Soft mobile robots with on-board chemical pressure generation." In: *International Symposium on Robotics Research*. 2011, pp. 1–16.

[64] Jifei Ou, Mélina Skouras, Nikolaos Vlavianos, Felix Heibeck, Chin-Yi Cheng, Jannik Peters, and Hiroshi Ishii. "aeroMorph-Heat-sealing Inflatable Shape-change Materials for Interaction Design." In: *Proceedings of the 29th Annual Symposium on User Interface Software and Technology*. ACM. 2016, pp. 121–132.

[65] Allen Pan. *Conductak*. https://www.kickstarter.com/projects/1474433053/conductak-stick-circuits-anywhere. Accessed: July 1, 2019. 2014.

[66] Jürgen Pauluhn. "Multi-walled carbon nanotubes (Baytubes®): Approach for derivation of occupational exposure limit." In: *Regulatory Toxicology and Pharmacology* 57.1 (2010), pp. 78 –89. ISSN: 0273-2300. DOI: 10.1016/j.yrtph.2009.12.012. URL: http://www.sciencedirect.com/science/article/pii/S0273230010000048.

[67] Ameya Phadke, Chao Zhang, Bedri Arman, Cheng-Chih Hsu, Raghunath A. Mashelkar, Ashish K. Lele, Michael J. Tauber, Gaurav Arya, and Shyni Varghese. "Rapid self-healing hydrogels." In: *Proceedings of the National Academy of Sciences* 109.12 (2012), pp. 4383–4388. ISSN: 0027-8424. DOI: 10.1073/pnas.1201122109. eprint: https://www.pnas.org/content/109/12/4383.full.pdf. URL: https://www.pnas.org/content/109/12/4383.

[68] Isabel P. S. Qamar, Rainer Groh, David Holman, and Anne Roudaut. "HCI Meets Material Science: A Literature Review of Morphing Materials for the Design of Shape-Changing Interfaces." In: *Proceedings of the 2018 CHI Conference on Human Factors in Computing Systems*. CHI '18. Montreal QC, Canada: ACM, 2018, 374:1–374:23. ISBN: 978-1-4503-5620-6. DOI: 10.1145/3173574.3173948. URL: http://doi.acm.org/10.1145/3173574.3173948.

[69] Majken K. Rasmussen, Esben W. Pedersen, Marianne G. Petersen, and Kasper Hornbæk. "Shape-changing Interfaces: A Review of the Design Space and Open Research Questions." In: *Proceedings of the SIGCHI Conference on Human Factors in Computing Systems*. CHI '12. Austin, Texas, USA: ACM, 2012, pp. 735–744. ISBN: 978-1-4503-1015-4. DOI: 10.1145/2207676.2207781. URL: http://doi.acm.org/10.1145/2207676.2207781.

[70] Jun Rekimoto. "Squama: Modular Visibility Control of Walls and Windows for Programmable Physical Architectures." In: *Proceedings of the International Working Conference on Advanced Visual Interfaces*. AVI '12. Capri Island, Italy: Association for Computing Machinery, 2012, 168–171. ISBN: 9781450312875. DOI: 10.1145/2254556.2254587. URL: https://doi.org/10.1145/2254556.2254587.

[71] Deepak Ranjan Sahoo, Timothy Neate, Yutaka Tokuda, Jennifer Pearson, Simon Robinson, Sriram Subramanian, and Matt Jones. "Tangible Drops: A Visio-Tactile Display Using Actuated Liquid-Metal Droplets." In: *Proceedings of the 2018 CHI Conference on Human Factors in Computing Systems*.

CHI '18. Montreal QC, Canada: ACM, 2018, 177:1–177:14. ISBN: 978-1-4503-5620-6. DOI: 10.1145/3173574.3173751. URL: http://doi.acm.org/10.1145/3173574.3173751.

[72] Liyang Shi, Pinghui Ding, Yuzhi Wang, Yu Zhang, Dmitri Ossipov, and Jöns Hilborn. "Self-Healing Polymeric Hydrogel Formed by Metal-Ligand Coordination Assembly: Design, Fabrication, and Biomedical Applications." In: *Macromolecular Rapid Communications* 40.7 (2019), p. 1800837. DOI: 10.1002/marc.201800837. eprint: https://onlinelibrary.wiley.com/doi/pdf/10.1002/marc.201800837. URL: https://onlinelibrary.wiley.com/doi/abs/10.1002/marc.201800837.

[73] Hiroki Shigemune, Shingo Maeda, Yusuke Hara, Uori Koike, and Shuji Hashimoto. "Kirigami robot: Making paper robot using desktop cutting plotter and inkjet printer." In: *Intelligent Robots and Systems (IROS), 2015 IEEE/RSJ International Conference on*. IEEE. 2015, pp. 1091–1096.

[74] Xu Sun, Samuel M Felton, Ryuma Niiyama, Robert J Wood, and Sangbae Kim. "Self-folding and self-actuating robots: a pneumatic approach." In: *2015 IEEE International Conference on Robotics and Automation (ICRA)*. IEEE. 2015, pp. 3160–3165.

[75] Ryo Suzuki, Junichi Yamaoka, Daniel Leithinger, Tom Yeh, Mark D. Gross, Yoshihiro Kawahara, and Yasuaki Kakehi. "Dynablock: Dynamic 3D Printing for Instant and Reconstructable Shape Formation." In: *Proceedings of the 31st Annual ACM Symposium on User Interface Software and Technology*. UIST '18. Berlin, Germany: ACM, 2018, pp. 99–111. ISBN: 978-1-4503-5948-1. DOI: 10.1145/3242587.3242659. URL: http://doi.acm.org/10.1145/3242587.3242659.

[76] Zhenghai Tang, Yingjun Liu, Qingyi Huang, Jinshan Zhao, Baochun Guo, and Liqun Zhang. "A real recycling loop of sulfur-cured rubber through transalkylation exchange of C–S bonds." In: *Green Chemistry* 20.24 (2018), pp. 5454–5458. DOI: 10.1039/C8GC02932F.

[77] Ye Tao, Youngwook Do, Humphrey Yang, Yi-Chin Lee, Guanyun Wang, Catherine Mondoa, Jianxun Cui, Wen Wang, and Lining Yao. "Morphlour: Personalized Flour-Based Morphing Food Induced by Dehydration or Hydration Method." In: *Proceedings of the 32nd Annual ACM Symposium on User Interface Software and Technology*. UIST '19. New Orleans, LA, USA: Association for Computing Machinery, 2019, 329–340. ISBN: 9781450368162. DOI: 10.1145/3332165.3347949. URL: https://doi.org/10.1145/3332165.3347949.

[78] Seppe Terryn, Joost Brancart, Dirk Lefeber, Guy Van Assche, and Bram Vanderborght. "Self-healing soft pneumatic robots." In: *Science Robotics* 2.9 (2017), eaan4268. DOI: 10.1126/scirobotics.aan4268.

[79] Yasuyuki Tsuji, Shujiro Dohta, Tetsuya Akagi, and Yuto Fujiwara. "Analysis of Flexible Thin Actuator Using Gas–Liquid Phase-Change of Low Boiling Point Liquid." In: *Proceedings of the 3rd International Conference on Intelligent Technologies and Engineering Systems (ICITES2014)*. Springer. 2016, pp. 67–73.

[80] Udayan Umapathi, Patrick Shin, Ken Nakagaki, Daniel Leithinger, and Hiroshi Ishii. "Programmable Droplets for Interaction." In: *Extended Abstracts of the 2018 CHI Conference on Human Factors in Computing Systems*. CHI EA '18. Montreal QC, Canada: ACM, 2018, VS15:1–VS15:1. ISBN: 978-1-4503-5621-3. DOI: 10.1145/3170427.3186607. URL: http://doi.acm.org/10.1145/3170427.3186607.

[81] Akira Wada, Hiroyuki Nabae, Takaaki Kitamori, and Koichi Suzumori. "Energy regenerative hose-free pneumatic actuator." In: *Sensors and Actuators A: Physical* 249 (2016), pp. 1–7.

[82] Akira Wakita, Akito Nakano, and Nobuhiro Kobayashi. "Programmable Blobs: A Rheologic Interface for Organic Shape Design." In: *Proceedings of the Fifth International Conference on Tangible, Embedded, and Embodied Interaction*. TEI '11. Funchal, Portugal: ACM, 2011, pp. 273–276. ISBN: 978-1-4503-0478-8. DOI: 10.1145/1935701.1935760. URL: http://doi.acm.org/10.1145/1935701.1935760.

[83] Guanyun Wang, Tingyu Cheng, Youngwook Do, Humphrey Yang, Ye Tao, Jianzhe Gu, Byoungkwon An, and Lining Yao. "Printed Paper Actuator: A Low-cost Reversible Actuation and Sensing Method for Shape Changing Interfaces." In: *Proceedings of the 2018 CHI Conference on Human Factors in Computing Systems*. ACM. 2018, p. 569.

[84] Yao Wang, Assaf Biderman, Ben Piper, Carlo Ratti, and Hiroshi Ishii. *SandScape*. https://tangible.media.mit.edu/project/sandscape/. Accessed: July 1, 2019. 2003.

[85] Michael Wehner, Ryan L Truby, Daniel J Fitzgerald, Bobak Mosadegh, George M Whitesides, Jennifer A Lewis, and Robert J Wood. "An integrated design and fabrication strategy for entirely soft, autonomous robots." In: *Nature* 536.7617 (2016), pp. 451–455.

[86] Martin Weigel, Tong Lu, Gilles Bailly, Antti Oulasvirta, Carmel Majidi, and Jürgen Steimle. "ISkin: Flexible, Stretchable and Visually Customizable On-Body Touch Sensors for Mobile Computing." In: *Proceedings of the 33rd Annual ACM Conference on Human Factors in Computing Systems*. CHI '15. Seoul, Republic of Korea: Association for Computing Machinery, 2015, 2991–3000. ISBN: 9781450331456. DOI: 10.1145/2702123.2702391. URL: https://doi.org/10.1145/2702123.2702391.

[87] Martin Weigel, Tong Lu, Gilles Bailly, Antti Oulasvirta, Carmel Majidi, and Jürgen Steimle. "iSkin: Flexible, Stretchable and Visually Customizable On-Body Touch Sensors for Mobile Computing." In: *Proceedings of the 33rd Annual ACM Conference on Human Factors in Computing Systems*. CHI '15. Seoul, Republic of Korea: ACM, 2015, pp. 2991–3000. ISBN: 978-1-4503-3145-6. DOI: 10.1145/2702123.2702391. URL: http://doi.acm.org/10.1145/2702123.2702391.

[88] Mark Weiser. "The computer for the 21st century." In: *ACM SIGMOBILE mobile computing and communications review* 3.3 (1999), pp. 3–11.

[89] Michael Wessely, Theophanis Tsandilas, and Wendy E. Mackay. "Stretchis: Fabricating Highly Stretchable User Interfaces." In: *Proceedings of the 29th Annual Symposium on User Interface Software and Technology*. UIST '16. Tokyo, Japan: ACM, 2016, pp. 697–704. ISBN: 978-1-4503-4189-9. DOI: 10.1145/2984511.2984521. URL: http://doi.acm.org/10.1145/2984511.2984521.

[90] Scott R. White, Nancy R. Sottos, Philippe H. Geubelle, Jeffrey S. Moore, Michael R. Kessler, S. R. Sriram, Eric N. Brown, and S. Viswanathan. "Autonomic healing of polymer composites." In: *Nature* 409.6822 (2001), p. 794. DOI: 10.1038/35057232.

[91] Anusha Withana, Daniel Groeger, and Jürgen Steimle. "Tacttoo: A Thin and Feel-Through Tattoo for On-Skin Tactile Output." In: *Proceedings of the 31st Annual ACM Symposium on User Interface Software and Technology*. UIST '18. Berlin, Germany: ACM, 2018, pp. 365–378. ISBN: 978-1-4503-5948-1. DOI: 10.1145/3242587.3242645. URL: http://doi.acm.org/10.1145/3242587.3242645.

[92] Tongfei Wu and Biqiong Chen. "Synthesis of Multiwalled Carbon Nanotube-Reinforced Polyborosiloxane Nanocomposites with Mechanically Adaptive and Self-Healing Capabilities for Flexible Conductors." In: *ACS Applied Materials & Interfaces* 8.36 (2016), pp. 24071–24078. DOI: 10.1021/acsami.6b06137. eprint: https://doi.org/10.1021/acsami.6b06137. URL: https://doi.org/10.1021/acsami.6b06137.

[93] Yu Yanagisawa, Yiling Nan, Kou Okuro, and Takuzo Aida. "Mechanically robust, readily repairable polymers via tailored noncovalent cross-linking." In: *Science* 359.6371 (2018), pp. 72–76. ISSN: 0036-8075. DOI: 10.1126/science.aam7588. eprint: https://science.sciencemag.org/content/359/6371/72.full.pdf. URL: https://science.sciencemag.org/content/359/6371/72.

[94] Lining Yao, Ryuma Niiyama, Jifei Ou, Sean Follmer, Clark Della Silva, and Hiroshi Ishii. "PneUI: pneumatically actuated soft composite materials for shape changing interfaces." In: *Proceedings of the 26th annual ACM symposium on User interface software and Technology*. ACM. 2013, pp. 13–22.

[95] Zhiwei Zhou, Qingwei Li, Luzhuo Chen, Changhong Liu, and Shoushan Fan. "A large-deformation phase transition electrothermal actuator based on carbon nanotube–elastomer composites." In: *Journal of Materials Chemistry B* 4.7 (2016), pp. 1228–1234.

PUBLICATION INCLUDED IN THIS THESIS

International Journal

[P1] Koya Narumi, Hiroki Sato, Kenichi Nakahara, Young ah Seong, Kunihiro Morinaga, Yasuaki Kakehi, Ryuma Niiyama, and Yoshihiro Kawahara, "Liquid Pouch Motors: Tube-less Planar Pneumatic Actuators Driven by Liquid-to-gas Phase Change." In: *IEEE Robotics and Automation Letters (RA-L)*, submitted on Oct. 16, 2019.

[P2] Takefumi Hiraki*, Kenichi Nakahara*, Koya Narumi*, Ryuma Niiyama, Noriaki Kida, Naoki Takamura, Hiroshi Okamoto, and Yoshihiro Kawahara, "Laser Pouch Motors: Selective and Wireless Activation of Soft Actuators by Laser-powered Liquid-to-gas Phase Change." In: *IEEE Robotics and Automation Letters (RA-L)*, submitted on Oct. 16, 2019 (* authors contributed equally).

International Conference

[P3] Kenichi Nakahara, Koya Narumi, Ryuma Niiyama, and Yoshihiro Kawahara, "Electric Phase-change Actuator with Inkjet Printed Flexible Circuit for Printable and Integrated Robot Prototyping." In: *2017 IEEE International Conference on Robotics and Automation (ICRA)*, pp.1856–1863, May 2017.

[P4] Koya Narumi*, Fang Qin*, Siyuan Liu, Huai-Yu Cheng, Jianzhe Gu, Yoshihiro Kawahara, Mohammad Islam, and Lining Yao, "Self-healing UI: Mechanically and Electrically Self-healing Materials for Sensing and Actuation Interfaces." In: *Proceedings of the 26th annual ACM symposium on User interface software and technology (UIST)*, pp.293–306, Oct. 2019 (* authors contributed equally).

International Demo / Poster

[P5] Koya Narumi*, Fang Qin*, Siyuan Liu, Huai-Yu Cheng, Jianzhe Gu, Yoshihiro Kawahara, Mohammad Islam, and Lining Yao, "Demonstration of Self-healing UI: Mechanically and Electrically Self-healing Materials for Sensing and Actuation Interfaces." In: *Proceedings of the 26th annual ACM symposium on User interface software and technology (UIST)*, Oct. 2019 (* authors contributed equally).

Domestic Workshop

[P6] 鳴海紘也, 中原健一, 佐藤宏樹, 新山龍馬, 川原圭博, "Liquid Pouch Motors: 紙のインタフェースのための薄く軽く柔軟なアクチュエータ." In: 第26回インタラクティブシステムとソフトウェアに関するワークショップ *(WISS)*, no.83, pp.1–6, Sept. 2018.

[P7] 鳴海紘也*, Fang Qin*, Siyuan Liu, Huai-Yu Cheng, Jianzhe Gu, 川原圭博，Mohammad Islam, Lining Yao, "Self-healing UI: 機械的かつ電気的に自己修復するセンシングインタフェース." In: 第27回インタラクティブシステムとソフトウェアに関するワークショップ *(WISS)*, pp.55–60, 2019 (* authors contributed equally).

Art Exhibition

[P8] Hiroki Sato, Kenichi Nakahara, Koya Narumi, Yasuaki Kakehi, Ryuma Niiyama, Yoshihiro Kawahara, "Papilion." In: *Ars Electronica*, Sept 2017.

[P9] アンリアレイジ, "A LIVE UN LIVE," In: 六本木クロッシング, 2019（技術協力）.

PUBLICATION EXCLUDED FROM THIS THESIS

Domestic & International Journal

[P10] 鳴海紘也, 中原健一, 川原圭博, "ConductAR: 導電性インク回路の試行錯誤的なデザインに向けたARツール." In: 情報処理学会論文誌, vol.58, no.10, pp.1628–1641, Oct. 2017.

[P11] Tingyu Cheng*, Koya Narumi*, Youngwook Do, Yang Zhang, Tung D. Ta, Takuya Sasatani, Eric Markvicka, Yoshihiro Kawahara, Lining Yao, Gregory D. Abowd, and Hyunjoo Oh, "Silver Tape: Inkjet Printed Circuits Peeled-and-Transferred on Versatile Substrates." In: *Proceedings of the ACM on Interactive, Mobile, Wearable and Ubiquitous Technologies (IMWUT)*, conditionally accepted, 2020 (* authors contributed equally).

International Conference

[P12] Koya Narumi, Steve Hodges, Yoshihiro Kawahara, "ConductAR: An Augmented Reality Based Tool for Iterative Design of Conductive Ink Circuits." In: *Proceedings of the 2015 ACM International Joint Conference on Pervasive and Ubiquitous Computing (UbiComp)*, pp.791–800, 2015.

[P13] Tung D. Ta, Masaaki Fukumoto, Koya Narumi, Shigeki Shino, Yoshihiro Kawahara, Tohru Asami, "Interconnection and Double Layer for Flexible Electronic Circuit with Instant Inkjet Circuits." In: *Proceedings of the 2015 ACM International Joint Conference on Pervasive and Ubiquitous Computing (UbiComp)*, pp.181–190, 2015.

[P14] Takahiro Hashizume Takuya Sasatani, Koya Narumi, Yoshiaki Narusue, Yoshihiro Kawahara, Tohru Asami, "Passive and Contactless Epidermal Pressure Sensor Printed with Silver Nano-particle Ink." In: *Proceedings of the 2016 ACM International Joint Conference on Pervasive and Ubiquitous Computing (UbiComp)*, pp.190–195, 2016.

[P15] Zekun Chang, Tung D. Ta, Koya Narumi, Heeju Kim, Fuminori Okuya, Dongchi Li, Kunihiro Kato, Jie Qi, Yoshinobu Miyamoto, Kazuya Saito, and Yoshihiro Kawahara, "Kirigami Haptic Swatches: Design Methods for Cut-and-Fold Haptic Feedback Mechanisms." In: *Proceedings of the 2020 CHI Conference on Human Factors in Computing Systems (CHI)*, To appear in Apr. 2020.

International Demo / Poster

[P16] Koya Narumi, Xinyang Shi, Steve Hodges, Yoshihiro Kawahara, Shinya Shimizu, Tohru Asami, "Circuit Eraser: A Tool for Iterative Design with Conductive Ink," In: *Proceedings of the 33rd Annual ACM Conference Extended Abstracts on Human Factors in Computing Systems (CHI)*, pp.2307–2312,

2015.

[P17] Tung D. Ta, Koya Narumi, Yoshihiro Kawahara, "Assistant Tools and Techniques for Conductive Inkjet Printing Technology." In: *Proceedings of the 2015 ACM International Joint Conference on Pervasive and Ubiquitous Computing (UbiComp)*, GadgetShow Plus Demo, Sept. 2015.

[P18] Takefumi Hiraki*, Koya Narumi*, Koji Yatani, Yoshihiro Kawahara, "Phones on Wheels: Exploring Interaction for Smartphones with Kinetic Capabilities." In: *Proceedings of the 29th Annual Symposium on User Interface Software and Technology (UIST)*, pp.121–122, 2016 (* authors contributed equally).

[P19] Zekun Chang*, Heeju Kim*, Kunihiro Kato, Kazuya Saito, Tung D. Ta, Weiwei Jiang, Koya Narumi, Yoshinobu Miyamoto, and Yoshihiro Kawahara, "Kirigami Keyboard: Inkjet Printable Paper Interface with Kirigami Structure Presenting Kinesthetic Feedback." In: *In Extended Abstracts of the 2019 CHI Conference on Human Factors in Computing Systems (CHI)*, p. LBW2113, 2019 (* authors contributed equally).

Domestic Conference

[P20] 鳴海紘也, 杉本雅明, 清水信哉, 川原圭博, 浅見徹, "銀ナノインクでの回路プロトタイピングにおける書き直し特性の計測." In: 電子情報通信学会ソサイエティ大会公演論文集, B-18-3, Sept. 2014.

[P21] 奥谷文徳, 鳴海紘也, 川原圭博, 浅見徹, "圧縮センシングを用いた心拍の計測手法における復元精度の評価." In: 電子情報通信学会ソサイエティ大会公演論文集, B-18-10, Sept. 2014.

[P22] 鳴海紘也, 川原圭博, 浅見徹, "手書き回路の解析が可能な CAD ソフトの実装に向けた導電性インクのシート抵抗の画像認識手法." In: 電子情報通信学会総合大会公演論文集, B-15-16, Mar. 2015.

[P23] 鳴海紘也, 小野寺宏, "In vivoでのマウス頭蓋骨透明化に向けた骨片透明化試験." In: 第77回応用物理学会秋季学術講演会, Sept. 2016.

[P24] 中原健一, 鳴海紘也, 川原圭博, 浅見徹, "銀ナノインク回路の過電流からの防護に向けた発熱量分布の可視化." In: 電子情報通信学会ソサイエティ大会公演論文集, B-18-5, Sept. 2016.

[P25] 中原健一, 鳴海紘也, 川原圭博, 浅見徹, "電気回路と一体で印刷可能なアクチュエータによる動的インターフェイス及びロボットの試作," In: 情報処理学会第79回全国大会, Mar. 2017.

[P26] 鳴海紘也, 岸野文昭, 根東覚, 大木研一, 小野寺宏, "哺乳類脳神経活動の*in vivo*観察に向けた透明化試薬による*in vitro*及び*in vivo*でのマウス頭蓋骨透明化." In: 第17回東京大学生命科学シンポジウム, Apr. 2017.

[P27] 鳴海紘也*, Tingyu Cheng*, Tung D. Ta, 川原 圭博, Lining Yao, "銀ナノ粒子インク回路を多様な基板に転写する手法とその評価." In: 電子情報通信学会ソサイエティ大会公演論文集, B-18-7, Sept. 2018 (* authors contributed equally).

[P28] 中原健一, 成末義哲, 笹谷拓也, 鳴海紘也, 川原圭博 , "渦電流を利用した非接触駆動による相転移アクチュエータの高速化." In: 電子情報通信学会ソサイエティ大会公演論文集, B-18-6, Sept. 2018.

[P29] 野間裕太, 鳴海紘也, 奥谷文徳, 川原圭博, "折りたたみ3D印刷の提案と形状に対する双安定性の評価," In: 電子情報通信学会ソサイエティ大会公演論文集, B-15-7, Sept. 2019.

[P30] 黒澤蓮, 笹谷拓也, 鳴海紘也, 川原圭博, "三次元無線給電システムにより駆動する空中浮遊デバイスに向けたペイロードと給電効率の検証." In: 電子情報通信学会ソサイエティ大会公演論文集, B-15-24, Sept. 2019.

[P31] 鳴海紘也, "銀ナノインクによるアドホックな回路作成のための支援ツール." In: 紙のエレクトロニクス応用研究会第5回技術研究発表会, Nov. 2015.

Domestic Demo

[P32] 野間裕太, 鳴海紘也, 奥谷文徳, 川原圭博, "先細り物体を折りたたみ3Dプリントするためのインタラクティブな設計ツール," In: インタラクション2020, To appear in Mar. 2020.

Introduction Article

[P33] 鳴海紘也, 川原圭博, "プラスチックフィルムと印刷技術による薄く柔軟なモータ," In: プラスチックス, vol.68, no.11, pp.68–72, Nov. 2017.

[P34] 鳴海紘也. "印刷技術を使った軽くてやわらかいモーター," サイエンスゲート, P22, Jan. 2018.

Domestic Patent

[P35] 特開2016-058460, AgIC株式会社, 国立大学法人東京大学, "導電パターン消去方法および消去具." 清水信哉, 杉本雅明, 川原圭博, 鳴海紘也, 浅見徹, 2016年4月21日公開

AWARDS

[A1] 東京大学工学部電子情報工学科 優秀卒業論文賞
鳴海紘也, "銀ナノインクでの反復的回路作成に向けた画像認識による抵抗値推定を利用したコンピュータ支援設計." Mar. 25, 2015.

[A2] Honorable Mention Award (top 5% of all the accepted papers)
Koya Narumi, Steve Hodges, and Yoshihiro Kawahara, "ConductAR: An Augmented Reality Based Tool for Iterative Design of Conductive Ink Circuits." In: *Proceedings of the 2015 ACM International Joint Conference on Pervasive and Ubiquitous Computing (UbiComp)*, Sept. 10, 2015.

[A3] 最優秀論文賞 (全論文中1件)
鳴海紘也, 中原健一, 佐藤宏樹, 新山龍馬, 川原圭博, "Liquid Pouch Motors: 紙のインタフェースのための薄く軽く柔軟なアクチュエータ." In: 第26回インタラクティブシステムとソフトウェアに関するワークショップ *(WISS)*, no.83, pp.1–6, Sept. 28, 2018.

[A4] 発表章 (全発表中2件)
鳴海紘也, 中原健一, 佐藤宏樹, 新山龍馬, 川原圭博, "Liquid Pouch Motors: 紙のインタフェースのための薄く軽く柔軟なアクチュエータ." In: 第26回インタラクティブシステムとソフトウェアに関するワークショップ *(WISS)*, no.83, pp.1–6, Sept. 28, 2018.

[A5] UbiComp Gaetano Outstanding Student Award Finalist (5 outstanding students per year)
Koya Narumi, "Animating Daily Objects and Environments." In: *Proceedings of the 2019 ACM International Joint Conference on Pervasive and Ubiquitous Computing (UbiComp)*, Sept. 9, 2019.

[A6] 最優秀論文賞 (全論文中1件)
鳴海紘也*, Fang Qin*, Siyuan Liu, Huai-Yu Cheng, Jianzhe Gu, 川原圭博，Mohammad Islam, Lining Yao, "Self-healing UI: 機械的かつ電気的に自己修復するセンシングインタフェース." In: 第27回インタラクティブシステムとソフトウェアに関するワークショップ *(WISS)*, pp.55–60, Sept. 27, 2019 (* authors contributed equally).